Development of Novel Scaffolds for Skeletal Muscle Tissue Engineering Applications

A DISSERTATION SUBMITTED TO THE
NATIONAL INSTITUTE OF TECHNOLOGY ROURKELA
IN PARTIAL FULFILMENT OF

Doctor of Philosophy

IN
BIOTECHNOLOGY AND MEDICAL ENGINEERING

BY

BISWADEEP CHAUDHURI
(ROLL NO. 511BM602)

Under the Supervision of
Prof. (Mrs.) Krishna Pramanik

April, 2016

Department of Biotechnology and Medical Engineering
NATIONAL INSTITUTE OF TECHNOLOGY, ROURKELA, INDIA

"No matter what conditions you encounter in life, your right is only to work not to the fruits thereof. You should not be impelled to act for selfish reasons, nor should you be attached to inaction"

The Bhagavad Gita 2/47

Dedicated

to

My Parents

Department of Biotechnology and Medical Engineering

NATIONAL INSTITUTE OF TECHNOLOGY, ROURKELA

August 31, 2016

Certificate of Examination

Roll Number: 511BM602
Name: Biswadeep Chaudhuri
Title of Dissertation: Development of Novel Scaffolds for Skeletal Muscle Tissue Engineering Applications

We the below signed, after checking the dissertation mentioned above and the official record book (s) of the student, hereby state our approval of the dissertation submitted in partial fulfillment of the requirements of the degree of Doctor of Philosophy in Biotechnology and Medical Engineering at National Institute of Technology Rourkela. We are satisfied with the volume, quality, correctness, and originality of the work.

Krishna Pramanik Principal Supervisor	**Samir Kumar Patra** Member (DSC)
Amit Biswas Member (DSC)	**Susmita Mishra** Member (DSC)
Mukesh Kumar Gupta Chairman (DSC)	**Sourabh Ghosh** Examiner

Department of Biotechnology and Medical Engineering

NATIONAL INSTITUTE OF TECHNOLOGY, ROURKELA

Supervisor's Certificate

This to certify that the work presented in this dissertation entitled "**Development of Novel Scaffolds for Skeletal Muscle Tissue Engineering Applications**" by "Biswadeep Chaudhuri", Roll Number 511BM602, is a record of original research carried out by him under my supervision and guidance in partial fulfillment of the requirements of the degree of *Doctor of Philosophy* in Biotechnology and Medical Engineering. Neither this dissertation nor any part of it has been submitted for any degree or diploma to any institute or university in India or abroad.

Krishna Pramanik
Professor
Dept. of Biotechnology & Medical Engineering
National Institute of Technology, Rourkela, Odisha, India

Place: NIT, Rourkela
Date:

Declaration of Originality

I, Biswadeep Chaudhuri, Roll Number 511BM602, hereby declare that this dissertation entitled ''***Development of Novel Scaffolds for Skeletal Muscle Tissue Engineering Applications***'' represents my original work carried out as a doctoral student of NIT Rourkela and, to the best of my knowledge, it contains no material previously published or written by another person, nor any material presented for the award of any other degree or diploma of NIT Rourkela or any other institution. Any contribution made to this research by others, with whom I have worked at NIT Rourkela or elsewhere, is explicitly acknowledged in the dissertation. Works of other authors cited in this dissertation have been duly acknowledged under the section ''References''. I have also submitted my original research records to the scrutiny committee for evaluation of my dissertation.

I am fully aware that in case of any non-compliance detected in future, the Senate of NIT Rourkela may withdraw the degree awarded to me on the basis of the present dissertation.

Biswadeep Chaudhuri

Place: NIT, Rourkela

Date:

ACKNOWLEDGEMENTS

There are always many wonderful people behind the scenes, with supports, sacrifice and good wishes in order to reach the goal. My Ph.D. Thesis would not have come to reality without all of those my well-wishers and supporters. Therefore, I would like to take the opportunity to convey my sincere thanks to all of them who helped me to carry out this thesis work and also all those who supported me with their good wishes to be what I am at present.

First and foremost, I would like to convey my deepest gratitude to my research guide, Professor (Mrs.) Krishna Pramanik, Department of Biotechnology and Medical Engineering for her valuable and inspiring guidance, in depth scholarly inputs, consistent encouragement, patience and providing me an excellent lab facility and atmosphere for doing research in this modern field of skeletal muscle tissue engineering. I am indebted to her for her love and concern during the past years. For this I would remain ever grateful to her with the hope of getting her blessings in all my life.

I am grateful to our Hon'ble Director, Professor S. K. Sarangi, who occasionally visited our department and encouraged us in our research and developmental work. I would also like to convey my regards to Professor B. Majhi (CS), Academic Dean, for his various suggestions and advice.

I also extend my sincere thanks to the Chairman and Head of the Department, Prof. M. K. Gupta (BM) and all the DSC members: Prof. S.K. Parta (LS), Prof. A. Biswas (BM), Prof. S. Mishra (CH) for their cordial supports and suggestions.

My sincere thanks are also extended to Prof. S. S. Ray, Prof. I. Banerjee, Prof. S. Paul and other teachers of Biotechnology and Medical Engineering Department, NIT, Rourkela. I am also grateful to Dr. D. Bhadra and Dr. B. Mondal of IACS, Kolkata, for their collaboration, Dr. S. Kumar of VITS University for various for various help and valuable suggestions. I am also thankful to Dr. J. Uddin for his help in HRTEM measurements at IIT, Kharagpur. I am especially grateful to Prof. Lorenzo Moroni, University of Twente, Tissue Regeneration Department, The Netherlands, for his collaboration and various suggestions.

I would like to extent my thanks and deepest love to my dear friends without whom I would not have survived the entire process: Dr. A. Bissoyi, Dr. N. Panda, Dr. N. Siddique, P. Majhi, B. N. Singh, V. Vishwanath, R. Kaur, D. Das and many other scholars of the Department, who stood with me throughout in suggesting solutions to all my academic and personal problems and giving me helpful suggestions.

I will always remember the support offered by our technicians associates Mr. Rabindra Maharana, Mr. Satyabrata Prusti, Mr. Haladar Behera, Mr. Chittaranjan Bhoi and Mr. Suresh Patra whose technical help was very much important to complete my research work.

I also take the opportunity to convey my sincere thanks to all my teachers and professor starting from school to university days. I am specially indebted to my MS thesis supervisor Prof. Tim Boswell (Newcastle University, U.K., School of Biology). Their blessings and suggestions are invaluable to build my carrier.

If there is any place where I get the highest help of all – appreciation, love, compassion and support, then that is my home. When my father stood firm for my education, my mother always took care and prayed for my personal life. I am grateful to my parents for their invaluable care and blessings.

I acknowledge The Department of Biotechnology (DBT), New Delhi, Government of India for providing research funds and fellowship to complete my research work.

Above all, I am indebted to the Almighty God for granting me the wisdom, health and strength to undertake this research task and enabling me to its completion.

Biswadeep Chaudhuri

NIT Rourkela

Development of Novel Scaffolds for Skeletal Muscle Tissue Engineering Applications

ABSTRACT

Tissue Engineering (TE) is emerging as an effective way of curing tissue oriented disorders through new tissue regeneration. Recently graphene oxide (GO composed of graphene oxide nanoplatelets, GOnPs) is widely being used for electronic and biomedical applications because of its favourable physicochemical properties. The present thesis work focuses on the fabrication of electrospun GO-poly (ε-caprolactone, PCL) and GO-poly (lactic-co-glycolic acid, PLGA) composite scaffolds for myoblast proliferation and differentiation of human cord blood derived mesenchymal stem cells (hMSCs), which is novel and challenging. The GO surface possessing different hydrophilic groups allowed it to be well dispersed in the polymer matrices for making electrospun fibrous scaffold meshes. Addition of GO in these polymers enhanced mechanical property, hydrophilicity and electrical conductivity of the GO-polymer composites. Electrical conductivity of the GO-PCL and GO-PLGA scaffolds increased by about two orders of magnitudes (from ~$5x10^{-9}$ to 2.3 x10^{-7} S/m^2) with the addition of low GO concentration (within non-toxicity limit <20 μg/ml for human cells). Such enhancement of conductivity along with nanostructural surface morphology of GO improved the biocompatibility and cell viability of the developed scaffolds. GO-polymer composites showed percolation behavior at low GO concentrations (~0.79 and 0.76wt%, respectively, for GO-PCL and GO-PLGA). High resolution TEM (HRTEM) and Raman G and D peak values indicated the presence of GO in the composite scaffold messes. *In-vitro* cell culture study confirmed excellent myoblast differentiation of hMSCs on these electrospun composite scaffolds. The GO-PCL composite scaffolds with suitable mechanical properties, little higher hydrophilicity as well as conductivity and dielectric constant (associated with GO surface charge) compared to those of GO-PLGA, exhibited better myoblast differentiation and promoted self-aligned myotubes formation, which were evident by cell attachment (FESEM studies), viability and proliferation (WST-8 assay), Immunohistochemical analysis etc. Moreover, IGF-1 cell signalling pathway study done on GO-PCL scaffolds also indicated superiority of the GO-PCL scaffolds for skeletal muscle tissue regeneration. It was revealed, for the first time,

that GO surface charge and significant enhancement of conductivity of the GO–polymer nanocomposite scaffolds, GO-PCL scaffold in particular, might be considered as potential candidates for the myoblast differentiation of hMSCs for the next generation human skeletal muscle tissue regeneration.

Keywords: ***Tissue Engineering; Myoblast differentiation; Graphene Oxide (GO); GO-Polymer Composites; Electrospun Scaffolds; Umbilical Cord Blood; Mesenchymal Stem Cells; Skeletal Muscle Tissue.***

Table of Contents

List of Figures

List of Tables

List of Abbreviations

AFM	Atomic Force Microscopy
Col	Collagen
CB-hMSCs	Cord blood derived mesenchymal stem cells
DMSO	Dimethyl sulfoxide
ECM	Extracellular matrices
DMF	N,N-dimethylformamide
FESEM	Field emission scanning electron microscopy
FTIR	Fourier transform-infrared spectroscopy,
FBS	Fetal bovine serum
FGF	Fibroblast Growth Factor
GO	Graphene oxide (GO)
GOnPs	Graphene oxide nanoplatets (GOnPs or GO)
GO sheet	Graphene oxide sheet composed of GOnPs
GF	Growth factor
HAP	Hydroxyapatite
IGF-1	Insulin-like growth factor 1
iPSCs	Induced pluripotent stem cells
LIF	Leukemia inhibitory factor
MMP-	Matrix metalloproteinase one
MHC	Myosin heavy chain
MNCs	Mononuclear cells
MSCs	Mesenchymal Stem Cells
hMSCs	Human mesenchymal stem cells
NMP	N-methyl-2-pyrrolidone
PDGF	Platelet Derived Growth Factor (PDGF
PVDF	Polyvinylidene fluoride
PBS	Phosphate buffer saline (solution)
PANi	Polyaniline
PVA	Polyvinyl alcohol

PLA	Poly-lactic acid
PE	Piezoelectricity
PLGA	Poly (lactic-co-glycolic acid)
PGA	Poly-glycolic acid
PCL	Poly (ε-caprolactone)
Q	GO surface charge
rGO	Reduced graphene oxide
SAED	Selected area electron diffraction
SkMCs	Skeletal myoblast cells
SMT	Skeletal Muscle Tissue
TE	Tissue Engineering
TGF	Transforming growth factor
THF	Tetrahydrofuran
TCP	Tissue culture plate
UCB	Umbilical cord blood
XDR	X-ray diffraction
ε	Dielectric constant of scaffold material
σ	Conductivity of the scaffold material

CHAPTER –1

General Introduction

1. General Introduction

This chapter provides a general introduction and brief discussion on different basic aspects of tissue engineering (TE), skeletal muscle structure and functions, muscle repair mechanism, challenges of skeletal muscle TE, significance and important properties of TE scaffolds, material aspect of scaffolds, stem cells and their importance in TE, future prospect of TE, its limitations and problems**.** A brief outline of the organization of the thesis is presented at the end of the chapter.

1.1. Background and Importance of the Study

With the advent of modern science and technology, conventional clinical fields of research and development have reached to a peak of excellence; various complicated tissue related diseases are being treated via medication and through surgeries with the aid of available modern sophisticated instrumental facilities. But, in several acute cases, precise clinical services with adequate advanced technological approaches are occasionally needed; especially when replacement or regeneration of tissue is of vital importance and where application of advanced TE becomes inevitable. Scientists and biotechnologists with their innovative ideas are engaged working in this highly demanding field of "Tissue Engineering", that regenerates, maintains and improves the functionality of the damaged or diseased tissues [1,2]. Currently, TE has become one of the rapidly emerging fields of clinical research contributing to the advancement of regenerative medicine to cure various diseases related to skeletal muscle [3,4], bone [5], cartilage [6,7], skin [8] and cardiac failure [9] to name a few.

The skeletal muscle tissue (SMT) is one of the most important tissue types responsible for the movements of different parts of human body. The main purpose of SMT engineering is to restore movements of defective limbs [10] or organs. The SMT damage might occur due to various causes like injuries, burns and disease like muscle trauma [11]. In such cases, large muscle tissues are lost or damaged thereby become non-functional. Moreover, there is also a chronic shortage of donor organs available for transplantation that highlights the urgency to develop novel strategies to address this problem. In general, medical treatment is performed by grafting of muscle from another part of the body to compensate the damaged area (auto graft) or by healthy tissues,

harvested from another animal or human (allograft), are used. Moreover, as mentioned above, there is also acute donor scarcity. In such cases, immunorejection and matching of identical physical structure are of major concerns [12]. Even if this procedure is carried out successfully, it may not provide natural orientation and functionality to the repaired or cured tissues [13]. Under such circumstances, patients might have to go through repeated surgeries that might sometimes be fatal [14]. To cope up with such adverse circumstances, TE has come forward with immense potential, not only to regain lost tissue, but also to maintain and provide tissue structure and strength without hampering its original functionality [15].

The most important requirements of successful tissue engineering are biocompatible scaffolds and live cells. Scaffolds must provide favorable environment for the differentiation and proliferation of the despised tissues. Such scaffolds should facilitate necessary guiding cues for tissue regeneration within the required time frame. For making skeletal muscle TE scaffolds, various biocompatible polymers have so far been used depending upon specific tissue types. Most popular biocompatible and widely studied polymers are both synthetic such as PCL (polycaprolactone) [3,4], PLA (poly-lactic acid) [16], PGA (poly-glycolic acid) [17], PLGA (poly-lactide-co-glycolide) [18] as well as natural polymers namely collagen, silk fibroin, chitosan [19,20]. But various problems related to biodegradability, mechanical stability, cell scaffold interaction, hydrophilicity, and conductivity of these scaffolds are needed to be tuned to develop a suitable scaffold for a particular tissue engineering application. A single polymer (natural or synthetic) scaffold has not been found, so far, to be suitable to provide all the desired properties (mechanical, biodegradability, conductivity etc.) to successfully regenerate a specific tissue type, for instance, skeletal muscle tissue. Therefore, continuous research and developments are still going on to find a suitable scaffold using novel materials that could effectively be employed to fulfil most of the required factors as mentioned above. Recently carbon based materials like carbon nanotubes (CNT) [3] or nanowire and nanocrystalline diamond have been widely tested for their potential toxicological risks and their possible uses in biomedical applications. The results of such studies involving carbon nanotubes (CNTs) are, however, not beyond contradiction, showing cytotoxic effects in some cases and improved cell growth in other case [21]. The toxicity of

nanotubes is apparently affected by their degree of dispersion, their level of functionalization and length [22-24]. Preparation of pure CNT is also difficult. Another recently discovered very important carbon based material is graphene and its derivatives. These novel graphene and graphene derivative, viz. graphene oxide (GO) and reduced graphene oxide (rGO) have drawn attention world-wide for applications in electronic devices, biosensors as well as in tissue engineering because of their favorable physicochemical properties as well as excellent biocompatibility that support skeletal muscle and other tissue growth and proliferation [24]. In graphene oxide, there are many hydrophilic groups on its surface (like carboxyl, hydroxyl and epoxy) so it can be dispersed in water and many other organic liquids, which are ideal solvents of several polymers. More importantly, GO is antibacterial and nontoxic (within 50µg/mL for human cells), ease to make composites with a wide range of conventional biopolymers which facilitate GO for TE and other biomedical applications. Graphene oxide nanoplatelets (GOnPs) form composites with many bioactive polymers [25], for examples, PCL, PLGA and PVA (polyvinyl alcohol). As usual, bioactive scaffolds composed of GOnPs and polymer can be prepared by various techniques. Electrospinning [26] is one of the latest popular modern techniques that had widely been used for the last decade to fabricate fibrous scaffolds with define and controlled characteristics [27]. This technique can also be successfully applied for the fabrications of GO-polymers or other polymer based composites for making scaffold meshes, similar to many other polymer meshes, for TE applications. To find a convenient and easily available source of stem cells for tissue regeneration is also of crucial importance [28-30].

1.2. Challenges in Skeletal Muscle Tissue Engineering

Tissue engineering is an emerging multidisciplinary field of research and development. There are various challenges which researchers encounter for the successful applications of TE. TE applies biological, chemical, mechanical, physical and engineering principles [28-31] towards the repair, regeneration or restoration of living tissues using biomaterials, cells, and growth factors. The most important issues related to the success of TE are the procurement of stem cells and the development of temporary holders providing favourable environment for cell growth and proliferation called ‘Scaffolds’. Cells are grown onto appropriate scaffolds with various optimized parameters to make

suitable constructs. Here, one of the major challenges is to design and fabricate the scaffolds using suitable biocompatible material that would provide necessary advantageous cues for the growth and proliferation of the desired muscle tissues. Moreover, one has to deal with various physicochemical parameters of the solid materials to find the best biocompatible scaffolds for the growth of specific cells on those scaffolds successfully [32-34] and also for the desired cells differentiation and proliferation before final implantation in the body. For tissue engineering, constant supply of living cells is also needed. In this connection, it is to be mentioned that among the various sources of human stem cells (viz. bone marrow, cord blood etc.), the use of human umbilical cord blood (UCB), considered as biological waste, would be highly significant if widely being used for TE purposes in a convenient way.

1.3. Skeletal Muscle Structure and Function

Skeletal muscles (SM) are responsible for locomotion of limbs and breathing and they also produce body heat called thermogenesis. Human body is comprised of 324 muscles and about 40-45% of human body mass consists of muscles. There are three types of muscles found in human body such as (a) skeletal muscle [3,4] (b) smooth muscle [35,36] located in the blood vessels, respiratory tract, iris of the eye, gastro-intestinal tract and (c) cardiac muscle [37] located in the heart that provides the contractile activity [38]. The SMT is composed of muscle fibers that are cylindrical-shaped having many nuclei per cell (multinucleated) which make up the entire skeletal muscle [30,38,39]. Muscle fibers or myotubes are made up of several muscle cells or myoblasts fused together. These fibers are again made up of number of myofilaments (~0.05-0.10mm of diameter and ~15cm in length). There is a layer of connective tissue called epimysium surrounding the entire skeletal muscle fiber [38]. But if this connective tissue is situated surrounding a bundle of muscle fibers, it is called perimysium while endomysium surrounds an individual muscle fiber. Each of the muscle fibers contains contractile machinery and cell organelles [38]. Skeletal muscle fibers contain blood vessels (capillaries) that enable flow supply of micronutrients and removal of waste. Through muscle contraction, skeletal muscle shortens and makes various parts of the skeleton moving. Muscle contraction is activated through specific signals carried out to the muscle via somatic nervous system [40].

1.4. Muscle Repair Mechanism

Natural muscle fibers cannot be repaired by their own. Muscle repairing cells, called satellite cells [41] are the main tools that involve in this complex mechanism of muscle tissue repair [42, 43]. Skeletal muscles repair themselves via fibrosis repair unlike skin or cardiac tissue repair [44]. Satellite cells are present in the outer layer of muscle fibers within the sarcolemmal basement membrane [45]. During muscle tissue repair, collagen-III is produced which plays an important role in muscle tissue regeneration. Researchers [46] later reported matrix metalloproteinase one (MMP-1) which destroyed previously produced collagen III and involved in the development of extracellular matrix (ECM) to migrate to the site of wounded/ injured tissue by releasing of MMP-2 [47]. Site specificity of MMP-1 was also reported by Wang and co-workers [48]. MMPs are naturally involved in the formation of ECM. But they can also be used by satellite cells to degrade basement membrane in order to migrate. On the other hand, expression of various transcription factors clearly indicate the current status of the muscle tissue. For example, MyoD is expressed until cell fusion occurs in muscle tissues. Similarly, myogenin marker also involves in myoblasts differentiation. After fusion of those satellite cells, MHC (myosin heavy chain) is expressed. So, Satellite cells are important tools to regenerate skeletal muscle tissue and to track myoblasts fusion for the formation of muscle fibers [49].

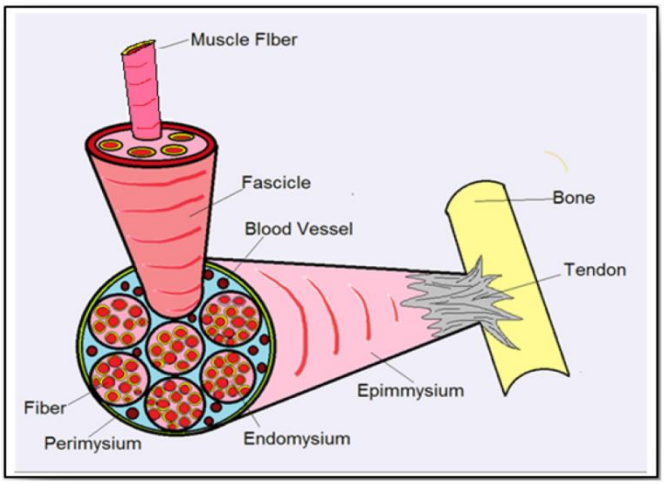

Figure 1.1. Schematic representation of human Skeletal Muscle Tissue (SMT) showing progression from muscle body surrounded by the epimysium. Bundles of muscle fibers are encapsulated by the endomysium and collected into fascicles by the perimysium.

1.5. Scaffolds for Skeletal Muscle Tissue Regeneration

On an average, skeletal muscle occupies 40-45% of total body mass. Skeletal muscle defects arising due to injury and/or diseases like muscle trauma are very much common and a major challenge to conventional therapeutic techniques. Various alternative techniques have been developed to cope up with the situation. Tissue regeneration is one of the most attractive and promising of them. However, for the success of TE, the design and development of suitable biocompatible scaffolds, as mentioned above, are of paramount importance. Skeletal muscle tissue engineering scaffolds have to be engineered in such a way so that cells can grow onto them and can form myotubes with natural orientation. In addition, scaffolds must facilitate muscle formation by stimulating cells adhesion, proliferation and differentiation. To prepare scaffolds, various biopolymers are used either in pure form or in the form of composite. As mentioned earlier, PCL [50] and PLGA [51] are among the most common synthetic biopolymers used for scaffolds preparation [52]. Various other polymers or solid materials are generally used as fillers to make these polymer composites suitable for TE applications. Recently graphene, a 2D monolayer of Sp^2 bonded carbon atoms and its derivatives like graphene oxide (GO) were found to be applicable in diverse fields for their excellent physicochemical, electro-chemical and mechanical properties [3, 53]. Interestingly, GO addition in polymer enhances the conductivity along with mechanical property of the GO-polymer composites. Conductivity enhancement of the scaffolds is important to induce myoblast differentiation and formation of self-aligned myotubes, a desirable factor for skeletal muscle tissue regeneration [28]. GO being nanomaterial like carbon nanotubes, there are several advantages of using such nanomaterial in TE [3, 54]. Graphene based materials are also utilized for various biomedical applications such as drug delivery [55], cancer therapy [56], and bio-sensing devices [57] because of their unique chemical and physical properties. Graphene based materials have also got application as a suitable implantable platform for electro conducting tissue engineering applications [3,58,59]. For example, fibroblast, osteoblasts and human mesenchymal stem cells (hMSCs) adhered well onto graphene based substrates and developed good cellular interaction [58,59]. Pristine graphene induced the osteogenesis of hMSCs [60] and differentiation of human neural stem cells into neurons [59,61]. GO stimulated the

differentiation of hMSCs to adiposities and the differentiation of induced pluripotent stem cells (iPSCs) into endodermal lineages [62]. GOnPs (or GO) form interesting nanocomposites with bioactive polymers like PCL [3] or PLGA [63] which can be electrospun to produce fibrous meshes for tissue regeneration. The GO-polymer composites with improved mechanical and electrical conductivity provide suitable cues for electro-responsive muscle tissue regeneration [64-67]. Biocompatibility and myoblast differentiation onto such composite meshes might also be very important for skeletal muscle or other tissue engineering applications. Because of excellent physicochemical properties, it has been proposed [59,67] to use these GO-polymer composite scaffolds as one of the potential candidates for myoblast differentiation and proliferation and also for myotubes formation.

In relation to scaffolds, cells-scaffold interaction also plays an important role in TE. Bone marrow (BM) derived stem cells have generally been used for various tissue engineering applications. Cord blood derived human mesenchymal stem cells (hMSCs) have also been reported to possess remarkable properties to differentiate into different cell types under suitable condition [68-70]. The study of cell adhesion, proliferation, and differentiation of hMSCs to skeletal myoblast cells (SkMCs) might be interesting. However, so far, very little work has been done on the differentiation of human mesenchymal stem cells (hMSCs) on GO sheet and GO-polymer composites (like GO-PCL, GO-PLGA or other polymers). Such investigation would establish the potential of GO and GO-polymer composites for myoblast differentiation and proliferation using cost effective hMSCs for tissue regeneration [71-74]. In this context, it might be argued that the availability of copious amount of stem cells from umbilical cord blood (UCB) would also increase the importance and feasibility of the TE research and applications in the field of regenerative medicine.

1.6. Important Properties of Skeletal Muscle Tissue (SMT) Engineering Scaffolds

The scaffolds used for TE applications must have certain well recognized basic properties as follows-

(a) Biocompatibility

It is to be noted that biocompatibility is associated with the characteristics of the biomaterials in different ways. It is actually the ability of biomaterial to response adequately (providing suitable environmental cues) with the host cells attached to it. Every scaffold material intended to apply in human or other animal body should be biocompatible to prevent blood clot leading to thrombosis or immunogenicity. All materials used for tissue engineering or drug delivery purposes should be excellent biocompatible. Scaffolds materials have to be free from toxins and non-immunogenic. Scaffolds (in-vivo) must be accepted by the body without any infection or immune response [75,76] . In this regard GOnPs appears to be an ideal biocompatible material.

(b) Biodegradability

It is actually a chemical dissolution of the biomaterial by biological means. Scaffold materials must have appropriate degradability inside the body (in-vivo). In most desirable case, the rate of degradation must match with new tissue formation. In addition, the rate of biodegradation must not be faster than cellular growth [77].

(c) Hydrophilicity

Hydrophilicity is the behavior of molecule that has tendency to attach or dissolve in water or other polar substances. Scaffolds must be hydrophilic (as much as possible) to accelerate cell adhesion and proliferation. Cells naturally prefer hydrophilic environment [78,79].

(d) Mechanical properties

Depending on the applications, scaffolds must have certain amount of mechanical strength. It is important mainly for the bone tissue regeneration. Hard tissues like bones require more mechanical strength compare to soft tissues like muscle tissues. But some researchers have reported mechanical stimulation improves skeletal muscle tissue regeneration [80]. For Go based GO-PCL composite films, Young's modulus varied from 13-19 +± 0.15 (MPs) and for graphene oxide it is around 10 MPs [64]. The addition of filler like graphene oxide in polymer composites enhances their mechanical properties along with conductivity which might also be varied depending on GOnPs contents in the composites [64-67]. Physical properties of the composite scaffolds depend on the

properties (nanostructure, size etc.) of the filler and the filler-polymer interaction [65-67].

(e) Conductivity (σ)

Conductivity (electronic or ionic) is a measure of the ability of scaffold material to conduct electric current, associated with movement of electron or ionic charge. Conductivity of scaffolds is an important physical property that contributes to the enhancement of biocompatibility and also influences specific cellular growth and their orientation. For skeletal muscle tissue regeneration, conducting scaffold materials accelerate cells adhesion and cell-cell interaction [81-83]. Biocompatibility of graphene oxide based insulating polymer composites is associated with unusual physicochemical properties of GO, namely, surface charge and dielectric permittivity similarly to many other scaffold materials [56,85,86]. Conductivity of PAV , PCL , PLGA, and MPPA are very small (5-10x10^{-9}S/m^2). In case of conducting polyaniline added PCL conductivity increases more than 5 times along with the increase of biocompatibility [84]. Similar increase of mechanical property, conductivity and dielectric constant of GO-PVA was also reported [65]. So an interdisciplinary approach of studying various physical properties (conductivity and dielectric constant associated with scaffold surface charge) of the scaffold materials is being currently made to explore the origin of biocompatibility of novel materials for the development of better scaffold materials for tissue engineering and other applications.

(f) Dielectric permittivity (ε)

Permittivity is a material property that affects the Coulomb force between two point charges in the material like graphene, polymers etc. Relative permittivity is the factor by which the electric field between the charges is decreased relative to vacuum. This property is associated with dipoles and surface charge present in the scaffold materials. In general, dielectric permittivity which is frequency and temperature dependent is very small (~5-10 at room temperature) for most of the biopolymers (PVA, PLGA, PCL, PVDF etc.). Addition of GO possessing surface charge to these polymers enhances both conductivity and permittivity along with biocompatibility of the composites [26,87] thereby showing percolating threshold behavior.

(g) Percolation behaviour of composites

Percolation is a random probabilistic process which exhibits a phase transition. Different percolation systems may contain clusters of different sizes and shapes. Studying the statistics of the clusters helps to understand the critical value of density when formation of finite or long range conductivity in random system first occurs. This is called the percolation threshold [87]. Figure 1.2 shows schematically the non-percolating and percolating network formation of equal size filler particles within a matrix (say, polymer) which indicates that as the concentration of the filler increases, clusters of individual particles are formed when the filler concentration approaches the percolation threshold, such clusters get self- connected and extend throughout the system. This theory has got great appreciation in material research as a powerful tool to account for the physical properties of heterogeneous material [87,88].

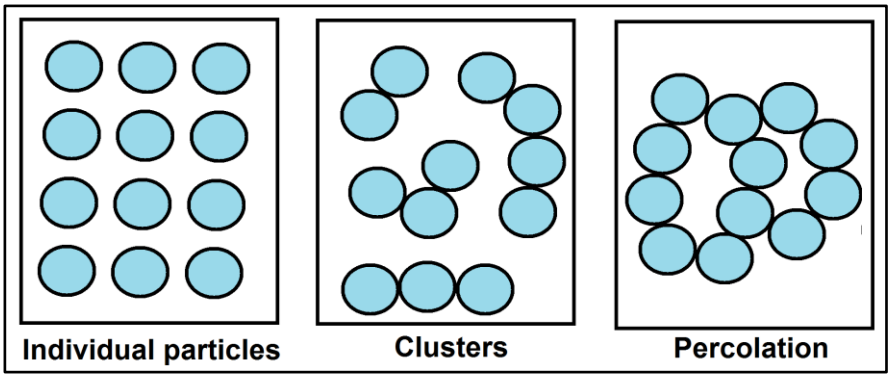

Figure 1.2. Representative diagram of the formation of non-percolating and percolating network composed of similar size fillers.

Percolation is a general phenomenon applicable in almost every area of science and technology as the simplest model for spatial disorder. Percolation has got wide applications in mathematics, physics, biology, geography, chemistry, hydrology, petroleum ecology and material sciences. Implication of percolation should be made to dielectric permittivity and electrical conductivity in polymer –graphene oxide composite scaffold. Percolation in polymer composites is highly important due to the potential to create electrically conducting material with an optimised dielectric permittivity with lowest possible filler (graphene oxide in the present investigation). Since one cannot use as much as possible GO in the composite because of the toxicity limit, the knowledge of percolation threshold would be important to find the lowest filler concentration with higher conductivity. A Lower percolation threshold is important for making

biocompatible substrates of desired mechanical strength. Higher concentration of the filler destroys mechanical property of the scaffold.

1.7. Scaffold Characterization

(a) Morphological studies

Morphological studies of the scaffolds and scaffold materials are very important for characterization of the material. Morphological studies are carried out by scanning electron microscopy (SEM), field emission scanning electron microscopy (FESEM), tunnelling electron microscopy (TEM), atomic force microscopy (AFM) and X-ray diffraction (XRD) studies [33].

(b) Porosity

Scaffolds must contain optimum porosity to facilitate nutrient diffusion to rejuvenate cells. Porosity of scaffolds depends on the type of cells they will carry and the type of tissues to be regenerated. Porosity and pore size may vary depending of application of that scaffolds and cell types. Porosity can also regulate mechanical behavior of a scaffold [33,89].

(c) Phase analysis and structural studies

Phase analysis of the prepared GO-polymer composite scaffolds is carried out by X-ray diffractometer (Model PA Analytical Philips, USA) using CuK_{α} radiation (λ=0.1542A^{o}) at room temperature [4,26,87,89].

(d) Contact angle

For the study of surface property (homogeneity, surface resistance, interaction of the scaffold surface) contact angle (CA) measurement is important [90]. There are several instruments available for the direct measurement of CA (both wetting and dewetting).

(e) Spectroscopic studies

Fourier transform infrared (FTIR) spectroscopy measurement is performed to estimate various structural properties and functional groups of the fabricated scaffolds. The machine is operated in transmitted mode in the frequency range within 500 -4000cm^{-1} [4,26,33].

1.8. Polymer Biomaterials for Skeletal Muscle Tissue Engineering Applications

Bioactive polymers are the major and most suitable components for the preparation and development of tissue engineering scaffolds [30]. There are mainly two types of biocompatible polymer materials viz. synthetic and natural along with their composites used to fabricate TE scaffolds that provide favorable cues for cells growth and proliferation [88]. Polymer being its own or in the form of polymer derivatives, blends, or copolymers are the building blocks of tissue engineering scaffolds.

(a) Natural polymer

These are abundantly available and resemble the components present in extracellular matrices (ECM) of cells. Natural polymers are obtained from natural living source such as animal shell, skin, plants etc. They are used for better cellular growth and proliferation. Recently, silk fibroin, chitosan, collagen, fibrin and gelatin are among the vastly useable natural polymers. These polymers are hydrophobic and non-immunogenic. But due to lack of strength and high swelling rate, they are not always desirable for every application. The higher cost of natural polymers is another disadvantage for rapid usages [91,92] of such polymers.

(b) Synthetic polymer

Synthetic polymers are easily available, versatile and comparatively cheaper synthetic polymers (PCL, PVA, PLA, PLGA, PMMA etc.) with predictable physicochemical properties, which are now widely being used in pure or mostly in the form of composites. These are highly stable for long term study and more non-immunogenic than natural ones [4,30].

(c) Composites

The composite materials can be defined as a composition of more than one distinct phase that is separated by interfaces. To take the advantage of more than one materials, many researchers are using composites instead of pure one [93-96]. For example, PCL is a suitable biopolymer for tissue engineering applications because of its biocompatibility, biodegradability, elasticity and mechanical properties [97]. But, lesser hydrophilicity, biodegradability and insulating (non-conducting) behavior limit its use in various

biomedical fields. During the last decade, researchers have made several attempts to make it more hydrophilic and electro conductive by preparing PCL-PANi (polyaniline) composites or by various surface coatings (via plasma treatment) to increase cellular activities [91]. There are also limitations for the use of organic polymeric scaffolds originating due to the release of acidic by-products that cause inflammation inside the human body and the lack of adhesion with the bone cells due to differences in their compositional properties [92]. The addition of a bioactive material to the polymeric system gives an added advantage of cell adhesion with the organic phase. Different biomaterials like hydroxyapatite, bioactive glasses, and glass-ceramics having bonelike mineral compositions are generally added to the polymers so as to make the tissue regeneration process faster by improving bone bonding *in vivo* [93-95]. Another advantage of using a filler is that the alkaline degradation products of the mineral help in neutralizing acidic by-products of the biopolymers thereby reducing inflammation. Thus polymeric scaffolds prepared from composites based on PLA, PCL and PLGA are expected to provide improved mechanical as well as physiological activity by way of initially reinforcing the polymer blend matrix and later as a bio-initiator. However, for the desired results, appropriate fillers supporting biocompatibility, biodegradability, cells-scaffold interactions, rate of cells proliferation etc. are to be chosen carefully. Biomaterial composites should create a favorable environment for cells to grow and develop tissues [93-95]. To prepare best possible scaffold for skeletal muscle tissue engineering, the material properties should provide favourable cues to grow muscle tissue. Although various biodegradable polymers are being used for skeletal muscle tissue engineering purpose, still there is urgent need for the development of novel and suitable electro-conductive biocompatible materials/composites providing necessary cues for the adequate growth and proliferation of skeletal muscle tissues. Experiments have been done with conductive matrix to understand their properties and usefulness as biomaterials. For better biocompatibility and specific tissue (like skeletal muscle) regeneration, as mentioned above, conductivity appears to be one of the important parameters to be acquired by the scaffolds [26, 93-95]. To improve conductivity of insulating biopolymers like PCL, researchers have used conducting polymers like polyaniline (PANi) which enhanced biocompatibility of the scaffolds [84]. So, different studies are being carried out for the discovery of new scaffolds with conducting

materials. In this context, graphene based polymer composite materials appear to be promising for the development of new scaffolds for future TE applications [26,97-101]. Interestingly, graphene oxide nanoplatelets (GOnPs) added polymer composite systems, hereafter also abbreviated as GO-polymer composites, are important for the enhancement of both mechanical stability and biocompatibility of the GO-polymer composites. GO-polymer composite electrospun meshes are also free from bead formation, a problem generally appears in polymer scaffolds [102-104]. The material properties of these composites can be optimized to enhance tissue regeneration. Composites composed of such novel GOnPs with suitable polymers are highly promising for skeletal muscle TE application discussed in the present thesis.

(d) GO-polymer composites and percolation behavior

With the addition of many solid fillers (GOnPs, for instance) in the polymers, mechanical electrical and dielectric properties are improved. But such enhancements showed limitation above a certain concentration of the filler (called percolation threshold concentration, f_c). Beyond that concentration, mechanical or electrical properties decline and such properties show anomalies at that concentration and mechanical and other properties of the polymer drastically change. The percolation concentration of the filler (GOnPs) depends on the physical properties (structure of the nanoparticles etc.) of the fillers as well as polymer character. It is desirable that the filler should be biocompatible and percolation threshold should be low without compromising the mechanical property (flexibility) of the scaffold materials. For nanomaterials like GOnPs the f_c is quite low [65]. Therefore, study of percolation behavior of composites is important to make composites with suitable mechanical stability as well as electrical conductivity.

1.9. Techniques Used for Scaffold Fabrication

There are several conventional techniques available to fabricate scaffolds. Such as Electrospinning, rapid prototyping, phase separation etc. which are briefly mentioned and discussed below.

(a) Electrospinning

This is the conventional and widely used method of producing nanofibers. Here electric field (with high voltage ~30-40kV) is applied to facilitate the fiber (nano or micro) formation. At the point when critical voltage is applied, surface tension of the polymeric solution is overcome by the charge imbalance that forces the solution towards target (collector) in the form of fiber. Here working distance, applied voltage, nozzle diameter are some of the important parameters [102-103] to be controlled. Various companies are making this machine such as Elmarco Nanospider, Czech Republic (Model: NS Lab 200 nano-spider), PICO Electrospinning machine, India (Model: ESPIN NANO). Electrospinning is the mostly used technique for making fibrous polymer or composite scaffold meshes.

(b) Rapid prototyping

Rapid prototyping or solid free fabrication (SFF) is the most technologically advanced method of producing 3D scaffolds with desired shape and structure. Computer aided design (CAD) is used to determine the structure of the scaffold using software and then RP machine generates the main structure. Layer by layer methodology is made to construct a 3D structure. Stereo-lithography, fused deposition modelling and laser sintering are among the most popular rapid prototyping methods. Scaffolds with complex geometry can be produced via this technique [98].

(c) Salt leaching

This is a simple method of preparing porous scaffolds. In this process, soluble salt particles are added in polymer solution as porogen and then casted into suitable moulds. After the solvent evaporates, the salt particles are removed by leaching and porous scaffolds are formed [105]. When salt particles are removed, the vacant areas appear in the form of pores. The major shortcomings of this method are difficulties in controlling pore size with porosity, low mechanical strength, pore interconnectivity, use of toxic solvents. To overcome the limitations of this process, more advanced methods were developed [99]. By controlling the pore size of the salt particle, it is possible to monitor the properties of the porous structure of scaffold material [106].

(d) Freeze drying

In this process, thermally induced phase separation (between two components) method is used. The pore size of the prepared scaffolds is established during this process. Freezing temperature can be varied from $-5^{o}C$ to $-80^{o}C$. The heating steps can be introduced to find the effects on the pore sizes. Annealing in the freeze drying process is associated with the rise of temperature of the frozen suspension as well as to boost the growth of ice crystals. The results indicated [105] that the pore size of the scaffolds are reduced along with the reduction of freezing temperature. It is also noticed that the introduction of annealing steps during freezing increased pore size (~30-40%). Phase separated mixture (water and the scaffold materials in most cases) is kept in low temperature and high vacuum atmosphere to sublime the solvent. Pores are generated by the removal of ice crystals. Here, by optimizing freezing temperature as well as concentration of the polymer solution, the solvent crystal (porogen) size can be controlled. The major drawback in this process is lower interconnectivity, production of toxins (residual solvent) and lower mechanical strength of the produced scaffolds [105]. Freeze drying works on the principle of thermally induced phase separation [107].

(e) Freeze gelation

This is a very common technique to produce porous 3D scaffolds and depends on the principle of thermally induced phase separation. This simple and effective method is vastly used to control pore size. Scaffold material solution is gelled and then dried to retain proper pore size thereby symmetry of scaffold remains intact. While the gel is warmed to melt the ice crystals, it makes the scaffold porous with comparatively continuous porosity with similar pore size and shape. On the other hand, this process is simple, cost effective and produces crack free scaffolds made up of various natural as well as synthetic polymers [101]. This is a simple effective technique where frozen polymer solution is immersed in a gelation environment at temperature lower than the freezing temperature of the polymer [86]. As the polymer matrix becomes gel before the drying stage, the porous structure can be retained without freeze drying. After freezing, the gel is warmed to melt the ice crystal and then dried [108]. This method overcomes many limitations of freeze drying like surface skin formation. It allows preparing low cost and crack-free 3D scaffolds in a convenient way [109].

1.10. Stem Cells for Tissue Engineering

Stem Cells have the unique property to differentiate into various cell types in the body [110]. Stem Cells are found in internal repair systems where they can divide unlimitedly to either repair or replace damaged cells throughout the body. Stem cells have the capability of forming a new cell which either has the potential of a stem cell or becomes a more dedicated type of cells having specific functionality. Stem Cells can be regarded as undifferentiated cells having high proliferative capability, ability of self-renewal and can form in multinuclear organisms. Stem cells have two unique properties compared to other cells namely, they are undifferentiated cells and capable of self-renewing for a longer period of time. Moreover, stem cells can be differentiated into different lineages with specific functionality. There are two types of stem cells: (a) Embryonic stem cells (ESCs) and (b) Adult or Somatic Stem Cells. ESCs can give rise to the whole body. On the other hand, an adult stem cell is undifferentiated cell found in different tissue or organ [111,112]. Adult Stem Cells maintain and repair the tissue in which they are found. Adult stem cells are immunocompatible, immunomodulators and immunosuppressant [110-114].

1.10.1. Mesenchymal stem cells

Mesenchymal stem cells have the ability to proliferate in-vitro and also differentiate into a number of mesoderm type lineages which include osteoblasts, chondrocytes, myocytes, adiposities cells [115-120]. hMSCs are potential source of TE because they are easily available in large quantity [118]. These cells also have high proliferation rate [116], immunocompatible and immunosuppresent. These are useful in allologous and autologous stem cells transplantation. hMSCs do not form teratoma or tumor as in the case of ESCs [121,122]. hMSCs were first identified in 1968 [123] from rat marrow. hMSCs in culture have fibroblastic morphology and can adhere on tissue culture plate (TCP) [124]. The important sources of hMSCs are bone marrow (BM), Umbilical Cord Blood (UCB), Placental Tissue (PT), Adipose Tissue (AT), Amniotic Fluid (AF) and others. It is to be noted that hMSCs derived from different sources might differ in proliferation and differentiation capabilities [125,126]. However, the most advantage of using UCB derived hMSCs are ease of their availability in large quantity and cost effectiveness (usually discarded as waste). Moreover, their ability to proliferate and maintain self-

renewal capability for long period of time in culture make these cells more useable for research and development [111]. One important characteristic of human mesenchymal stem cells (hMSCs) is their adherence to plastic surface (>90% expression of CD105, CD73, CD90) and differentiation to chondrocytes, adiposities, osteoblasts, myoblasts [127].

1.10.2. Site specificity of hMSCs

Site specificity is another important factor of tissue growth. Regeneration of new tissue has to be highly précised and should also be at the required injured site where replacement of old tissue with the new one is only needed. It has also been observed that under proper conditions, hMSCs can differentiate to specific tissues that had already been injured and urgently needed to be regenerated to support normal muscle function. Most importantly, the site specificity and efficiency are highly desirable to regenerate the damaged part without disturbing the rest where no further regeneration is required. Recently, it has been demonstrated [128-132] that hMSCs might differentiate selectively into tissue types that have only been injured. These tissues have systemically administered the growth of hMSCs to clone into immune deficient mice after subsequent carbon tetrachloride hepatic injury. Further to add, differentiation of hMSCs only into albumin expressing hepatocyte-like cells was also observed in those mice. All these are strong evidences that hMSCs possess some unique properties that are specific to the site of injury.

1.11. Future Prospects of Tissue Engineering (TE)

As mentioned earlier, TE is a parallel branch of medical technology that tries to overcome various difficulties of conventional therapeutic methods. In USA alone, 55% of all sports injuries are related to muscle damage caused by contusion, strain, or laceration [133]. Tissue engineering has the potential to cure organs with its original structure and functionalities. Till today, researchers have reported its tremendous benefit and prospects towards clinical science. Several tissue engineered and regenerative medicine products have been successfully developed prior to clinical trials in the United States alone [134] to overcome various difficulties regarding quality

control, ethical complications and in-vitro transplantation. Besides the therapeutic values of tissue engineering, in 2010, Journal of the Royal Society Interface [135] reported tremendous industrial impacts of this field due to an urgent need to overcome certain limitations of the conventional medical practices. They have also highlighted an emergency need for tissue engineering industries. USA alone has spent ~$2.5 billion in 2007 to develop this field that includes over 167 companies along with ~6000 employees. But this is not enough to serve the entire population of the world. Moreover, there are various ethical and approval (FDA) issues that still limit researchers as well as business personnel working in this areas [136]. But, the urgent need for an alternative therapy is taking this new field forward both in research and industrial level. Thus, it is highly expected that in the near future TE would make a parallel way beside conventional therapies [137]. Use of cord blood derived mesenchymal stem cells instead of bone marrow (BM) derived stem cells would further make this field of TE more attractive. A comparative study had already been done [138,139] which demonstrated the increasing growth rate of tissue engineering and number of employees involved in these industries. So, it is quite clear that TE industries are at constant growth. Another study also reported overall TE and stem cell sectors that spent ~$3.6 billion and employing almost ~14,000 employees during mid-2011 [139,140].

1.12. Tissue Engineering Limitations

The first scientific meeting on TE held in 1988 at Lake Tahoe, California [137,138], established the concept and importance of tissue engineering. Though TE is immerging as the next generation clinical practices capable of curing various diseases, this new field has several limitations and various challenges yet to overcome. First of all, there is immense gap between *in-vitro* and *in-vivo* experiments to know the actual efficiency of biomaterials due to lack of laboratory setup, research funds and expertise working in this area. Even after vigorous testing in sophisticated laboratories, FDA approval to functionalize a new product is another difficult procedure which various industries encounter. Furthermore, there are ethical issues involved that sometimes make barriers to the researchers. Beside developed laboratory facilities in USA and Europe, many Asian developing countries are nowadays conducing various research on this emerging area with limited research funds. Cost effective chemicals and lack of sophisticated

laboratories for in-vivo testing often make such kind of studies quite difficult. However, still there is increasing interest in research as well as in building industries. It has been noticed that most of the investors are from private sector or small scale organizations with limited financial capabilities [141-143]. The major industrial difficulties such as: (1) excessively high manufacturing and maintaining costs, (2) insufficient attention to reimbursement, (3) poorly structured agreements with marketing partners or Government, (4) unrealistic assessments of the cost-to-benefit ratio of the early products, (in developmental stage), (5) unrealistic sales forecasts leading to excessive fixed costs of sales, (6) financial exhaustion after protracted regulatory approval (FDA) processes, (7) less significant products with higher costs compare to conventional proven medication, (8) competition with existing well established companies (J&J, Pfizer, GSK, P&G etc.) who make pharmaceutical drugs and successfully treating diseases with conventional therapeutic products over centuries. In such a case, acceptance of tissue engineering products would be in doubt for majority of patients as well as doctors [140, 144-146]. However, researchers are now in contact with various related industries to enhance the growth of tissue engineering facilities both in research as well as in industrial scale production to bring the benefits of this novel field of biotechnology serving the mass.

1.13. Thesis Outline

Present study was intended to establish excellent cellular interaction and myoblast differentiation of cord blood derived human mesenchymal stem cells (hMSCs) on GO sheet composed of graphene oxide nanoplatelets (GOnPs), electrospun GO-PCL and GO-PLGA composite scaffold meshes which might be considered as potential candidates for skeletal muscle regenerations. The organization of the thesis is briefly described below:

The thesis consists of nine chapters(General introduction and literature review–Chapters 1 and 2, Experimental part –Chapter 3, Results and Discussion–Chapters 4-8 and Summary and Conclusion– Chapter 9).

Chapter 1 considers the fundamental concepts of TE and describes skeletal muscle structure and function, skeletal muscle repair mechanism and various types of scaffolds used in TE applications. Different types of biomaterials including the novelty of graphene

oxide (GO) based biocompatible composites, human stem cells used for TE applications are also briefly discussed in this chapter.

Chapter 2 consists of the summary of previous work done mainly on skeletal muscle tissue engineering scaffolds and mesenchymal stem cells used in TE for the regeneration of skeletal muscle tissue. Biocompatible composite biopolymer scaffolds used for skeletal muscle regeneration, importance of graphene oxide based polymers composite scaffold for TE applications have been briefly elucidated. The scope and objective of the thesis have been discussed at the end of this chapter.

Chapter 3 deals with the experimental part of the thesis. Synthesis of graphene oxide nanoplatelets (GOnPs), preparations of GO sheets, electrospun GO-polymer composite meshes (GO-PCL and GO-PLGA scaffolds), different characterization techniques have been discussed. Apparatus used for cells characterization and immunostaining analysis have been briefly mentioned in this chapter. Isolation of cord blood derived mesenchymal stem cells (hMSCs) from umbilical cord blood (UCB), used for myoblast differentiation on GO-based polymer composite meshes, has also been discussed.

Chapter 4 represents morphological characterizations of GOnPs (abbreviated simply as GO) sheet and GO-PCL composite scaffolds. Structural, vibration spectroscopic, mechanical and other characterizations (XRD, SEM, FESEM, HRTEM, Raman, FTIR, UV-VIS spectroscopic studies) of the prepared GO sheet and GO-PCL composite meshes have been discussed.

Chapter 5 deals with the in-vitro cell culture study on the fabricated scaffolds (GO sheets and electrospun GO-PCL scaffold meshes). Myoblast differentiation of cord blood derived stem cells, hMSCs and myotubes formation on thin GO sheet and GO-PCL scaffolds. In this part an attempt has been made to demonstrate myogenic proteins and gene expression on GO sheet and GO-PCL scaffolds along with IGF-1 cell signaling pathway analysis on these substrates. Importance of IGF-1 pathway on skeletal muscle differentiation and maturation has been explained.

Chapter 6 describes characterization of graphene oxide-PLGA composite scaffolds. Morphological and different other physical characterizations of the fabricated composite

(GO-PLGA) meshes (using, XRD, SEM. FESEM, HRTEM, Raman, FTIR, UV-VIS spectroscopic studies) have been presented.

Chapter 7 represents *in-vitro* myoblast differentiation and proliferation of cord blood derived stem cells, hMSCs, and myotubes formation on GO-PLGA scaffolds similar to that done on GO-PCL meshes. Myoblast differential potential of GO-PLGA composite scaffold has also been examined along with immunophenotypic characterizations, cell viability assay and flow cytometric analysis.

Chapter 8 highlighted the origin of excellent biocompatibility of the GO-polymer composites. From the study of GO surface charge, capacitance–voltage and current–voltage characteristics, an attempt has been made to elucidate the importance of conductivity and GO surface charge for the enhancement of conductivity and its contribution towards biocompatibility of GO added polymer composites .

Chapter 9 briefly summarizes the results obtained from the experimental work.

CHAPTER –2

Literature Review

2. Literature Review

This chapter deals with the current scenario of skeletal muscle (SM) tissue regeneration, some conventional polymer scaffolds used for skeletal muscle tissue engineering (SMTE), growth factors, novel aspects of new generation graphene in tissue engineering applications, graphene oxide nanoplatelets (GOnPs)-polymer composite scaffolds for tissue engineering and other applications. The scope and objectives of the thesis have been highlighted at the end of this chapter.

2.1. Skeletal Muscle Tissue Regeneration

The statement of purpose defined for tissue engineering (fabrication of artificial tissue and organs) is very promising with numerous scientific and technological challenges. Cells and biomaterial (which stimulate mammalian extranuclear matrix) are important components of artificial organs fabricated using tissue engineering strategies. Though the conventional medical therapeutic methods used in skeletal muscle repair and regeneration have now reached at an optimum state of remediation, still it is necessary to find an alternative method of tissue regeneration as there is large demand of skeletal muscle tissue repair and regeneration. Tissue damage generally occurs by various ways viz. injury, high degree burns etc. [3-5,147,148]. Though current therapeutics might cure such muscle disorders, but to acquire natural orientation maintaining functionality of the cured muscles, have not been discovered by the clinical practitioners yet. There is need of engineering living tissues which can be directly implanted inside the body [6, 54,72,148-150]. The main issue of tissue engineering is to precisely and safely regenerate or reconstruct injured tissues of skeletal muscle, bone, teeth, neural, cardiac, cartilage etc. [5,149,150]. One of the primary requirements for the development of tissue engineering is a constant source of supplementary stem cells which have the ability to be differentiated into various tissue types such as chondrocyte, osteoblast or myoblast cells. In modern tissue engineering, mesenchymal stem cells (derived from bone marrow or other sources) play the most important part [151] for in-vitro growth or regeneration of the required tissues. Researchers have already made various ingenious attempts focusing on the beneficial issues of mesenchymal stem cells [152] for the skeletal muscle regeneration and repair tissues with suitable scaffold materials that

would provide favourable environment including structural orientation [153] for muscle tissue regeneration.

Though the detailed process how dystrophic muscles are replaced or regenerated by fibrotic tissues inside the living organs is still not very clearly understood, skeletal muscle tissue engineering has been proved as one of the most important fields of regenerative medicine, a parallel potential therapeutic approach [154-156] to the conventional clinical practices, for the benefit of next generation human society. Myoblast cells or satellite cells are myogenic stem cells. These cells can multiply, align themselves and fuse to form multinucleated myotubes and then to myofibrils [38]. In vitro myoblast cells are stimulated to fuse and form myotubes by reducing the mitogen content in the growth medium [38]. The reaction of satellite cells to injury is similar to that of myoblast differentiation with regards to transcription factor. Several transcription factors that are part of the MRF (myogenic regulatory factor family) stand out from the plethora of molecular mechanisms involved in MyoD, and myf5 expressions which are involved in satellite cell/myoblast activation resulting in terminal differentiation of myoblast cells [157]. The transcription factors are often used as markers for proliferative or differentiated myoblasts. Modulating or maintaining the level of these transcription factors rely on cell-cell communication and also factors available in the ECM environment. Differentiation is negatively regulated by a host of mitogens and growth factors like Hepatocyte growth factor (HGF), fibroblast growth factor (FGF), transforming growth factor -β (TGF-β) and various cytokines, to name a few, which have enormous effects on the expression of transcription factors. HGF was shown to be associated with the maintenance of the proliferative state of myoblasts and also to stimulate satellite cells to enter the cell cycle. This was shown when injected in to the injured muscle. HGF blocked regeneration but increased the myoblast population [158]. FGF has been shown to interact with MyoD transcription factor. Yablonka-Reuveni and Rivera studied [159] primary cell lines and cultured immortal cell lines from the lineage and they found that with primary cell lines FGF had no difference on MyoD expression, but the cells maintained proliferation [159]. In immortalised cell lines, FGF only effects cells [160] not expressing MyoD to maintain the proliferative state.

2.1.1. Skeletal muscle tissue regeneration on electrospun scaffolds

For the development of tissue engineering and regenerative medicine, the importance of biocompatible polymer scaffolds (for instance, cell adhesion, differentiation, protein adsorption etc.) is unimaginable [33,161,162]. In stem cell therapy, scaffold material and appropriate scaffold design contribute in a most significant way to determine the desired shape and structure of the neo tissue [163]. Recently computer aided scaffold designing is becoming more popular [164,165]. Scientists working with suitable biomaterials are giving efforts to control over pore geometry and architecture of the scaffolds that would be favourable for the cell growth [164-166]. Bioengineered scaffolds made up of porous polyvinyl alcohol (PVA), silk, polycaprolactone (PCL), chitosan, polyhydroxylbutyrate, collagen, heparin, gelatin etc. had been used efficiently for scaffold preparations [167-170]. Earlier non-toxic polyvinyl alcohol (PVA) was used [164] as it tended to dissolve quickly after implantation. There are several convenient techniques which are in use for scaffold preparation viz. solvent casting [171,172], polymerization [173], melt quenching and moulding [174], phase separation [175] and freeze drying [176]. Regeneration of new muscle and degradation of scaffold should take place simultaneously. Ultimately the scaffold should be degraded within appropriate time frame and that space would gradually be occupied by the neo muscles [177,178]. This phenomenon might be compared with the phagocytosis of artificial (scaffold) basement membrane by neo muscles. It has recently been reported that surface charge, conductivity etc. also play important role in cellular interactions which may be beneficial for skeletal muscle tissue engineering application [26,179]. New generation scaffolds with new materials are being developed taking all these factors under consideration.

2.1.2. Some conventional polymers and composites for skeletal muscle tissue regeneration

Researchers are in constant search of an ideal material for specific tissue regeneration and their clinical applications. Vandenberg and his group [180] first used collagen gel as the substrate for skeletal muscle tissue engineering applications. Later, their work was modified by Huang [181] through the use of biocompatible silk fibrin gel as the matrix for muscle cells growth. The fibrin was degraded in three to four weeks as cells grew onto them maintaining their own ECM. The same research group [182,183] also

prepared 3D silk fibrin gel with better cellular activities and force transduction properties. Force measured at around ~40 kN/m^2 was similar to soleus muscle (~44 kN/m^2) in 1 day old wistar rats. This study also suggested how much force muscle produces in relation to specific occupied muscle area. However, some drawbacks were found that inhibited researchers from using such scaffolds for the application to skeletal muscle tissue engineering. The major drawback of using fibrin gels as a scaffold for skeletal muscle tissue regeneration is that they convey no template for muscle alignment and orientation.

Lam and his co-workers [183] had successfully used PDMS (polydimethylsiloxane) aligned scaffold and coated with 2μg/ml of laminin to accelerate myoblast attachment and gave rise to proper alignment on them. At the time when ~80% myotubes formed, a thin silk fibroin layer was applied onto them to create a natural extra cellular matrix. But the results did not show desirable alignments. Later, Dennis and co-workers [184,185] fabricated electrospun aligned PDMS scaffolds using a rotating drum collector aiming to give rise proper alignment of myotubes. Here electrospun scaffolds were used for the initial stage on which cells grew and a thin gel applied for better 3D myotube expansion on them. But, the main drawback of fibrin was immunogenic that caused infection leading to cells death. Another study [186,187] described that flexibility of the scaffold had an impact on myoblasts differentiation as well as myotubes orientation. Engler and co-workers [185,186] reported that myoblasts differentiated into myotubes were better and they also resembled natural muscle more closely on elastic scaffolds. They compared glass slides with collagen coated poly-acrylamide gels and collagen gels maintaining similar stiffness to natural muscle (~12kPa). Myoblasts differentiation was accelerated on elastic substrates. Levy-Mishali and his group [188] also did some research on this topic. This study was on polyelectrolyte multilayer films made from poly(l-lysine)/hyaluronan with various cross linkers to modify/regulate the stiffness of the scaffolds. They found myoblasts were detached earlier from soft gels because of formation of fewer focal adhesions on those flexible substrates. Levy-Mishali and co-workers [188] used PLGA foams with various PLA:GA ratios and concluded that scaffolds with Young's modulus of greater than 200kPa along with a higher lactic acid content showed better results for myoblasts differentiation in comparison to scaffolds with a greater glycolic acid content. That was an important finding to be considered for future

researchers for the fabrication of scaffolds for skeletal muscle tissue engineering [27,189]. Random and aligned fibers possess tensile strength of ~4 and ~5MPa, respectively. This finding demonstrates that random fibers are more elastic than aligned one suggesting the random one could be better for skeletal muscle tissue engineering if elasticity is considered.

Producing and maintaining the myotubes morphology both *in-vivo* and *in-vitro* are challenging problems of TE [190-191]. Cell growth and proliferation were done by using a scaffold [192,193]. Electrospun PLGA scaffold provided guidance for alignment of myoblasts [194,195] and an elastic substrate for myotube differentiation. A comprehensive review of the electrospinning process was carried out by Subbiah and co-worker [196]. High-speed rotating mandrel was used to create aligned fibers [53,195-198]. To date PCL, PLA, PGA, and their co-polymer PLGA have been used in the form of foams, films, and electrospun fibers for tissue engineering applications [199-201]. They used a sponge of PLLA and PLGA to form a highly porous three-dimensional (3D) scaffold for skeletal muscle development. Choi and co-workers [27] used electrospun PCL with collagen fibrous scaffold to induce myotube formation. Previous reports showed that flat, inflexible scaffolds were not suitable for myoblasts differentiation [202]. PLGA might overcome this problem making scaffolds suitable for myoblast cells growth. An elastomeric polymer like PLGA might show elastic deformation. Scaffold must withstand the stresses and strains of a monolayer of differentiating myoblasts into myotubes [185,203]. Graphene oxide –PLGA or PCL produced suitable electrospun scaffolds for myoblast differentiation and myotube formations [67].

2.1.3. New generation graphene in TE: Novel opportunities for skeletal muscle tissue engineering (SMTE) applications

Graphene has planer nanoflakes that consist of rings of carbon atoms with a hexagonal lattice structure [204]. It is the basic building block for other graphitic materials such as few layer graphene, graphene oxide (GO), and reduced graphene oxide (rGO). Few layer graphene is a flake-like stack of 2-10 graphene layers. When graphene undergoes oxidation, it becomes a chemically modified graphene; GO. Graphene oxide can be further reduced to produce reduced graphene oxide, rGO. Over the last several years graphene has emerged as a promising nano-platform with enormous potential for

biomedical applications and translational research because of its chemical, physical and mechanical properties, which make graphene and its derivatives ideal candidates for many biomedical applications including tissue engineering [51,58,62] and drug delivery [205]. Graphene is a newly added material for the use in Biomedicine and TE [206], its discovery won 2010 Nobel prize. Graphene and its derivatives have found their ways towards the interests of researchers working in different fields across the world. Interesting electrical, mechanical, optical, and chemical properties of graphene have further widen the application in a various interdisciplinary fields like electronic devices, biosensors, drug delivery, cancer therapy as well as in tissue engineering.

2.2. Characteristics of Graphene

Graphene possesses distinct properties different from any other carbon molecule, such as benzene and other allotropies. With such properties, graphene has provided advantages in TE and in much other applications. Its noble properties, such as electrical conductivity, elasticity, dielectric constant, surface charge, and adsorption of protein and low molecular weight substances, may favour the stem cells differentiation and neural or myoblast cells proliferation [206-208].

2.2.1. Electroconductivity of graphene

Electrical conductivity of graphene is due to sp^2 hybridized carbon atoms. Three of the outer carbon atoms form sigma bonds with neighbouring three electrons. The remaining one electron forms a π bond. In accordance with the Pauli Exclusion Principle, the outermost shells of the C-atoms are filled. σ -bond forms a solid and stable bond. In the π bond only half of the each C-atom p- orbital is filled. The electrical conductivity of graphene arises due to such bond formation.

2.2.2. Adsorption of proteins and low molecular weight substances

Graphene has the unique property that can be utilized for tissue engineering which is its ability to adsorb protein and low molecular weight chemicals. In order to either grow or communicate with neighbouring cells, cells secret various substances. Such substances are adsorbed onto the graphene surfaces and affect cell proliferation and differentiation [206-209].

2.2.3. Graphene promotes mesenchymal stem cells proliferation and differentiation

Marie Kalbacova and co-workers [58] showed that graphene based substrates promote the growth of hMSCs. Their study was based on hMSCs adhesion and proliferation. They found that hMSCs proliferated much better when cultured on graphene films compare to other substrates [58]. Though graphene is usually hydrophobic in nature, but other parameters such as surface chemistry, roughness and texture in combination create a favourable platform for the hMSCs to grow better. Cellular attachment involves physicochemical linkages between the cells (hMSCs) and the graphene surface through ionic forces or adsorption of any conditioning molecules such as proteins. Furthermore, differentiation of mouse skeletal myoblasts cells [67] have been done on graphene based substrates and these cells have grown better on GO because of their important physicochemical properties.

2.2.4. Exfoliation of isocyanate-treated GO nanoplatelets (GOnPs)

Researchers also have exfoliated functionalized GO nanoplatelets [204] that formed very stable dispersion in polar aprotic solvents. Treatment of GO with organic isocyanates forms new class of GO possessing reduced hydrophilic properties that are able to exfoliate in polar aprotic solvents thereby yields derivative of graphene oxide nanoplatelets. That was the first findings of complete exfoliation of chemically derived GO importantly in organic solvents. Use of cyano, keto, azidosulfonyl also modified the surface properties and chemistry of GO that can be further utilized for better cellular attachment and proliferation.

2.3. Graphene Oxide Based Skeletal Muscle Tissue Engineering

2.3.1. Graphene oxide and polymer composites for tissue engineering

This is a tedious work to find a novel material for specific applications. However, intensive and continued researches carried out all over the world thereby discovered different carbon based bioactive materials like carbon nanotubes, graphene and diamond. For skeletal muscle tissue engineering applications, the biomaterials have to be biocompatible, non-immunogenic and electro-conducting and also flexible with suitable mechanical strength. Recently, graphene and its derivatives are found to be very

suitable for tissue engineering applications. GO itself is non-toxic within the limit (~50μg/mL for human cells) which is suitable for use as an additive for the preparation of electro-responsive tissue engineering polymer composite scaffolds and other clinical applications [210]. GO can also form homogeneous composites with various biocompatible polymers suitable for producing composite meshes [51].

Yang and his co-workers [211] prepared GO-PVA composite films and characterized them using SEM, XRD, FTIR and thermogravemetric analysis. Films were prepared by reducing graphene oxide in polymer matrix using simple solution processing. Their interesting findings from structural and study of physical properties indicated the dispersion of graphene on molecular scale and aligned in PVA matrix which exhibited strong interfacial interactions among graphene and PVA via strong hydrogen bonding. Interestingly, this phenomenon was responsible for changing the structure and properties of the composite such as increasing glass transition temperature (T_g) and decrease in the level of crystallization. Though no study was done on cellular interaction or biocompatibility, this is well reported findings that helped future researchers. Recently, intensive study indicated enhancement of conductivity of polymer composites enhanced biocompatibility of the composite that are important for skeletal muscle tissue regeneration [4,212].

2.3.2. Graphene oxide nanoplatelets (GOnPs)–polymer composites enhanced mechanical, electrical and dielectric properties

Recently, intensive study of the GOnPs-PVA composite films have been done [56,66] showing enhancement of conductivity and dielectric constant in the composite. GOnPs form homogeneous composites with many bioactive polymers [213] are suitable for tissue engineering application because of their enhanced mechanical, electrical and dielectric properties [213]. Bhadra and co-workers [214] studied GO-PVA polymer composites and their percolating behaviour. Their results demonstrated that compared to pure PVA polymer, the GO-PVA composite significantly increased electrical conductivity and dielectric properties even at very low GO concentration. Low percolation threshold value was also estimated from the concentration dependent transport and dielectric data. Nearly 300 time increase in dielectric permittivity (compare to pure PVA) was observed which could be very much suitable for the growth

of cells, which are electro conducting such as skeletal myoblast cells and neural cells. The percolation threshold values of PLGA and PCL-GO composites were also found to be very small (~0.78 and ~0.81wt%, respectively for the PLGA and PCL composites. The enhancement of conductivity is very interesting indeed and could be very useful for enhancing biocompatibility of the composite scaffold (as in the case of conducting polyaniline added PCL composite scaffolds [172]) and hence such scaffold would be suitable for TE applications.

A few detailed studies on the relationship between human stem cell and graphene have drawn a tremendous impetus in the field of different TE applications [54]. These investigations were carried out mainly with bone marrow derived mesenchymal stem cells, induced pluripotent stem cells and neural cells. Although mouse myoblast proliferation on reduced graphene oxide deposited modified glass substrate was reported [67], no study was focused on the proliferation and differentiation of human mesenchymal stem cells to skeletal myoblast cells on GO sheet or GO-polymer fibrous scaffold. These studies are important for exploring the possibility of fabricating different GO-polymer based biocompatible conducting electrospun scaffolds for the repair and regeneration of skeletal muscle and other tissues using human stem cells.

2.3.3. Graphene oxide nanoplatelets (GOnPs)-polymer composites for tissue engineering

Graphite, a single atomic layer of sp^2-hybridized carbon covalently bonded in a hexagonal lattice is a naturally abundant material composed of stacked graphene layers (figure 2.1). Recently, GO based materials are being given high importance for their ability to differentiate and proliferate mesenchymal stem cells to different tissue types. Therefore, GO and GO based polymer composites are being used as potential biomaterial candidates for TE applications.

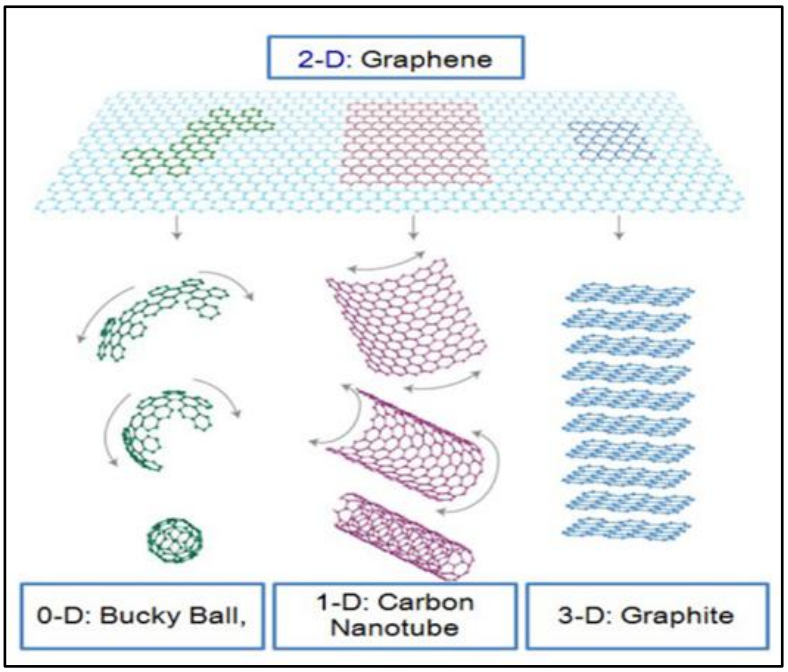

Figure 2.1. Schematic representation of graphene and carbon based materials. The hexagonal honeycomb structure with chemically active edges, graphene is a single layer of carbon atoms. The folded single carbon layer for carbon forms nanotubes. Graphene oxide is the oxidized form of graphene, increasing stiffness with number of layers.

Graphene has zero band gap with very high carrier concentration and mobility that results in remarkable electrical property that is suitable for various biomedical applications as well. Materials for such scaffolds should have suitable mechanical properties, chemical and biological compatibility and degrade in an appropriate time window [215-217]. During the last couple of decades many electrospun nano fibrous scaffolds [3,25,64,97,218-220] and carbon based nanomaterials (e.g. carbon nanotubes (CNTs) [221-223], graphene and its derivatives [58,224]) have widely been investigated for different clinical and TE applications. The CNT and GO incorporated scaffolds have good mechanical property and are useful for stimulating cell growth [221]. However, the metal catalysts used in the fabrication of CNTs are generally trapped inside the nanotubes [222] which have negative effects on their cytotoxicity [223]. Currently, graphene and its derivatives have drawn special attention as novel nanomaterials with great potential in applications and utilizations such as photonics and optoelectronics [225], sensors [55,86], biomedical as well as TE [56,87,226-228] because of their extraordinary physicochemical properties and favourable bioactivity. These properties further extended their intensive applications for the differentiation of human neural stem cells [56], osteogenic differentiation of human stem cells, drug delivery [227,228].

An injectable graphene/hydrogel-based gene delivery system has been developed for vasculogenesis and cardiac tissue repair [229]. The antibacterial property [230,231], anti-inflammatory effects [232] and biocompatibility [233] of graphene and graphene GOnPs were also tested with mammalian cells [95,101,117] by different research groups. Induced pluripotent stem cells (iPSCs) cultured on GO surface were found to adhere and proliferate even at a faster rate than graphene [60]. Graphene showed controlled and accelerated osteogenic differentiation of human mesenchymal stem cells [60,62]. All these favourable results revealed superior biocompatibility of graphene based materials for tissue culture and other biomedical applications compared to many bioactive polymer scaffolds [234]. Moreover, in contrast to carbon nanotubes and nano-diamond, GOnPs can be more easily prepared in pure form [235]. GO forms homogeneous composites with many bioactive polymers which are biocompatible and suitable for tissue engineering applications. A schematic representation of GO-polymer composite is shown in figure 2.2. Some important aspects of GO favouring TE application are mentioned in Table-2.1.

2.3.4. Importance of PCL and PLGA polymers for making biocompatible composites

It has already been mentioned that PCL and PLGA have been vastly used in TE and in other biomedical applications [236-242] because of their biocompatibility and solubility in different solutions for making fibrous scaffolds (Table 2.2). It is also important to note that the biocompatibility of graphene and graphene derivatives appear to be related to their different physical properties namely electrical conductivity (σ), surface charge (Q) which favours cells growth and proliferation [51,81,97,179]. Myoblast differentiation is also stimulated by electrically conductive scaffold fibers. In case of TE, the cells growth is improved in presence of electro-responsive materials [38]. Insulating PCL blended with conducting nanofibers formed excellent conducting biocompatible composites which enhanced cells proliferation [219]. Tables (2.1) and (2.2) describe some other important features of PCL, PLGA and GO for their favourable properties, suitability for making composite scaffolds for TE and other biomedical applications. Similar characteristic

behaviour is also exhibited by PLGA [51]. Over the last decade, PLGA composites have also been used extensively as artificial scaffold materials [243-246]. So, study of composites of PLGA and PCL with any new filler (like GO) for skeletal muscle TE application would be important. However, the filler used must be biocompatible and should have low percolation threshold for conductivity/dielectric permittivity. GO is biocompatible and GO-polymer composites have also shown low percolating threshold [214], higher conductivity and dielectric with low GO content. Therefore, graphene oxide nanoplatelets are promising fillers for the fabrication of biocompatible PCL and PLGA nano-composite scaffolds [247,248].

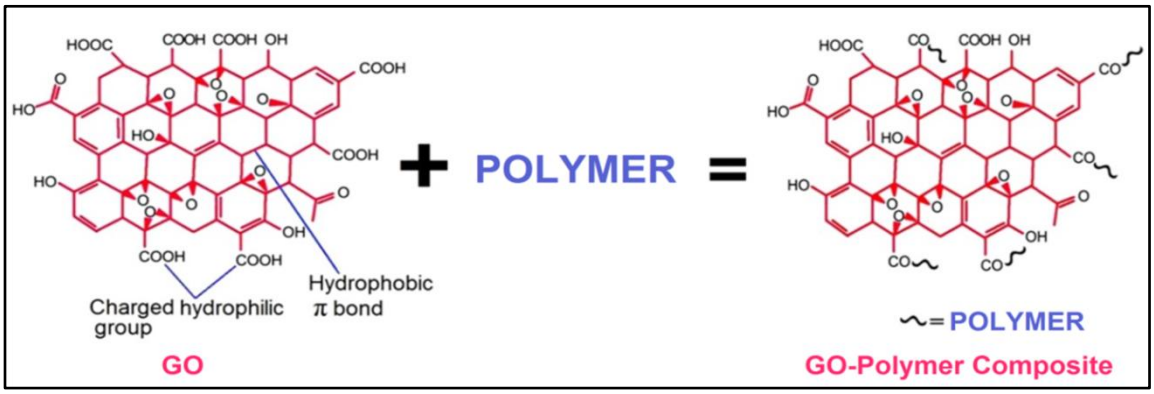

Figure 2.2. Schematic representation of graphene oxide (GO) and polymer interacting to form composites (edges are chemically active). It shows honeycomb structure with hydrophobic π bond. The polymer interacts with OH and carbon bonds. Uncharged polar groups (OH, -O) are seen on the basal surface.

It is reported that all the carboxyl groups cannot interact with the polymer chain. Only unbounded or free carboxyl groups interact. Unhindered -COOH groups bond covalently with the ester functional groups of the polymer [27,51,81,82,88,179]. Discussion on the interaction of graphene oxide and polymer has been made by Kim and his group [25] where strong interaction of GO and polymer has been shown. Both covalent and non-covalent functionalization of GO platelets has been reported to generate stable dispersions of chemically modified graphene platelets in organic solvents and also to enhance their compatibility with various polymer matrices. Among others, reactions using amines and isocyanates [27,51] have also been reported for small molecule functionalization of GO platelets because of the facility of the reactions and the ability to react in multiple ways (e.g., amidations, nucleophilic epoxide ring-

openings, carbamate formation, etc.). However, covalent functionalization of GO platelets could adversely affect the electrical conductivity of the platelets as these functionalizations disrupt (or retain the disruption already present in) the sp^2 hybridized network required for good electron conduction [27]. Non-covalent functionalization of GO nanoplatelets via, for example, pep stacking could minimize disruption of the conductive and conjugated structure [61,81].

Enzymatic degradation of graphene/PCL for tissue engineering was studied by Murry and co-workers [71] exploring the effects of graphene addition on the degradation rates of the correspondent nanocomposite scaffolds. In addition to electrical and topographical cues, piezoelectric (related to dielectric constant ε) responses of scaffold materials might also control the addition and differentiation of specific cell types [27]. Hydrophobicity is the only major drawback of pure PCL that prevents cell attachment which can, however, be overcome with surface coating of PCL or blending of PCL with other suitable materials such as gelatin, collagen, PANi, chitosan etc. Till now, researchers and scientists have given tremendous efforts to successfully regenerate skeletal muscle tissue construct. There is immense scope of research and development in this field of tissue engineering in terms of finding Novel materials like graphene and its derivatives that provide suitable physicochemical and biological properties required for skeletal muscle tissue regeneration. A few detailed studies on the relationship between human stem cell and graphene have drawn a tremendous impetus in the field of different TE applications [4,230,234]. These investigations were carried out mainly with bone marrow derived mesenchymal stem cells, induced pluripotent stem cells and neural cells. Although mouse myoblast proliferation on reduced graphene oxide deposited modified glass substrate was reported [67], no study has focused on the proliferation and differentiation of human mesenchymal stem cells to skeletal myoblast cells on such novel GO based composite scaffold. These studies are important for exploring the possibility of fabricating different GO-polymer based biocompatible conducting electrospun scaffolds for the repair and regeneration of electro-responsive skeletal muscle and other tissues using human stem cells.

Polymer blends and composites are the main composition for the preparation of various scaffolds. Recently, considerable interest has been paid on the skeletal muscle regeneration by tissue engineering to overcome various limitations of conventional medical approaches [4]. It has been demonstrated that conducting graphene oxide (GO) accelerates myoblast differentiation showing the potentiality of GO in the field of skeletal muscle tissue engineering. Graphene-based nanomaterials have obtained much interest in the field of biomedical and drug/gene delivery, cancers remedy, image resolution, as well as cells engineering. Beside dose dependent biocompatibility, GO is nontoxic and implantable within its nontoxic limit. But, their own influence on myogenic differentiation has almost never been learnt earlier other than the culture of neural cells and stem cells [207]. Many researchers explained graphene-based nanomaterials, particularly GO as well as reduced graphene oxide (rGO) as the emerging bioactive materials. Some important aspects of GO favouring TE applications are shown in Table 2.1. Recent reviews discussed many important biomedical and related applications of graphene and graphene based materials such as superior anticancer activity of graphene nanoplatelets [249,250].

2.3.5. Biocompatibility and toxicity of graphene and graphene based materials

Biocompatibility of GO and graphene–polymer composites have already been mentioned. Though graphene and its derivatives are in use for quite some time, biocompatibility and toxicity of graphene in case of human cells have recently been discovered. Wang and co-workers in 2011 [210] examined on this topic and put some valuable findings for further research and development. Graphene oxide was prepared from modified Hummers method and biocompatibility was measured on them using human fibroblast cells. Previously cells were cultured on various graphene substrates with different graphene concentration (low, middle to higher dose). In addition, they have also injected various amounts (dose) of graphene oxide to animal model (mice) to observe the biocompatibility of graphene oxide. Finally, they concluded that graphene oxide with dose less than 20μg/ml did not cause any adverse effect on human fibroblast cells. But, same way, it shows toxicity if dose is increased to more than 50μg/ml. Similarly, graphene oxide (0.1 to 0.25mg) injected in mice did not show any toxicity to

their body. But, if 0.4mg was injected onto them, there was some amount of adverse effects reported. Higher concentration of graphene oxide caused mice death due to lung granuloma formation in liver, kidney, spleen [210]. Another study with fibroblast cells showed that higher dose of graphene oxide caused cell apoptosis and disruption of cells causing cell death [210]. In conclusion, it is very much clear that careful selection of the amount of graphene oxide addition is very much important to enhance the biocompatibility.

2.4. Growth Factors for Skeletal Muscle Tissue Engineering

Growth factors play important role in skeletal muscle tissue engineering. Skeletal or other muscle regeneration needs collective action of cells, scaffolds, signalling molecules and growth factors [250]. Growth factors are soluble-secreted signalling polypeptides which instruct specific cellular responses in a biological environment. Under various circumstances, for instance, to regenerate affected tissues, cells secreted growth factors (GFs) protein perform various cellular actions viz. control over migration, differentiation or proliferation of a specific subset of cells and cell survival. Localized delivery of GFs is believed to be therapeutically effective for replication of cellular components directly involved in tissue regeneration and healing process [250-253]. Though all growth factors are important, some have more specific importance over the others for skeletal muscle regeneration. One important GF is Transforming growth factor (TGF)-beta1 which is very effective for fibroblast tissue regeneration. Immunohistochemical results predict TFG-beta as local stimulators for the tissue repairing process [253]. It has been shown that TFG-beta1 is one of the best fibrogenic mediators and it is over expressed in human dystrophic muscle [250-253]. Some important GFs are Angiopoietin-related growth factor (AGF), bFGF (basic fibroblast growth factor), Hepatocyte growth factor (HGF), Trand growth factor (TGF), Insulin-like growth factor (IGF), Platelet-derive growth factor (PDGF), Colony stimulating growth factor (CSF), Leukaemia inhibitory growth factor (LF) etc. It has been shown that TFG-beta1 is one of the best fibrogenic mediators and it is over expressed in human dystrophic muscle [250-253]. With increased TFG-beta1, mRNA levels are directly associated with initial stage [27] of tissue fibrosis which could be a positive indicator that the starting point of muscular tissue regeneration occurs through the TFG-beta1. It has also been shown that plasma TGF-beta1 level is elevated in

patients with DMD and congenital muscular dystrophy [254-256]. TFG-beta also shows positive effect on reorganization of extracellular matrix and basement membrane surrounding the damaged myofibers. By stimulating the synthesis of collagens, fibronectin and novel matrix proteins, TFG-beta directly induces angiogenesis to regenerate new blood vessels [257]. For example, it has been examined that TFG-beta is expressed by regenerating skeletal muscle within a few days after trauma. So, TFG-beta is undoubtedly one of the major multifunctional growth factors that can motivate the entire skeletal muscle regeneration process. Moreover, TFG-beta also stimulates the production of Platelet Derived Growth Factor (PDGF) that is well known to cause cell migration to the injured tissues thereby accelerate regeneration [258]. PDGF also acts as a potent stimulator of cell division in fibroblast-like cells. So PDGF is likely to accelerate fracture repair in early stages. Similarly, after tissue disruption, Fibroblast Growth Factor (FGF) released during inflammation which induces the satellite cells to further proliferate and hence accelerate the regeneration process [259]. Like TFG-beta, it has also been found that FGFs are angiogenic in nature. So, they can also be involved in the growth process of new blood vessel from pre-existing vessels, which gives another new aspect that TFG-beta not only regenerates new tissues but also helps in the formation of new blood vessels [68,204]. So it is quite evident that Transforming growth factor TGF-beta1 has some potentiality to directly influence the fibrotic process of human muscular dystrophy. Leukaemia inhibitory factor (LIF) has also been well examined and found to have some most important role in the regeneration of injured muscle [78]. LIF is also addressed as multifunctional cytokine that directly stimulates the growth of skeletal muscle after damage. Finally, growth factors have a great influence in proper growth and development of skeletal muscle regeneration.

Table 2.1. Some important aspects of graphene oxide (GO) for TE applications

Sl no.	Properties	Advantages of GO
1	Structural stability	Structurally high stable, doesn't breakdown during processing, can withstand high pressure & temperature [4,214].
2	Biocompatible	Suitable for in-vitro & in-vivo applications, non-immunogenic [4,67,260,261].
3	Electroconductivity	Excellent myoblast attachment and supports proliferation towards formation of myotubes. Declared as one of the BEST materials for SMTE. [4,67, 214,261].
4	Nontoxic (dose dependent)	Dose dependent toxicity has been observed [4,67, 72,84].
5	Self-Antibacterial	Additional benefit to prevent contaminations & infections [67,72].
6	Anti-cancer activity	Researchers have done some work on GO that indicates its anti-cancer activity which will be beneficial to support normal cells growth [13,67] 72].
7	Supports myoblast differentiation	GO supports myoblast differentiation and fusion to obtain multinucleated myotubes [53, 194,243].
8	Induces formation of multinucleated myotubes	GO supports myoblast differentiation and fusion to obtain multinucleated myotubes [13,53,194,243]

Table 2.2. Some important aspects of PCL and PLGA for TE applications

Sl No	Some Important aspects of PCL for TE Applications	
	Properties	**Advantages**
1	Highly biocompatible	One of the most suitable scaffold materials that is highly biocompatible and non-immunogenic therefore suitable for *in-vivo* applications. This remarkable property enables PCL to be used intensively for the fabrication of various tissue engineering scaffolds in the form of films or electrospun meshes [5,197].
2	Blendability	PCL can be blended with several natural and synthetic polymers. Moreover, PCL can be solubilized by various solvents like DMSO, chloroform etc. that makes it easier to blend with various other polymers for the preparation of scaffolds. It has also been observed that PCL makes uniform blend with other polymers which is useful to fabricate scaffolds with uniform distribution of polymers [4,260-264]
3	Structurally stable	Suitable for long term culture without breaking down the structure. This property enables PCL to sustain scaffolds properties while being used as composites [4,64].
4	Electrical conductivity of PCL composite scaffolds	Though pure PCL is less favourable towards cellular attachment, increased electrical conductivity with addition of Polyaniline (PANi) with PCL increased muscle cells growth of this composite. Electrical conductivity is an interesting feature that qualifies those materials for electro-responsive muscle tissue engineering [26,82,179,219].
5	Easy to fabricate	PCL by its own as well as in the form of composites can be easily fabricated by electrospinning for the preparation of fibrous meshes or for the preparation of films. This ease the scaffold fabrication process [64,261-264].
6	Used as composites	PCL as one of the popular scaffold materials used in the form of composites in tissue engineering and other biomedical applications. PCL can be blended homogeneously with silk-fibroin, PLGA, Chitosan, PLLA, collagen, gelatin etc. that increases its potential to be used as a scaffold material [5,260-264].
7	Non-acidic degradation	PCL does not produce any harmful by-products along with its degradation. This property does not put strain on growing cells and hence improves cellular interaction of the PCL-composite [5,260-264].
8	Economical	PCL is one of the cheapest biocompatible polymers being used Today for the preparation of tissue engineering scaffolds or in other biomedical applications. Use of PCL is thus beneficial especially for research purpose in developing countries [4,260-266].
Some important aspects of PLGA for TE applications:		
Both PCL and PLGA are similarly important for TE and other biomedical applications [67,260-265]. Amongst most of the biopolymer, PLGA has shown immense potential as a drug delivery carrier and as scaffold material for tissue engineering. Conductivity, biodegradability, and mechanical stability of PLGA can be improved by making composites with GO similar to that of PCL. PLGA is often described in terms of the relative percentage of two monomers (PLA and PGA); PLA and PGA ratio of 50:50, used in the present work, refers to 50%lactic acid and 50% glycolic acid [266]. One of the main advantages of PLGA is the non-toxicity of its degradation products. Both of which are easily metabolized by the body [266]. The ability to control the degradation kinetics of PLGA has made it a suitable biomaterial for control release strategies. PLGA has also been widely used as porous scaffolds for various TE applications [266].		

2.5. Scope and Objectives of the Work

From the literature survey, it appears that graphene and its derivatives (graphene oxide) are emerging as important biocompatible materials for tissue engineering applications. Graphene oxide has many oxygen-containing functional moieties, such as hydroxyl, carboxyl and epoxy groups. GO based composites are more conducting than the pure polymer scaffolds. The addition of GO enhances conductivity and mechanical stability of the polymer substrates as well as improve their cellular behavior. GO has antibacterial property and it is also non-toxic within certain limit (within 50 μg/mL) for human cells and provides necessary environment for TE applications. Therefore, GO is potential for use as a bio-building block for the fabrication of scaffolds for skeletal muscle regeneration. Because of the unique physicochemical characteristics such as electrical conductivity, high elasticity and good molecule adsorption of graphene oxides (GO and reduced graphene oxide, rGO) have drawn interest worldwide for their applications in tissue engineering and biomedical science. Graphene derivatives have been demonstrated as biocompatible substrates for the promotion of growth and spontaneous differentiation of various stem cells such as hMSCs, iPSCs, and neural cells. These investigations were carried out mainly with bone marrow derived mesenchymal stem cells, induced pluripotent stem cells and neural cells. Mouse myoblast proliferation on reduced graphene oxide (rGO) deposited on modified glass substrate was also investigated showing potential for myoblast differentiation. Elaborate investigation focused on the proliferation and differentiation of human mesenchymal stem cells (hMSCs) to myoblast cells on such novel GO based polymer composite fibrous scaffolds are highly important. Previous studies stimulated to explore the possibility of fabricating different GO-biopolymer biocompatible composite scaffolds for the repair and regeneration of skeletal muscle and other tissue types using human mesenchymal stem cells. These studies are challenging and demanding. Therefore, within the present scenario, the main objectives of the present thesis work are:

- To develop electrospun biopolymer based composite scaffolds
- To characterize the developed scaffolds from the studies of morphological, physicochemical and mechanical properties
- To assess in-vitro biocompatibility of the prepared scaffolds
- To differentiate mesenchymal stem cells seeded on these scaffolds to skeletal myoblast cells

E X P E R I M E N T A L

P A R T

CHAPTER-3

Materials and Methods

3. Materials and Methods

This chapter deals with the preparation of graphene oxide nanoplatelets (GOnPs) from natural graphite and electrospun GO–biopolymer composite (GO-PCL and GO-PLGA) meshes. A brief description of the different experimental techniques used for the characterization of prepared scaffolds used for cell culture was also briefly elucidated. Other than morphological, structural characterizations, standard methods were also used for the study of some physical properties (viz. measurements of conductivity, dielectric constants and surface charge behaviour) of GO and GO-polymer composites.

3.1 Materials

(a) Scaffold materials

Chemicals used for the prepration of GOnPs were analaytical grade graphite powder, H_2O_2, H_2SO_4, $KMnO_4$ (each of purity better than 99.9%) from E Merck (India). PCL (Mol wt. 65,000 g/mol), PLGA (PLGA: 50/50, MW=70-110kDa), chloroform and N, N-Dimethyleformamide (DMF) were purchased from Sigma-Aldrich , USA.

(b) Cell culture media and reagents

Dulbecco's modified eagle medium (DMEM), Penicillin-Streptomycin solution, fetal bovine serum (FBS), Dulbecco's phosphate buffered saline (DPBS), horse serum, antibiotic-antimycotic solution, phosphate buffer saline (PBS) solution, 0.25% Trypsin /ethylene diamine tetra acetic acid (EDTA) solution were purchased from (GIBCO, USA); paraformaldehyde, dimethyl sulfoxide (DMSO) from Sigma Aldrich, USA, All CD-markers were procured from BD pharminogen (Becton Dickenson, San Jose, CA). Tissue culture plates (TCP) ware from BD falcon and MP Biomedical-USA. Skeletal muscle growth media and skeletal muscle differentiation media (Promocell, Germany); insulin like growth factor 1 (IGF-1) (Invitrogen, USA); Ficoll Histopaque, paraformaldehyde, dimethyl sulfoxide (DMSO), WST-8 [2-(2-methoxy-4-nitrophenyl)-3-(4-nitrophenyl)-5-(2,4-disulfophenyl)-2H-tetrazolium, monosodium salt], collagen type-1 (rat tail) and FITC-phalloidin (Sigma Aldrich, USA); all primary and secondary antibodies (Abcam, United Kingdom) were purchased and used as received.

3.2. Preparation of Graphene Oxide Nanoplatelets (GOnPs)

High quality uniform shaped nanoflakes of GOnPs were prepared from pure (99.99%) natural graphite powder by the modified Hummers method [267,268] using $NaNO_3$, H_2SO_4, and $KMnO_4$. The oxidation product was purified by rinsing with 10% HCl solution, repeatedly washing with copious amounts of Milli-Q water, and filtering through standard filter paper. The filtered material was dried under vacuum (80°C, 3 h) and finally peeled off from the filter paper in the form of a ~0.5-mm-thick film. For the preparation of GOnPs dispersions in different solvents, the said dried product was first grounded and then added to the solvent followed by sonication in an ultrasound bath cleaner (J. P. Selecta Ultrasonic system, 40kHz) for 1 hr. To allow direct comparison between the dispersing behavior of the different solvents, a certain amount of graphite oxide powder (~5 mg) was added to a given volume of solvent (~10mL) in such a way that the resulting nominal concentration was adjusted to 0.5 mg mL^{-1} for all of the solvents. Graphene oxide dispersions were tested in different organic solvents such as acetone, methanol, ethanol, 1-propanol, ethylene glycol, dimethyl sulfoxide (DMSO), N, N-dimethylformamide (DMF), N-methyl-2-pyrrolidone (NMP), pyridine, tetrahydrofuran (THF), dichloromethane, o-xylene, and n-hexane. The water content of the solvents was below 0.1%. Because the common solvent for the preparation of graphite oxide dispersion is water, aqueous dispersions of the as-prepared graphite oxide materials were also made under exactly the same conditions as those used in the case of the organic solvents. Such water dispersion served as a reference against which the organic solvent dispersions were compared.

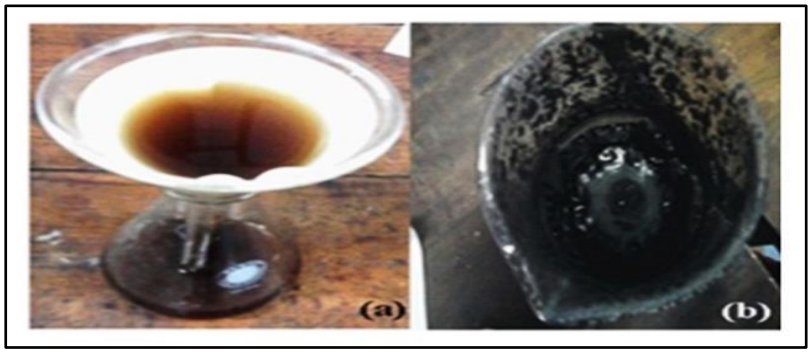

Figure 3.1. (a) Filtration of graphene oxide suspension, (b) graphene oxide suspension after hydrothermal treatment. The dried GOnPs were used for the fabrication of GO-polymer composites (GO-PCL or GO-PLGA).

A pictorial view of the preparation procedure of GOnPs suspension used for making GO sheet and GO-PCL composite meshes was presented in Figure (3.1) for demonstration.

3.2.1. Fabrication of thin GO sheets and hybrid composite materials with biocompatible polymers (PCL and PLGA)

The pure GO sheet was obtained from graphene oxide hydrosol prepared by ultrasonic peeling of GOnPs in aqueous suspension. The solution was dried in vacuum oven for making the GO sheet by spin coating. Graphene oxide solution in water was applied to a 2cm/2cm clean glass slide or Teflon plate which was mounted on a spin coater (Scientific India) attached with local vacuum unit. The sample was spun at 1500rpm for 20 seconds to fully cover the glass or Teflon slides with thin film of GO. The sample was then placed inside fume hood overnight before being placed in vacuum for complete evaporation of solvent and film formation [4,28]. To prepare GO-PCL or PLGA composites, the percolation threshold concentration of GO-PCL and GO-PLGA composites were studied. For this purpose, GO-polymer composite solutions were made in DMF (20v/v%) and chloroform (80v/v%) solutions with different GO concentration (0-1wt% GO) and were treated with ultrasound for 45 minutes to make a homogenous brown dispersion. PLGA (50:50) (or PCL) was dissolved at ~80^{o}C and the solution was subsequently cooled to room temperature (RT). The GOnPs were gradually added to the polymer solution (for instance DMF, for PLGA) with stirring and sonicated at RT for 45 minutes to obtain homogeneous GOnPs/polymer solutions. Finally, the above solutions were allowed to stand overnight to remove air bubbles, then poured into glass dishes and kept at ~40^{o}C for film formation until its weight equilibrated [4,28]. Similarly GO-PCL composite films of different GO concentrations were prepared. The final disc-shaped composite films for different GOnPs concentrations were prepared each having ~10-20mm in diameter and ~0.1mm in thickness. The concentrations of the GOnPs fillers were varied systematically to investigate the influence of GOnPs on the dielectric and electrical properties of the composite.

3.2.2. Preparation of electrospun GO-polymer (PCL and PLGA) composite meshes

To prepare electrospun GO-PLGA composite meshes, for cell culture, specific amount of GOnPs (20µg/ml) was dissolved in calculated amount of DMF (20v/v)/Chloroform(80v/v%) mixture under continuous stirring for three h. GOnPs were added at a concentration of 20µg/ml PLGA solution (to keep GO concentration within non-toxicity limits) and stirred again for another 1 h. making homogeneous solution. The final colloidal solution thus obtained was loaded into a 12ml plastic syringe with a stainless-steel needle (diameter ~0.60mm) and used for making fibrous meshes by using electrospinning machine (PICO ESPIN, India). The needle for electrospinning was connected to a high voltage supply (~25kV) and the flow rate of the solution was adjusted to 1.5ml/h. The fibrous meshes were collected on aluminium foil placed at a distance of 12 cm from the needle tip. Electrospun collagen (0.10g/ml acetic acid) meshes were also prepared for control using similar technique and sterilized for one hr by UV (wavelength ~254nm and power 15W). GO-PCL electrospun fibrous meshes were also similarly prepared from GO-PCL solution using PCL (1gm /100ml) and GO (20µg/ml). The final colloidal solution was used for making scaffolds by electrospinning as mentioned above.

3.3. Characterization of Scaffolds

Graphene oxide and graphene oxide polymer composites have been characterised by using different techniques like XRD, SEM, FESEM, AFM, Raman, FTIR and UV-VIS. The porosity of the electrospun scaffolds was measured by Mercury intrusion porosimeter.

3.3.1. Phase analysis

X-ray powder diffraction (XRPD) is a rapid analytical technique primarily used for phase identification of a crystalline or amorphous material and can provide information on the unit cell dimensions. The monochromatic collimated beam of X-ray from the source interact with the sample producing constructive interference (and a diffraction ray) when conditions satisfy Bragg's Law:

$$2d\sin\theta = n\lambda \qquad (3.1)$$

Where d is the inter-planer spacing, θ is the incident angle, n is the order of diffraction and λ is the wave length of the incident X-ray. Samples for XRD were taken in the form of powder in the holder and placed in the radiation chamber for obtaining the diffraction patterns indicating different phases of the samples. Conversion of the diffraction peaks to d-spacing allows identification of the material because each material has a different set of d-spacing. Typically, this is achieved by comparison with d-spacing of the standard pattern [269]. To ensure phase purity of the sample, XRD was performed for all GO and GO-polymer composite samples and materials at room temperature by a PHILIPS SHIFFERT 3710 diffractometer using Cu K_α radiation source (λ =1.5418 Å and 35kV, 30mA) [269]. The samples were scanned from 20° (2θ) to 70° (2θ) at a scanning rate of 3.0θ/min. Crystallinity was determined by integration using Kaleida Graph (Synergy Software).

3.3.2. FTIR analysis

Fourier-transform infrared (FTIR) spectroscopy is a measurement technique whereby the spectra are collected based on measurement of the coherence of a radioactive source, using time-domain or space domain measurements of the electromagnetic radiation or other type of radiation [270,271]. The FTIR spectra were recorded using the Perkin–Elmer spectrum 100 FTIR spectrometer with a 4 cm^{-1} resolution. FTIR spectrum (in the range of 500-4000cm^{-1} was obtained for the prepared graphene oxide and GO-polymer composites. FTIR spectroscopic study of pure PCL, PLGA, GO and the composites were done using Shimadzu 800 spectrometer.

3.3.3. UV-Visible spectral analysis

Solutions of transition metal ions can be coloured (i.e. absorb visible light) because d electrons within the metal atoms can be excited from one electronic state to another. Organic compounds, especially with a high degree of conjugation, also absorb light in the UV or visible region of the electromagnetic spectrum. For the UV-Vis measurements GO samples were taken in solution (water, chloroform and DMSO). The UV–visible spectrophotometric measurements of nanocomposite solution [272] were done within the wavelength range from 400-700nm by using a double beam spectrophotometer (Model No. EI2375).

3.3.4. Atomic force microscopy (AFM) studies

The AFM measures the forces acting between a fine tip and a sample surface. The tip is attached to the free end of a cantilever and is brought very close to a surface [273,274]. Attractive or repulsive forces resulting from interactions between the tip and the surface will cause a positive or negative bending of the cantilever. Atomic force microscopy (di CP-II, Veeco) was used to characterize the samples. AFM imaging of the dispersions deposited onto silicon wafer was performed and the corresponding tapping mode AFM images of graphene oxide nanoplatelets were detected. The fractured surfaces were coated with gold before analysis. FM tapping mode image of graphene oxide nanoplatelets from aqueous dispersion(spin coated on mica substrate at 2000rpm) with superimposed cross section measurements was taken along blue and cyanine indicating ~1567nm in radial diameter and GO sheet thickness around 450nm.

3.3.5. Scanning electron microscopic (SEM) analysis

Scanning electron microscopic studies were made to observe the morphology of the developed GO sheet, GO-PCL and GO-PLGA meshes using SEM model (SEM: JEOL JSM 6480) following standard procedure [269,272]. The traces of moisture present in the scaffolds were removed by drying in a vacuum drier for 2 h. at 40°C. Platinum coating was done prior to imaging. A minimum of 25 pores were considered for calculating the pore size of the developed scaffolds along with the estimation of fiber diameter by using Image J (USA) software.

3.3.6. Field emission scanning electron microscopy (FESEM)

Field emission scanning electron microscopy was used for better analysis of the nanostructure feature of the graphene oxide nanoplatelets (GOnPs) and GO embedded in PCL and PLGA polymer composite meshes using the FESEM (FEI Nova NanoSEM 230 FESEM), following standard procedures [269,272]. Almost similar procedure was adopted for the SEM and FESEM studies. The fractured surfaces of the GOnPs/polymer composite films were also observed via field emission scanning electron microscopy (FEI Nova NanoSEM 230 FESEM). The samples were dried in vacuum dryer for two h. at 40^{O}C and platinum (Pt) sputter coating was done prior to imaging.

3.3.7. High resolution transmission electron microscopy (HRTEM) analysis

High resolution transmission electron microscopic (HRTEM) analysis was made to study the presence and morphology of the GOnPs embedded in the GO-Polymer composite meshes. Small grains of GOnPs and composite samples were placed on copper grid using alcoholic solution and dried before use as usual. Selected area electron diffraction (SAED) confirmed the structure. The high resolution transmission electron microscope (Model: JEM-2010, JEOL) was used for the HRTEM analysis [275].

3.3.8. Raman spectroscopy

This is a vibration spectroscopic technique suitable for characterizing carbon based materials like graphene and graphene based composites with their characteristic peaks [276]. The laser Raman spectroscopic study was carried out for characterizing the graphene oxide and graphene oxide–polymer composites providing information about the GO band present in GO-polymer composite. Raman spectroscopy (HORIBA JOBIN Yuon: Exciting wavelength 514nm with Argon ion laser) was used. Raman spectra were taken in water solution of GOnPs and in chloroform solution of GO-PCL and GO-PLGA meshes. All measurements were made at ambient temperature.

3.3.9. Electrical conductivity and dielectric constant measurement

Frequency dependent electrical conductivity and dielectric measurements were carried out with the help of an impedance analyser (HP 4192A) [277]. To look for the origin of excellent cellular interaction of GO sheet and GO-polymer composite meshes, surface charge, current- voltage (I–V) and capacitance -voltage (C-V) characteristics were measured using standard methods [278]. Samples were cut in rectangular shape and both sides were coated with conducting paint which acted as electrodes. A two terminal capacitor configuration was employed for this measurement.

3.3.10. Conductivity and dielectric constant stability of the composite samples

The conductivity and dielectric constant stabilities related to degradation of the scaffolds [279] meshes were assessed by immersing in physiological solution (PBS) at ~37^{o}C for about one week. in vitro degradation of electrical conductivity and dielectric constant stabilities of the electrospun samples in PBS solution were determined from

the morphological changes and also by surface electrical conductivity and dielectric constant measurements. The dried electrospun fiber meshes with a thickness of 50-60 µm were cut into small rectangular pieces (~20x20mm^2) and the specimen were immersed in phosphate buffered saline (PBS) solution at pH ~7.4 in test beakers. These samples were incubated in a water bath at ~37^{o}C. After one week, each sample was retrieved from the beaker, rinsed several times with deionized water to remove adhered PBS solution and kept in a vacuum chamber before the measurements of resistivity, dielectric constant and the morphology study using SEM measurements.

3.3.11. Mechanical property

Mechanical tests were performed to define tensile strength (from load - elongation curves) of the scaffolds by using a Universal Testing Machine (Model: Instron Electro Puls E1000) with a 1 kN load cell at room temperature (~30^{o}C). Samples were prepared with an average length of ~15mm, width ~10mm and thickness of ~0.5mm. All tests were carried out at room temperature (RT) [4]. Mechanical characterization of the GO sheet was performed by uniaxial tensile testing. GO sheets were carefully cut into rectangular stripes (15×30mm) and loaded with an Instron 3369 tensile strength measuring system. A segment of electrospun meshes (10×25mm) was fixed at the cut ends for the axial testing (n=5).

3.3.12. Water contact angle measurement

Contact angle measurement of a water droplet on the scaffold surface can provide information about hydrophobicity [280]. Water contact angle (CA) measurements against distilled water were performed using a sessile drop method (DAS100S: KRUSS GMbH, Germany). The advancing (wetting CA_w) and receding (dewetting CA_{dw}) contact angles were measured at room temperature at different locations for the GO sheets and GO-polymer meshes. The advancing CA of liquid on homogeneous surface is mostly dependent on the surface resistance to wetting-presence of hydrophobic domains in the case of water. Conversely, the receding contact angle is most strongly controlled by the strength of the interaction between the liquid and the surface, that is, the presence of hydrophilic domains.

3.3.13. Porosity measurement

The porosity of the composite scaffolds was measured by Mercury intrusion porosimeter (Poremaster-33, Quanta chrome, USA). The bulk density of samples was calculated by equation, B_D = D/W-S, where D = dry weight, S = suspended Weight, W = soaked Weight [281]. The percentage porosity was calculated from intrusion data. For all types of scaffolds, experiments were carried out in triplicates.

3.4. Swelling Behaviour and Biodegradation Study

Each rectangular shaped sample film (initial weight W_o) was cut and immersed in deionized water for 12h. After retrieving from immersion, water from the scaffold surface was removed with water soaking paper and the sample was weighed in wet condition (W_1) [282]. Swelling ratio S_r (%) was calculated from the following relation.

$$S_r\ (\%) = [(W_1 - W_o)/W_o\ ] \times 100$$

Each such experiment was repeated three times.

For biodegradation study, the fabricated scaffolds were cut into small pieces (6mm/8mm) with initial weight M_o and immersed in PBS at ~37^oC (pH ~7.4). The samples were soaked in PBS solution for different periods. Then the scaffold samples were taken out of the solution and properly dried at 40^oC in an oven for 24h and the weights of dried scaffolds were again measured as M_t.

Whereas the biodegradation (B) was calculated as:

$$B\ (\%) = [(M_o - M_t)/M_t] \times 100$$

3.5. *In-Vitro* Cell Study

3.5.1. Human umbilical cord blood (UCB) collection

UCB was collected from ISPAT General Hospital, Rourkela with prior patient's consent. All procedures were approved by the Institutional (National Institute of Technology, Rourkela, India) Ethical Committee. In brief, UCB sample was collected in a blood bag containing ~15ml of Citrate Phosphate Dextrose Adenine (CPDA) anticoagulant agent to prevent blood clot and processed in laboratory.

3.5.2. Isolation and culture of mononuclear cells (MNCs)

Mononuclear cells (MNCs) were isolated directly from UCB following standard Ficol Hypaque density gradient method [4,261,283]. In brief, first, 30ml of UCB (diluted with RPMI 1640 in the ratio of 4:1 (v/v)) and 25ml of Ficol was added in sterile tube. This solution was centrifuged at 430×g at 4^{o}C for 30 min. Then the solution inside the tube was found separated into three various layers. Just above the Ficol layer (middle layer – buffy coat) a smoky white layer was produced where MNCs were present. This smoky layer was then carefully pipette out without hampering the other layers and kept in another sterile tube. Next, 25ml of D-PBS was added with this solution and again centrifuged for 15 min at 300×g. The supernatant was removed and bottom part (about ~5ml) was collected where the density of the MNCs were the highest. This solution was then mixed with 45ml of DMEM media consisting of 10% FBS, 2mM glutamine and 1% 100-x antibiotic-antimycotic solution in another sterile 50ml tube. The entire solution was mixed gently and poured in three sterile T75 culture flux and placed in a CO_2 Incubator. After 24h, the cells were washed with D-PBS to remove non adherent cells and fresh media was introduced. These cells were cultured for up to 5^{th} passaging. The media change was carried out twice a week.

3.6. Characterization of Umbilical Cord Blood (UCB) Derived hMSCs

3. 6.1. Morphological characterization

Morphological characterization of the cultured hMSCs were observed from the culture flask under phase-contrast inverted microscope. Images were captured using a Carl Zeiss Axiovert 40 microscope without any kind of specific staining.

3.6.2. Immunophenotypic characterization

This is one of the major techniques used in modern research for the acknowledgement of specific cells type using cell surface markers. Specific surface antigens expressed by hMSCs were characterized by flow cytometry analysis. UCB derived cells were stained with human monoclonal antibodies against CD90-FITC, CD73-PE, CD105-APC, CD34-FITC, HLA DR-APC, and CD45-PE [4,261]. This experiment was carried out using a flow cytometer (Becton Dickinson and Co, San Jose, CA, USA).

3.6.3. Proliferation of hMSCs (DNA quantification assay)

Proliferation of hMSCs was assessed by DNA quantification assay. Cell scaffold constructs from each predetermined time period of culture (3, 7, 11 days) were collected and washed with serum free DMEM to remove the traces of serum components. The constructs were washed twice with PBS and the cells were lysed using 0.4ml of Lysis buffer containing 10mM tris and 2% triton for about an hour. Quant-it PicoGreen reagent was used following the manufacturer's protocol. In brief, 100µL of Quant-it PicoGreen reagent was added to 100µL of sonicated cell lysate and incubated at RT for 10 minutes. The fluorescence was measured with a spectrofluorometric plate reader (Model: LS 55 Perkin Elmer, USA) at excitation and emission wave lengths of 528nm and 485nm, respectively.

3.7. Differentiation Potential of Umbilical Cord Blood (UCB) derived hMSCs

3.7.1. Cells seeding and culturing

UCB derived hMSCs (5×10^3cells/well) were directly seeded (following static seeding method) onto the thin film like GO sheet (~30µm thick) and GO-polymer mesh (areas ~45mm^2) as well as on control in a 12 well plate.

3.7.2. Cell attachment and morphology

Cells adhesion on the different substrates was studied by SEM or FESEM analysis. After specific days of culture, the cells seeded on all the substrates were carefully washed twice with PBS, fixed with 2.5% glutaraldehyde for 4h. and then dehydrated through a gradient series of ethanol from 70% to 100%. All the said substrates were then carefully dried using a vacuum desiccator to make them moisture free prior to SEM or FESEM analysis.

3.7.3. Cell viability and proliferation assay

Cell viability and proliferation on GO-PCL composite meshes, thin GO sheet and controls were measured by water-soluble tetrazolium salt (WST-8) assay after 3, 7 and 11 days of cell seeding in 96 well culture plate. 10µl of cell proliferation reagent (WST-8) was added into each well containing sample with 100µl of culture medium and

incubated for 4h. at 37^{o}C. Absorbance (OD) of the solution was then measured at 450nm by a microplate reader (Varioskan Flash, Thermo Scientific). The cells seeded on tissue culture plate and/or collagen mesh were evaluated as controls.

3.7.4. Myogenic differentiation

hMSCs grown onto the scaffolds were cultured with skeletal muscle differentiation media (90 v/v%) supplemented with FBS (10 v/v%) and 100x antibiotic-antimycotic solution (1 v/v% approximately), and incubated at 37^{o}C and 5% CO_2 atmospheric condition. In addition, insulin like growth factor-1 (IGF-1) was added (5ng/ml) to enhance the myogenic differentiation process. After 12-15 days of culture, cell morphology was found to change towards bipolar skeletal myoblasts. Low serum (2% horse serum) media was introduced to enhance myoblast fusion and formation of myotubes [4,261].

3.8. Characterization of Myoblast Cells

3.8.1. Immunohistochemical characterization of myoblasts

Fluorescence (Zeiss Axivert 40 CFL) and Confocal (Leica TCS SP2) microscopes were used for the detection of fluorescence spectra of the cells. The fluorescent images were analysed for the expression of muscle specific antigens such as Desmin, MyoD, Dystrophin and Myosin Heavy Chain (MHC) to assess the expression of myogenic cell specific antibodies. A computer monitor was attached with the microscope camera for the capture of images [4,261]. Immunohistochemical analysis was done directly on cells grown on scaffold samples along with tissue culture plate (TCP) taken as control.

3.8.2. Immunophenotypic characterization of myoblasts

Specific surface antigens expressed by skeletal myoblasts were characterized by Fluorescence-activated cell sorter (FACS) analysis. The skeletal myoblast cells adhered onto the GO sheet, GO-PCL meshes and control were trypsinized and flow cytometry analysis was performed to verify the expression of skeletal muscle differentiation markers like CD56 and desmin. For all antibodies, 5×10^5 cells were incubated in 100 ml of PBS containing 1% FBS and the dilution of primary antibodies was ranged from 1:15 to 1:100. The cells after being incubated with primary antibody on ice for 30 min, were

washed with 1% FBS in PBS, re-suspended in 100 ml of FITC-labelled secondary antibody and diluted 1:100 in 1% FBS in PBS. Finally, the cells were incubated again for 30 min on ice and washed with PBS containing 1% FBS prior to re-suspension in PBS with 1% FBS for FACS analysis. Isotype-matching immunoglobulin (IgG) and FITC-labelled secondary antibody were used to determine nonspecific signals. The flow cytometric analyses were performed using a flow cytometer (BD LSR Fortessa, San Jose, CA, USA) equipped with an air cooled argon laser. FACS data were analysed by FCS Express software.

3.9. Myogenic Protein Expression

Western Blotting method was used for this experiment. To study the expression of myogenic specific proteins, the trypsinized cells from specific cell-seeded scaffolds were suspended in buffer containing 20mM TRIS, 2mM EDTA, 150mM NaCl, 0.5%Triton X-100 and protease inhibitors (Sigma). The samples were then sonicated, centrifuged and the pellets were discarded. Cells were assayed for protein concentration following standard Bradford- assay. Protein extracts of approximately 45-50µg/sample were separated onto the 10% SDS PAGE and transferred to nitrocellulose membrane followed by incubation with primary and secondary antibodies following the manufacturer's protocol and visualized on film with the ECL substrate kit (Abcam Inc., Cambridge, MA, USA) [284].

3.9.1. Myogenic gene expression

Myoblast cells grown on scaffolds were analyzed via the expression level of myogenic genes such as Desmin, MyoD and MHC using Quantitative real-time RT-PCR. Synthesis of cDNA synthesis was performed from cells cultured on control, GO-PCL and GO-PLGA meshes separately using FastLane cDNA synthesis kit (Qiagen, Germany). Real time RT-PCR was carried out using Quantitect SYBR Green (Quigen, Germany) with BioRad CFX96 Real Time detection system (Bio-Rad, USA). Thermocycling conditions followed were 95^{o}C for 15 min, 40 cycles of denaturation (15s, 94^{o}C), annealing (30s, 55^{o}C) and extension 30s, 72^{o}C). The sense and antisense primers used were: MyoD, sense 5'-AAG CGC CAT CTC TTG AGG TA-3' and antisense 5'-GCG CCT TTA TTT TGA CC-3' (PCR product, 500 bp); Desmin, sense5'-CCAGCTCTCAGTGGCCATGCAGA-3' and antisense 5'ACCTCCAGCACTGTGAGCACCG-3' (PCR product, 400bp) and myosin heavy chain (MHC), sense 5'-TGT GAA TGC CAA ATG TGC TT-3' and antisense 5'- GTG GAG CTG GGT ATC CTT GA-3' (PCR product, 750 bp). Relative expression level of each gene compared with that

of beta-actin was calculated and normalized by the value for cells cultured on tissue culture plate taken as control [285-287].

3.9.2. Cell signalling pathway analysis

Insulin-like growth factor 1 (IGF-1) pathway is one of the important cell signaling pathways to assess myogenesis that is related to skeletal muscle differentiation and maturation [285,287,288]. The main pathway proteins involved here are IRS-1, PI(3)K, p-Akt and MyoD, sequentially. Expressions of these proteins were assessed by western blotting analysis. In addition, inhibition of Akt, present in this pathway, was done via chemical inhibition to assess the final expression of MyoD for confirmation of this pathway.

3.10. Statistical Analysis

All data were presented as mean ± standard deviation (SD). Single factor analysis of variance (ANOVA) was carried out to compare the mean of different data sets and a value of $p \leq 0.05$ was considered significant.

R E S U L T S

A N D

D I S C U S S I O N

CHAPTER-4

Characterization of GO Sheet and Electrospun GO-PCL Composite Meshes

4. Characterization of the Prepared Graphene Oxide Sheet and GO-PCL Composite Scaffolds.

This chapter deals with the experimental characterization of the prepared GO sheet (composed of grapheme oxide nanoplatelets, GOnPs) and electrospun GO-PCL composite meshes from the studies of XRD, SEM, TEM, HRTEM, FTIR, Raman spectra, mechanical property, contact angle measurement, and electrical properties (conductivity and dielectric constant). These properties indicated GO and GO-PCL electrospun scaffold meshes as suitable candidates for skeletal muscle tissue engineering and other biomedical applications.

Detailed discussion on the preparation of pure GO sheet and electrospun GO-PCL composite meshes has already been made (chapter-3). These novel bioactive composite materials have drawn special attention because of their great potential in applications for the differentiation of human neural stem cells [31], drug delivery [227,229], TE [56,60,233] and also in cancer therapy [248]. More discussion on the importance GO and GO-polymer composites for skeletal muscle tissue engineering applications have already been discussed in chapters 1 and 2. The GO concentration in the prepared GO-PCL composite scaffold meshes used for the present investigation was kept within the percolation limit.

4.1.1. Percolation threshold behaviour of GO-PCL composite

The percolation behaviour of GO-PCL composite was investigated from the study of GO (or GOnPs) concentration dependent conductivity and dielectric constant measurements of the composite at room temperature. The GO-PCL composite scaffolds were prepared with different GO concentrations (0-1wt%). Figure (4.1a) showed the well dispersed GO-PCL solution, spin coated GO film on glass and as prepared thin GO sheet (composed of GOnPs).

GO concentration (f_{GO}) dependent dielectric permittivity (ε) and frequency dependent conductivity (σ) of the GO-PCL composites showed maximum values (figure 4.1b and c, respectively) and a typical anomalous behaviour (phase transition) around $f_{GO} = f_c$ ~0.79wt%. As GO concentration (f_{GO}) in GO-PCL composite was increased to 0.79wt%, dielectric constant and conductivity decreased to a lower conducting regime.

This anomalous transition occurred at the percolation threshold value (f_c = 0.79wt% GO) which is associated with the formation of semiconducting network [87,88].

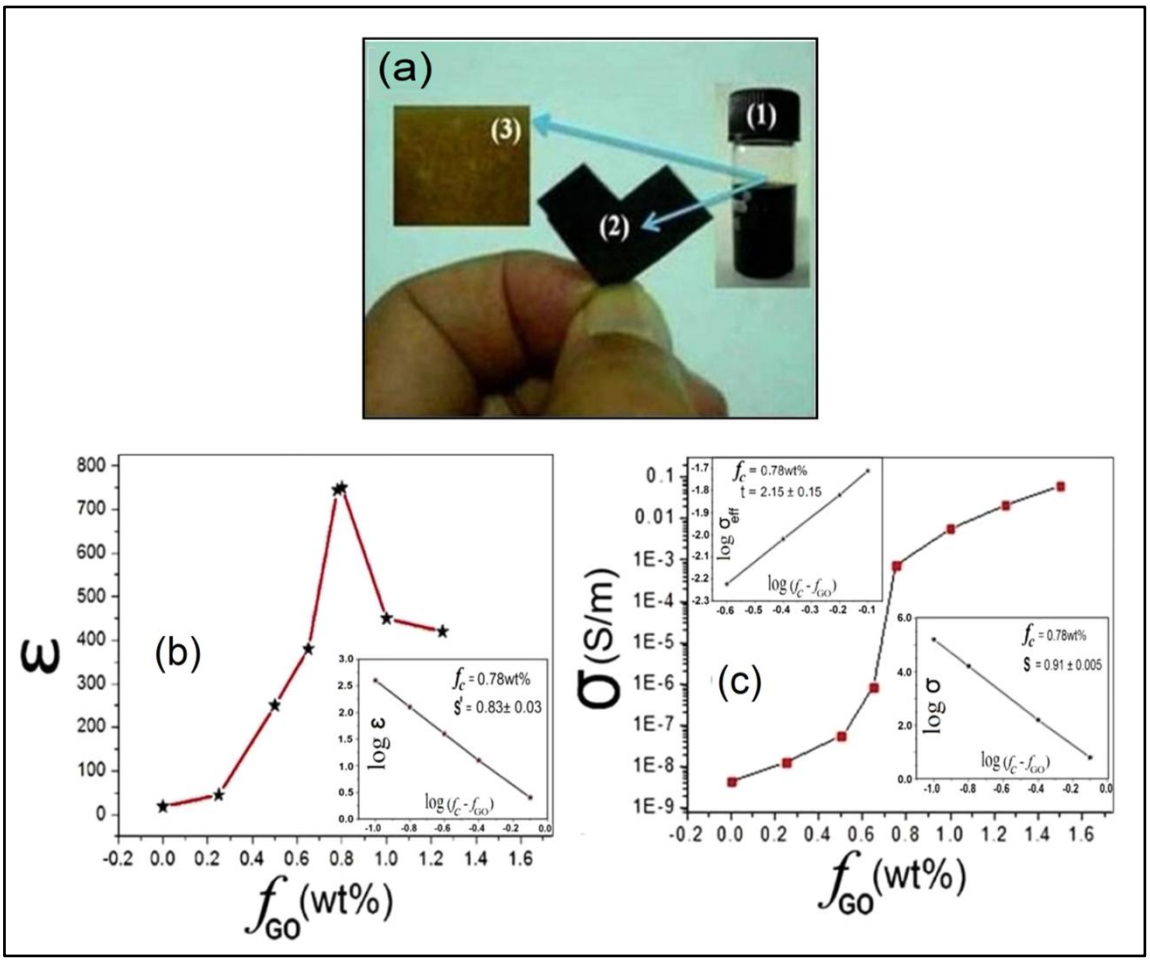

Figure 4.1. (a) Well dispersed GO-PCL solution (1), a free standing bendable tin GO sheet composed of GOnPs prepared by solution casting (2) which can be dispersed in water and spin coated GO sheet on cover glass (3) produced from GO solution.(b) Dependence of effective dielectric constant (ε) and (c) conductivity (σ) of the GO-PCL composite on GO concentration $f_{GO.}$ Inset of (b) shows the best fit dielectric constant with Eq.1 (with f_c~0.79). The inset of (c) shows the best fit conductivity data with Esq. 2 and 3 (with f_c~0.79).

The observed value of f_c is comparable with that of GO-PVA (polyvinyl alcohol) composite [214, 289]. For nanomaterials like GO, the threshold concentration is generally low [289,290]. The percolation threshold, f_c is a key parameter. Below this concentration, GO-PCL will remain mechanically stable as well as maintain their flexibility suitable for tissue engineering application or electronic applications. In order to estimate f_c, the experimental σ and ε data were fitted to the following equations [290-292] to establish the percolation behaviour followed by the GO-polymer composites.

$$\varepsilon \propto (f_c, - f_{GO})^{-s} \qquad \text{for } f_{GO}<f_c \qquad (1)$$

$$\sigma \propto (f_c, - f_{GO})^{-s'} \quad \text{for } f_{GO}<f_c \quad (2)$$

$$\sigma \propto (f_{GO} - f_c)^{-t} \quad \text{for } f_{GO}>f_c \quad (3)$$

Where t is the critical exponent in the semiconducting region and s' is the critical exponent in the insulating region. A sharp increase in dielectric permittivity was found when GO content reaches the percolation threshold, ~0.79wt% which was ascribed to the formation of numerous micro-capacitors in the self-assembled polymer composite at f_c. Linear regression fit of experimental data using Eq.1 yields a critical exponent of s ~0.831 and f_c of ~0.78wt% (shown in the insets of figure 4.1b) which was consistent with the universal one ($s_{un} \approx 0.8$-1.0) and also observed in practical continuum systems [290]. The best linear fit of the conductivity data to the log-log plot of the power low with Eqs. (2 and 3) gives $f_c = 0.79$, t ~ 2.15 ± 0.15, s'= ~0.91 (inset of figure 4.1.c). The critical exponent (t) showed little higher value along with (s') which agreed with the estimated values (t = 1.59-2 and s'_{un}= ~ 0.8-1). GOnPs nanosheets provided percolated pathways for electron transfer, making the GO-PCL composites electrically more conductive than insulating PCL matrix. In the presence of oxygen (potential acceptor sites), there might be possible ionic channels of charge transfer form GO across the semi-conductive network with many cross-linked connections. Similar techniques can be achieved with other conductive carbon fillers such as carbon black [293], carbon nanofibers (CNF), and expanded graphite (EG). Though GO-PCL composites showed percolation threshold around ~0.79wt% exhibiting maximum σ and ε values, for human cell culture, the non-toxicity limit was reported [210] to be (~20µg/ml solution). This concentration of GO, used for the preparation of GO-PCL electrospun meshes, was also within the percolation threshold concentration. For electronic applications, higher GO concentration around the threshold value might be important. However, electrospun GO-PCL composite scaffold meshes for myoblast differentiation were prepared within this non-toxicity and percolation limits, as mentioned earlier.

4.1.2. Structural analysis

X-ray diffraction is used most frequently to investigate the structure of bio-composites with embedded nanostructure. The XRD spectra of GO sheet showed (figure 4.2a) the characteristic GO peak appearing at $2\theta = 11.1^{o}$, corresponding to a lattice d-spacing of

0.78 nm. For the GO-PCL meshes, an XRD peak (figure 4.2b) appeared at 21.65^{o} representing the crystalline phase of the polymer [294]. The XRD pattern of GO-PCL indicated only PCL diffraction peak with no peak for GO around 2θ=11.1^{o}. The absence of GO peak was also reported earlier in case of GO-PVA composite [289,290]. These results demonstrated the disappearance of the regular and periodic structure of graphene oxide, the formation of fully exfoliated structures, and the homogeneous distribution of GOnPs in the polymer matrix [294,295]. As revealed from these data, well-dispersed GOnPs acted as nucleating agents and thus the crystallinity of the composites was also improved.

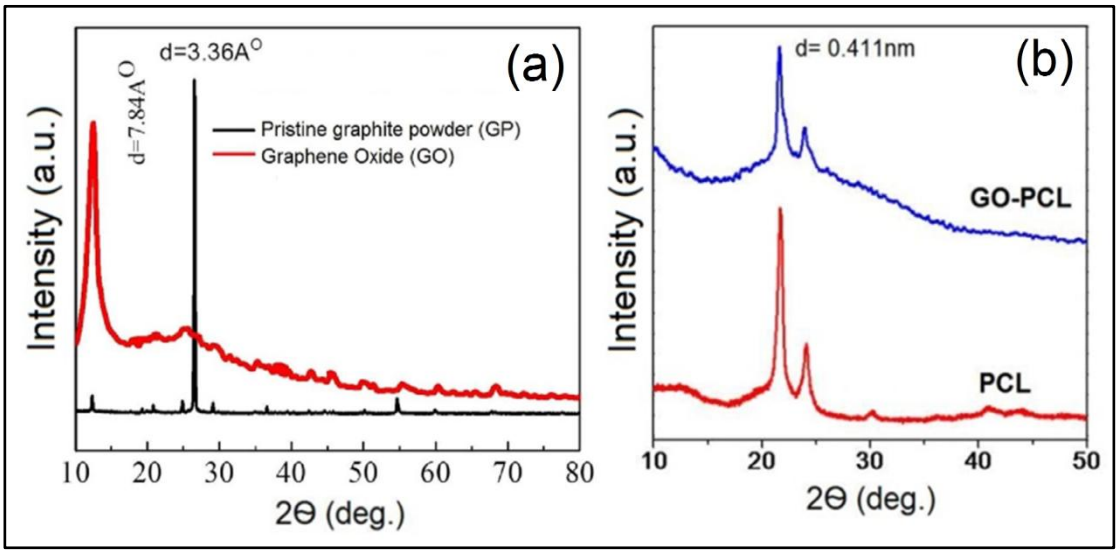

Figure 4.2. (a) The X-Ray diffraction patterns of GO and pristine graphite powder, (b) GO-PCL and PCL , respectively.

The peak around 22^{o} decreased in intensity after GO addition to PCL was due to the hydrogen bonding which are responsible for the change of structure and properties of the polymer-graphene nanocomposites [289]. At the same time Tg (glass transition temperature) was increased with decrease in the level of crystallization. This led to the decrease in intensity after GO is added to PCL. Similar phenomenon was also observed in the case of GO-PVA (polyvinyl alcohol) composites reported earlier [289,291,294,295].

4.1.3. SEM and TEM micrographs of GO sheet and GO-PCL meshes

The SEM micrograph of the GO sheet surface shown in figure (4.3a) indicated uniformly rough surface morphology. Inset of figure (4.3a) also presented FESEM micrograph showing the surface morphology of thin GO sheet which indicated wrinkles stacked in

multiple GOnPs layers. It was reported [296] that such surface morphology might favour cell adhesion and growth. Figure (4.3b) represented the SEM micrograph of the electrospun fibrous meshes and the selected area electron diffraction (SAED) pattern (inset of figure 4.3b) indicating the presence of sharp diffraction spot of nanocrystalline GO in GO-PCL mesh (estimated average fiber diameter of 490±125nm) with porosity ~80-85%. Figure (4.4c) presented the FESEM micrograph showing morphology of the broken edge of a GO sheet and inset of figure (4.3c) showed the HRTEM image of a single layer of the GOnPs film.

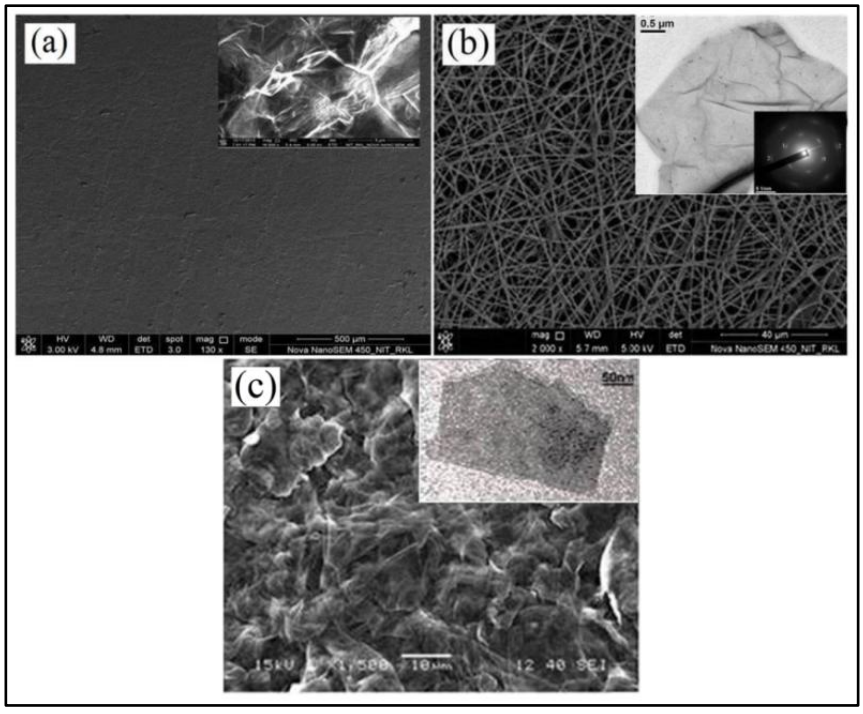

Figure 4.3. (a) SEM micrograph showing surface morphology of thin GO sheet (inset shows the FESEM micrographs of a particular point on the surface). (b) SEM micrograph of the GO-PCL electrospun meshes (inset shows the HRTEM image of GO present in GO-PCL along with the selected area electron diffraction (SAED) image). (c) FESEM micrographs of a broken edge of thin GO sheet (inset shows the HRTEM image of a single layer GO film).

4.1.4. AFM analysis of graphene oxide nanoplatelets (GOnPs)

Atomic force microscopy (AFM) was used to characterize the microstructural features of GO. To assess the degree of exfoliation of the GO in water, AFM images of the dispersions deposited onto silicon wafer surface was taken and the corresponding tapping mode AFM images of the GO nanoplatelets was shown in figure (4.4a). As indicated in figure (4.4b), marked by blue line, the thickness of the sheet resides between 400-500nm, which is in agreement with the previously prepared single layered

GO sheets explained earlier [297,298]. Analysis of AFM images shows most GO had length ~165np, the part marked by cyan line in figure (4.4c).

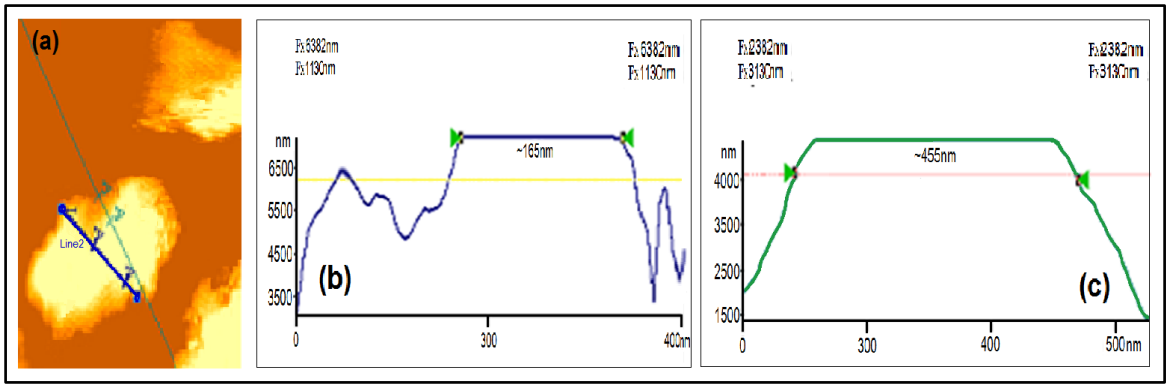

Figure 4.4. Atomic force microscopic (AFM) tapping mode image of the graphene oxide nanoplatelets sheets from an aqueous dispersion with superimposed cross section measurements taken along blue and cyan line indicating ~167 nm in radial diameter (b) and (c) sheet thickness of approximately 450nm.

4.1.5. Raman spectroscopic analysis of GO and GO-PCL composite meshes

This is the vibrational spectroscopic technique used to characterize GO and identify the presence of GO in GO-PCL composite. Raman spectra of GO sheet as shown in figure (4.5), indicated the characteristic feature of GO peaks at frequencies around 1345 and 1597cm^{-1}, respectively, for the G and D band usually assigned to the E_{2g} phonon of Csp^2 atoms and a phonon breathing mode of symmetry A_{1g}. The presence of GO peaks was also observed from the GO-PCL Raman spectra (inset of figure 4.5). Characteristic frequencies corresponding to the well-studied G and D bands agreed with the literature values [296-299] and also indicated little lattice distortion of the GO nanostructure. The intensity ratio I_D/I_G of the two peaks was widely used as characterizing the defect quantity within the GO materials [298,299]. By controlling the amount of defect quantity, the electronic and mechanical properties of the GO sheets might also be tuned as per user's requirement [300]. In single and/or multilayer graphene, Raman spectra showed 2D characteristic peak around 2700cm^{-1} [301-304]. The observed D and G bands were comparable with those of previously reported values for graphene oxide [303,304]. The D band was reported to be associated with the structural imperfections created by the attachment of hydroxyl and epoxide groups on the carbon basal plane [305]. The G band corresponds to the ordered sp^2 bonded carbon. Graphene oxide conduction was

also reported to occur through sp^2 regions via Klein tunnelling [306]. In figure 4.5a, the 2D band corresponding to 2700cm^{-1} was hardly observed, which indicated either absence or negligible presence of pure conducting graphene in the GO sheet of present investigation.

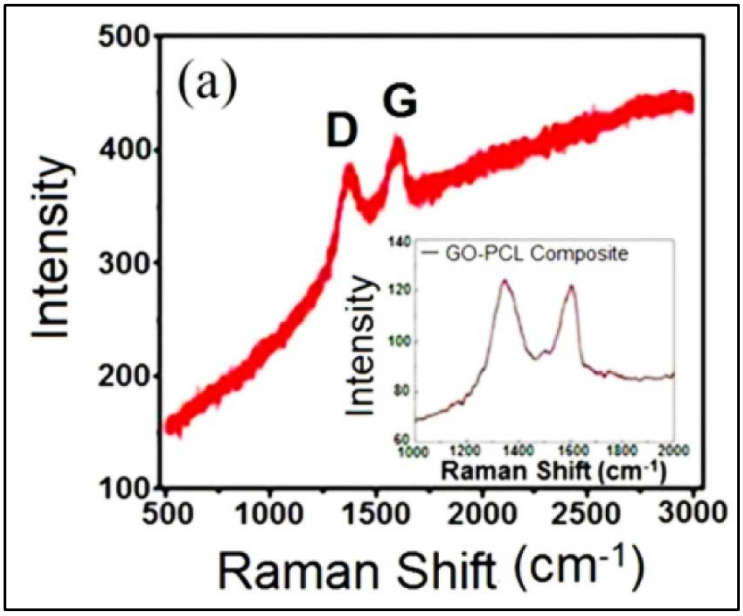

Figure 4.5. Raman spectra of GO (a) and GO-PCL (inset). The characteristic D ($2E_g$) and G (A_{1g}) peaks of graphene are shown both in GO and in the GO-polymer composite. There is no detectable peak corresponding to 2D around ~2700cm $^{-1}$ indicating that graphene is almost fully oxidised.

4.1.6. FTIR analysis of GO sheet and GO-PCL meshes

FTIR is one of the most common vibrational spectroscopic techniques used to obtain an infrared spectrum of absorption for the verification of GO and GO-PCL. Far infra-red (FTIR) spectra of GO and pristine graphite powder were shown in figure (4.6). The intense band at 3438cm^{-1} is attributed to the O-H band of CO-H. The band at 1639cm^{-1} is associated with the stretching of the C-O bond of carbonyl and carboxyl group.

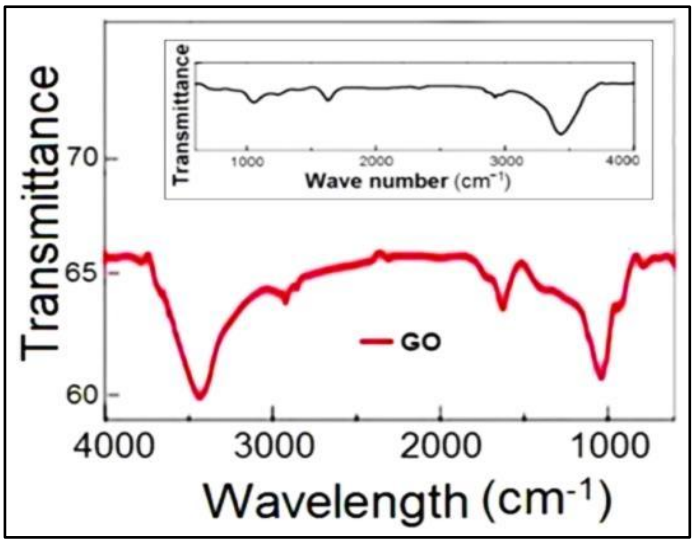

Figure 4.6. FTIR spectra of GO sheets and pristine graphite powder (inset) distinguishing the behaviour of graphene and graphite powder. In GO intense bond around 3438cm^{-1} corresponding to O-H band of CO-H is observed.

Deformation of the C-O band is observed at the band present at 1070 cm^{-1}. FTIR spectra (figure 4.7) of GO-PCL showed absorption band at 1727cm^{-1} indicating carbonyl stretching. The bands appearing at 1295cm^{-1} and 1240cm^{1} represented the C-O and C-C stretching bonds [307]. The bands at 1239cm^{-1} and 1175cm^{-1} were comparable with the asymmetric C-O-C stretching bonds indicating characteristic absorption [307] of PCL. The band at 1639cm^{-1} was associated with stretching of the C-O bond of carbonyl groups. Deformation of the C-O band was observed at around 1017cm^{-1}. From FTIR spectroscopy, evidence of different types of oxygen functionalities on GO were exhibited.

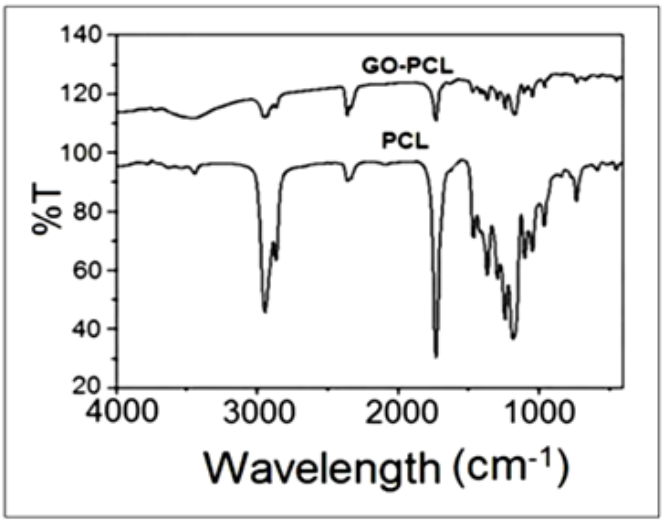

Figure 4.7. FTIR spectra of PCL and GO-PCL mesh distinguishing the behaviour of the two spectra. The spectra of GO-PCL if different from those of PCL and GO indicating strong coupling of GO and the PCL polymer. GO-PCL showed absorption bands at 1727cm^{-1} indicating carbonyl stretching.

It is well known that both the O-H stretching and the –C-OH stretching bonds are sensitive to the hydrogen bonding. The decrease of the intensity of the peak at 1727cm^{-1} was due to the dissociation of the hydrogen bonding among the hydroxyl groups in the polymer [1,2]. This result also indicates strong bonding between the polymer and graphene to the detriment of hydrogen bonding among polymer chains and diminishing the crystallinity of the polymer [305-307].

4.1.7. UV-visible analysis

UV spectroscopic studies are important for the molecular structural analysis (chemical bonding etc.) of the scaffold materials [303]. The UV spectrum of GO exhibited maximum at 371nm [289,290] which is characteristic feature of the π-π transition of aromatic C-C bonds. The corresponding peak in GO-PCL in chloroform solution was observed around 450nm (figure4.8). The π-π stacking force created by the sp^2 bonding and hydrophobic interaction between molecules allow graphene to be conducting [306-308] which provides important cues for the biocompatibility of GO added polymer composites.

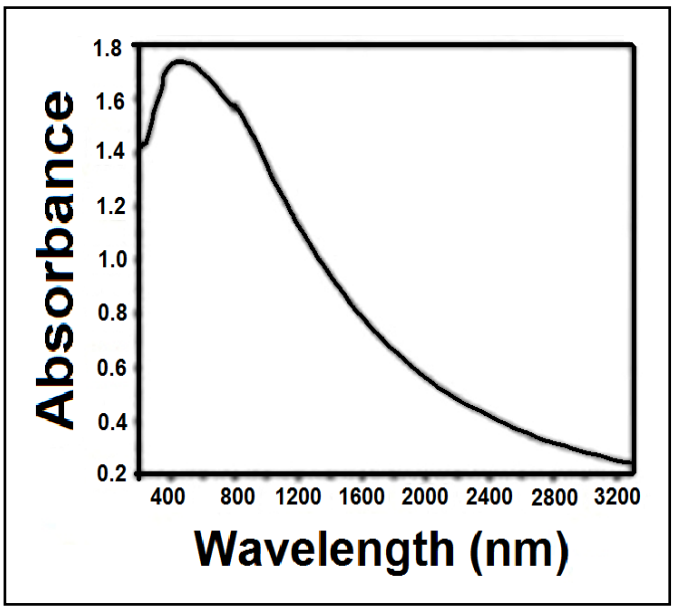

Figure 4.8. UV-visible spectra of GO-PCL composite. The GO peak exhibits maximum around 371 nm, the characteristic feature of the π-π transition of aromatic C-C bonds.

The corresponding peak of the composite (dissolved in chloroform solution) was observed at around 450nm. The ionic bonds, the π-π stacking forces formed by the sp^2 bonding and hydrophobic interaction among molecules allowed graphene to be conducting and also adsorb proteins and low molecular weight chemicals which provided important cues for biocompatibility of GO and GO based composites.

4.1.8. *In-vitro* biodegradability

The degradation behaviour of scaffold plays an important role in the formation of new tissue at the site of an implant. The *in-vitro* degradation pattern of PCL and GO-PCL composite scaffolds shown in the figure (4.9) indicated electrospun GO-PCL composite meshes degraded upto ~16% whereas electrospun PCL mesh degrade ~9% after 30 days of time interval. Slower rate of pure PCL is due to its lesser degradability and rigidity that hamper its use in pure form. But, On the other hand, GO-PCL composite mesh showed optimised degradability rate that is suitable for cellular growth. Optimized degradation of scaffolds eases the longevity of the scaffold implants at the site of the implant [309]. GO-PCL composite scaffold can thus provide support to the growing tissue for a long period of time in an optimised way which may be useful for *in-vivo* applications.

4.1.9. Contact angle measurement

Contact angle (CA) measurements provides important information about the surface roughness and hydrophilicity [90]. CA also indicates a measure of solid-liquid interaction. Wetting (CA_w) and dewetting (CA_{dw}) contact angles (discussed in chapter-3) of thin GO sheet and GO-PCL mesh were shown in figure (4.9 inset).

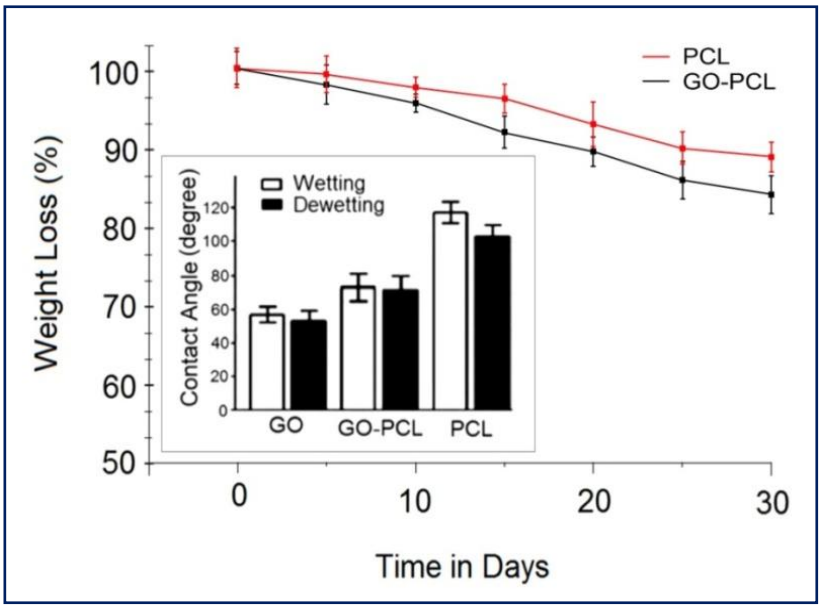

Figure 4.9. *In-vitro* degradation pattern of electrospun PCL and GO-PCL composite scaffolds in SBF (simulated body fluid) for 30 days. Inset shows contact angle analysis (in degrees) representing both advancing (wetting) and receding (dewetting) water sessile drop on GO sheets, GO-PCL and PCL meshes. Error bars present standard deviation.

In case of thin GO sheets, CA_w was found to be around ~58.7^o with hysteresis (CA_w-CA_{dw}) of ~4^o which might be a measure of the solid-liquid interaction [310]. For the GO-PCL meshes, the contact angle (CA) was ~78^o. Due to the presence of GO with abundant hydroxyl group, CA of GO-PCL significantly ($p<0.05$) decreased compared to PCL, (CA ~119^o). It is suggested that GO-PCL composite fibrous meshes could enhance cell adhesion as they are more hydrophilic due to the presence of GOnPs .

4.1.10. Mechanical property

The mechanical stability of the polymer scaffolds is important for cell adhesion and proliferation. Studies of mechanical properties of GO sheet and GO-PCL meshes were carried out indicating suitable mechanical strength of the scaffolds. The stress-strain curves of GO sheets and GO-PCL meshes were shown in figure 4.10. The tensile strength of PCL (~1.88 ± 0.25MPa) was found to increase significantly with addition of GO (~4.8± 0.25MPa). Mechanical property of the tensile strength is also known to increase with increasing GO concentration [64]. Favourable mechanical property supported GO sheet and GO-PCL meshes for tissue engineering applications.

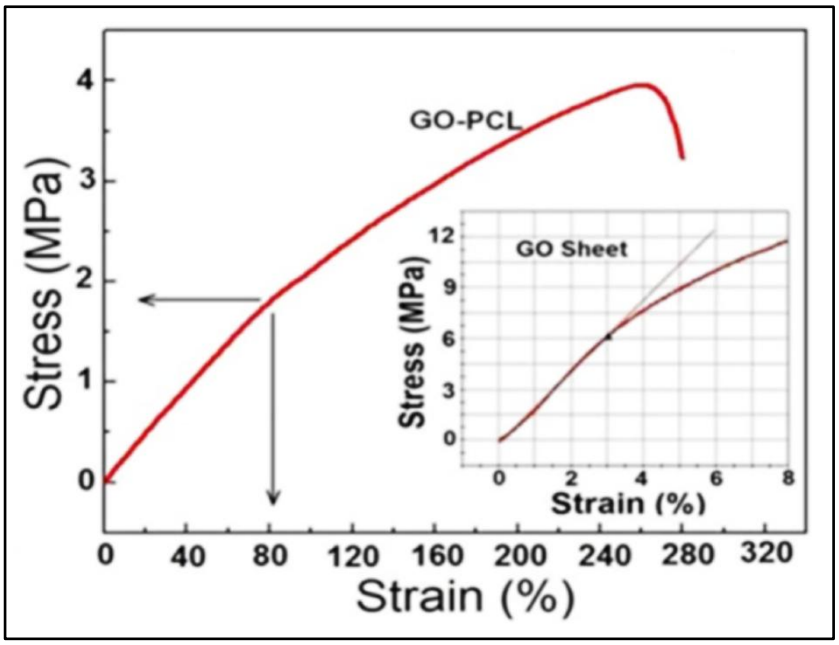

Figure 4.10. The stress-strain curve of the GO sheet and GO-PCL meshes carried out at room temperature with GO concentration within the non-toxic limit (~20µg/ml).

4.1.11. Conductivity (σ), dielectric constant (ε) of thin GO sheet and GO-PCL meshes

Figures 4.11 and 4.12 demonstrated room temperature (RT) σ value of GO sheet (~10^{-7} S/m). Quite high value of ε (~900) was also reported [15] for GO sheet which might be attributed to its high charge trap density [311,312] (~1.2×10^{18} cm^{-3}/eV) that influenced its σ, ε and even the piezoelectric (PE) behaviour [313] of GO that influenced improved cellular interaction. GO conductivity arises through the sp^2 regions via Klein Tunnelling mechanism [306].

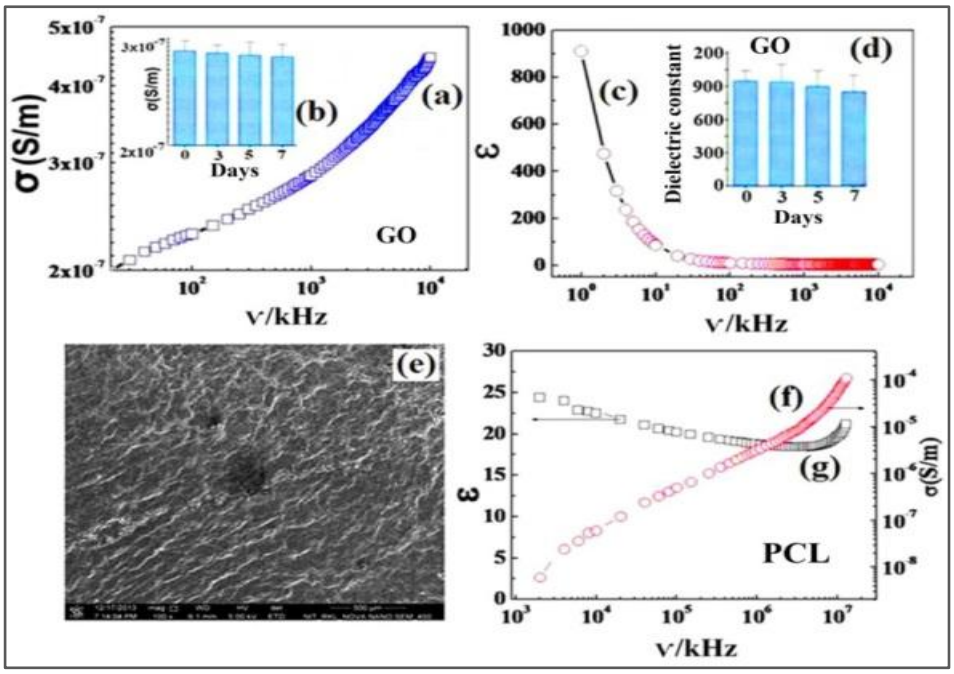

Figure 4.11. Room temperature (RT~30^{0}C) conductivity (σ) data of a GO sheet as a function of frequency (a) and corresponding conductivity data of the same sheet (measured at 1000 kHz) after immersion in PBS solution for up to 7 days (b) . (c) RT dielectric constant (ε) data of the GO sheet as a function of frequency. (d) Corresponding ε data of the sheet (measured at 1 kHz) after immersion in PBS solution. (e) FESEM micrograph showing morphology of the GO sheet surface after immersion in PBS upto 7 days. (f) RT variation of electrical conductivity and (g) dielectric constant of PCL fibrous meshes as a function of frequency. In (b) and (d), 0 days indicate, respectively, RT σ and ε data of GO before immersion in PBS (shown for comparison).

From the study of room temperature conductivity and dielectric constant data as shown in figures 4.11 (a-d), GO added PCL (GO-PCL composite) exhibited appreciably large increase of both ε (~300 for GO-PCL and only ~25 for PCL) and σ (more than two orders of magnitude higher in GO-PCL compared to GO sheet). Similar enhancement of σ and ε was also observed in GO-polyvinyl alcohol (PVA) and other GO-polymer composites [289,290,313]. Similar conductivity increment in GO-PMMA (poly-methyl methacrylate) was suggested to be due to deformed graphene nanosheets (considered to be the effect of agglomeration of GOnPs in polymer matrix) [313-315]. Enhancement of σ and ε in GO-PCL and other GO-polymer composites might , therefore, be associated with the formation of conducting pathways between the more conducting deformed GOnPs sheets (enhancing σ) and micro-capacitors with insulating polymer (PCL) as insulating dielectric films (enhancing effective ε) similar to those reported in case of other polymer composites [313-317].

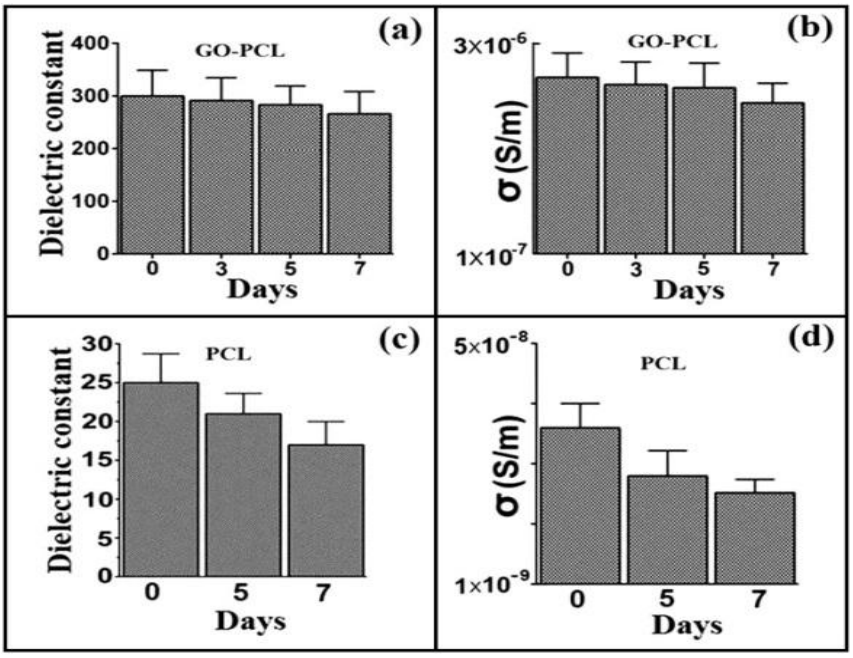

Figure 4.12. (a) Room temperature (RT) dielectric constant (ε) and (b) conductivity (σ) data of GO-PCL meshes before (0 days) and after immersion in PBS solution for up to 7 days. RT ε (c) and σ (d) data of PCL meshes before (indicated by the O days) and after immersion in PBS solution (all measurements were performed 1 kHz).

In pure GO there is a mixture of both positive and negative charges which lead to a decrease of σ but increases polarizability and hence ε value of GO [289,290,318]. It is further noticed from figures 4.12 that both σ and ε values of GO and GO-PCL mesh decreased only a little with increase of immersion time in PBS solution (up to one week in our present study) indicating *in-vitro* stability of the GO and the GO-PCL composite mesh. Moreover, no significant morphological change of the thin GO sheet was observed as revealed from the unchanged FESEM micrograph of the sheet after immersion in PBS solution (figure 4.11e). The room temperature (RT) variation of electrical conductivity and (figure 4.11f) dielectric constant (Figure 4.11g) of PCL fibrous meshes considered as a function of frequency. The addition of GO also reduced the degradation rate of GO-PCL (compared to PCL) in PBS solution (Figure 12a and b) which is indicated by the lesser decreasing rates of σ and ε compared to those of pure PCL (Figure 12 c and d). Thus, along with enhancement of σ and ε, the stability of GO-PCL mesh was also improved by the GO filler. The little decrease of both ε and σ of GO-PCL after immersion might be associated with a small amount of material leaching from the scaffolds as in the case of polyaniline doped PCL [272].

4.2. Conclusion

Addition of GO in PCL enhanced the mechanical property, contact angle and hydrophilicity of the GO-PCL composites. Structural characterization indicated well-dispersed GOnPs acted as nucleating agents and thus the crystallinity of the composites was also improved. FTIR study showed stretching of the C-O bond of carbonyl groups. Deformation of the C-O band was observed at around 1017cm^{-1}. From FTIR spectroscopy, evidence of different types of oxygen functionalities on GO were exhibited necessary for better cell scaffold interaction. UV-visible spectra indicated the π-π stacking forces formed by the sp^2 bonding and hydrophobic interaction among molecules allowed graphene to be conducting and also adsorb proteins and low molecular weight chemicals which provided important cues for biocompatibility of GO and GO based composites. Both conductivity and dielectric constant (associated with GO surface charge) increase in the GO-PCL composites. Enhancement of conductivity is important for the enhancement of biocompatibility [84]. The composite showed percolation threshold behaviour with GO concentration around 0.79wt% which was quite low. Below this concentration GO-PCL composite retains its mechanical stability. This study confirmed that both GOnPs and GO-PCL meshes retained their σ and ε values almost unaltered after immersion in PBS solution for about a week and, therefore, the cellular interaction associated with the biocompatibility of such composites appeared to remain almost unaltered even after immersion in PBS solution over one week. Controllable enzymatic degradation of graphene/PCL materials was studied by Murry and his collaborators [71] and these substrates were proved to be promising biodegradable electro-responsive type scaffolds for TE applications as discussed in the next chapter. Even the degradation products of the composite materials were reported [71] to exhibit less inhibition to cell metabolism and proliferation than the degradation product of pure PCL. Controllable non-toxic degradation and unique physical properties confirmed that covalently-linked PCL-graphene oxide based composites are ideal materials for the development of scaffold for skeletal muscle TE applications.

CHAPTER-5

Myoblast Differentiation on GO Sheet and GO-PCL Electrospun Scaffold Meshes

5. Myoblast Differentiation of Cord Blood Derived hMSCs on GO Sheet and Electrospun GO-PCL Composite Meshes

In the previous chapter (4) characterization of the GO films and GO-PCL electrospun meshes have been described. This chapter describes myoblast differentiation of cord blood-derived mesenchymal stem cells on the well characterized graphene oxide nanoplatelets sheets and GO–polycaprolactone (PCL) electrospun meshes. The expression of myogenic proteins and IGF-1 cell signalling pathway analysis has also been presented.

5.1. *In-vitro* Cell Culture Study

Differentiation of human umbilical cord blood (UCB) derived multipotent mesenchymal stem cells to myoblasts and formation of myotubes on the GO added electroconducting polymer scaffolds described in this thesis are new and challenging one. Excellent myoblast differentiation of hMSCs on GO sheet and GO-PCL meshes have been reported, for the first, to elucidate their potentiality for skeletal muscle tissue regeneration.

5.1.1. Isolation and culture of mononuclear cells (MNCs) from UCB

The mononuclear stem cells (MNCs) were isolated from UCB (figure 5.1a) and cultured in DMEM media (90v/v%) containing FBS (10v/v%) supplemented with 100x antibiotic-antimycotic solution (~1v/v%) for cell culture study and myoblast differentiation. The morphology of MNCs was initially round shaped (after 48 h of culture) as observed under phase contrast microscope (Figure 5.1b). These MNCs were cultured upto the formation of mesenchymal stem cells (hMSCs) up to 5^{th} passage.

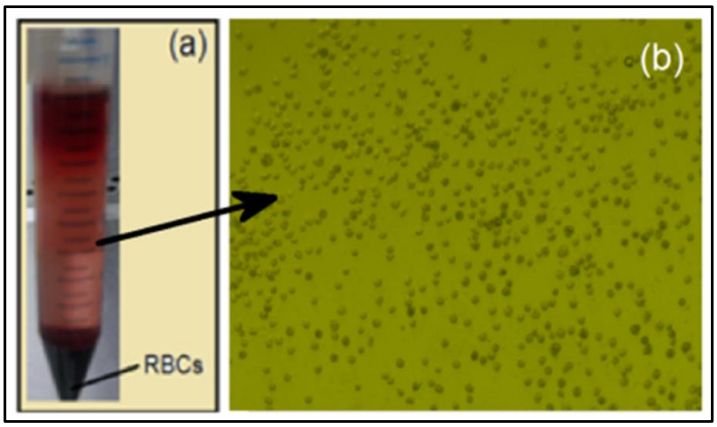

Figure 5.1. (a) Mononuclear cells (MNCs) layer (middle) and red blood cells (RBC) precipitated at the bottom in a 50ml culture tube. (b) Isolation of MNCs being cultured in a cell culture plate.

5.1.2. Morphological characterization of hMSCs

The cultured hMSCs isolated from UCB were used for the cell culture study to examine the cell supportive property of the developed composite scaffolds. The morphological variation in the cultured cells was studied by phase contrast microscopic images as shown in Figure 5.2. After initial culture, the hMSCs were observed to be round/ spherical shaped during the initial days of culture and turned gradually towards elongated fibroblast shape like morphology after 5th passage (Figure 5.2.a-d). These cells were used for further characterization as well as for myogenic differentiation.

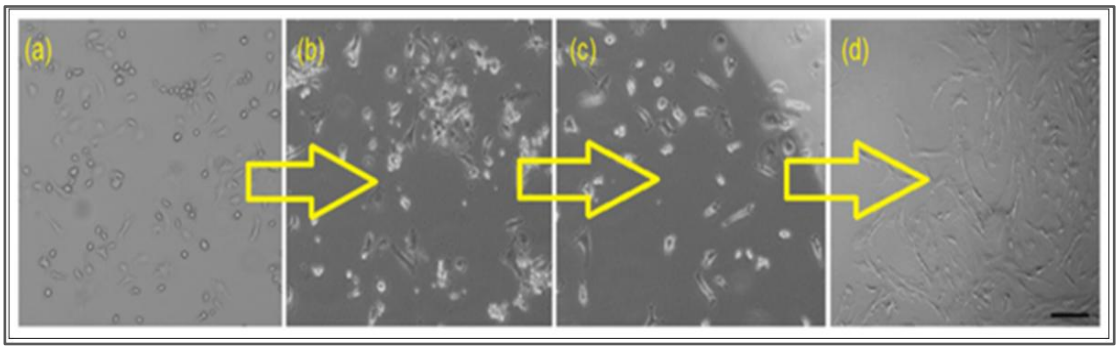

Figure 5.2. Gradual morphological changes of umbilical cord blood derived mesenchymal stem cells (hMSCs). After 5thpassage fibroblast like morphology (d) of the cultured cells were observed under phase contrast microscope.

The morphology of cells was also analyzed using cytoskeleton staining of actin filaments (Figure 5.3). Cells (stained with FITC-phalloidin) were observed under a Zeiss Axivert 40 CFL fluorescence microscope.

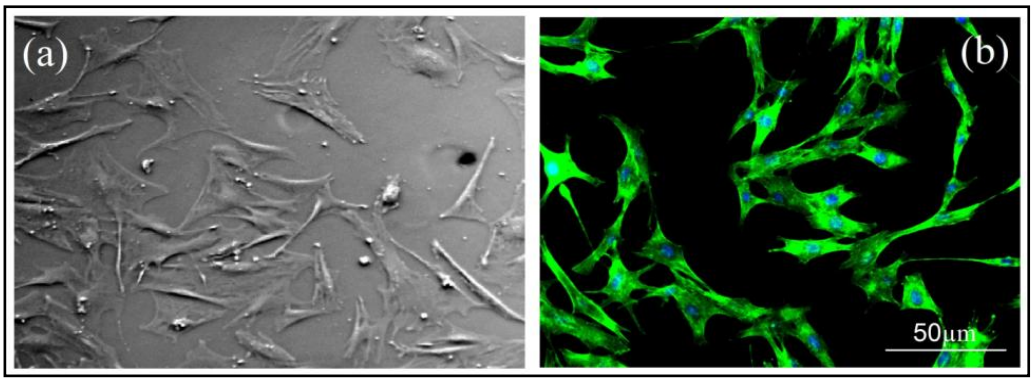

Figure 5.3. Morphology of hMSCs was analysed using phase contrast microscope (a) and cytoskeleton staining of actin filaments (b) along with Nuclei counterstained with DAPI.

5.1.3. Immunophenotypic characterization of hMSCs

Besides morphology, Immunophenotypic characterizations of hMSCs were assessed by performing flow cytometry analysis. The immunophenotypic characterizations shown in figure (5.4) were found to be positive for CD90 (99.2%), CD73 (98.5%), CD105 (98%) and negligible for hematopoietic markers like CD45 (1.5%), CD45 (0.5%) and HLA-DR (1.0%) indicating mesenchymal stem cells phenotype. The stem cells thus isolated from human umbilical cord blood were used for *in-vitro* skeletal myoblast cells differentiation on GO sheet and GO-polymer composite scaffolds.

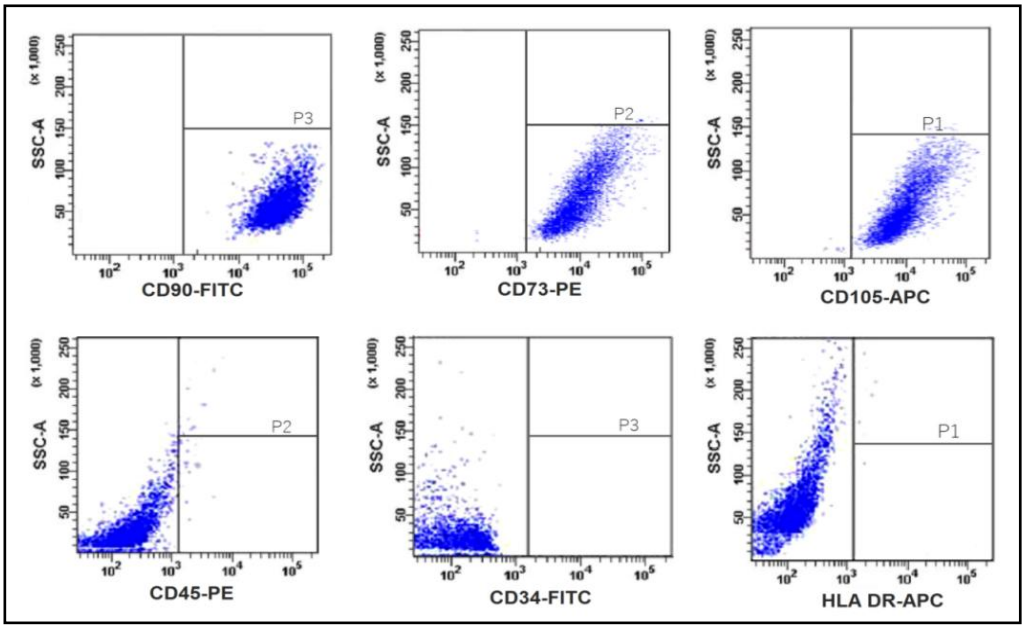

Figure 5.4. The immunophenotypic analysis was found to be positive for CD90 (99.2%), CD73 (98.5%), CD105 (98%) and negative for CD45 (1.5%), CD34 (0.5%) and HLA-DR (1.0%) indicating mesenchymal stem cells phenotype.

5.1.4. hMSCs seeding, attachment and spreading

After seeding of hMSCs (by static seeding method with ~2×10^4 cells/ml), attachment and spreading of these cells onto the scaffold surface were evaluated by scanning electron microscope (SEM) on various time intervals. SEM micrographs revealed excellent cell adherence as well as proliferation of hMSCs on the developed scaffolds after three, five and seven days of culture as shown in figure (5.5). Cellular attachment and spreading also indicat their compatibility to the scaffold environment.

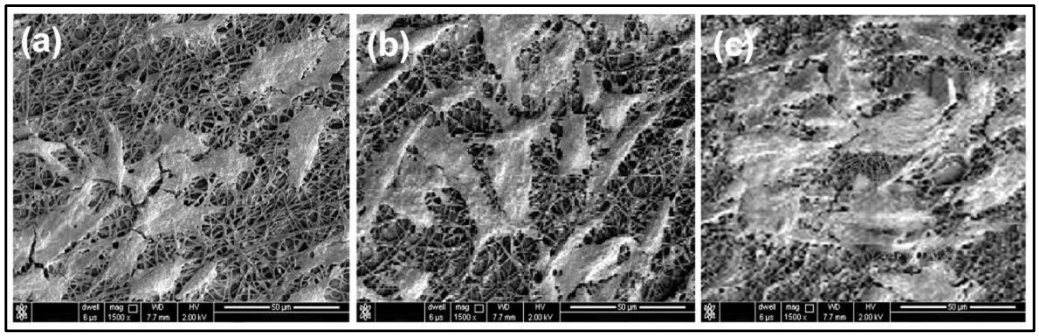

Figure 5.5. Attachment and Spreading of hMSCs on GO-PCL composite scaffolds on Day 3(fig. a), 5(fig. b) and 7(fig. c) days of culture. The cells are well visualized from the micrographs.

5.1.5. Cell metabolic activity

The cellular viability in terms of metabolic activity of the cultured hMSCs on the prepared GO based scaffold was further evaluated quantitatively by WST-8 assay as shown in figure (5.6). Difference in the increase of O.D (optical density) values with culture period have been observed for hMSCs grown on different substrates (GO sheet, GO-PCL composite mesh and tissue culture plate as control). The higher O.D value representing higher metabolic activity is obtained with GO based substrates. The increase in metabolic activity achieved with GO-PCL composite mesh can be attributed to the addition of GOnPs that provided essential physicochemical properties suitable for better cellular interaction. The amount of formazan dye generated (by the activities of dehydrogenases) was directly proportional to the number of living cells. Thus, GO based substrates proved their superior biocompatibility.

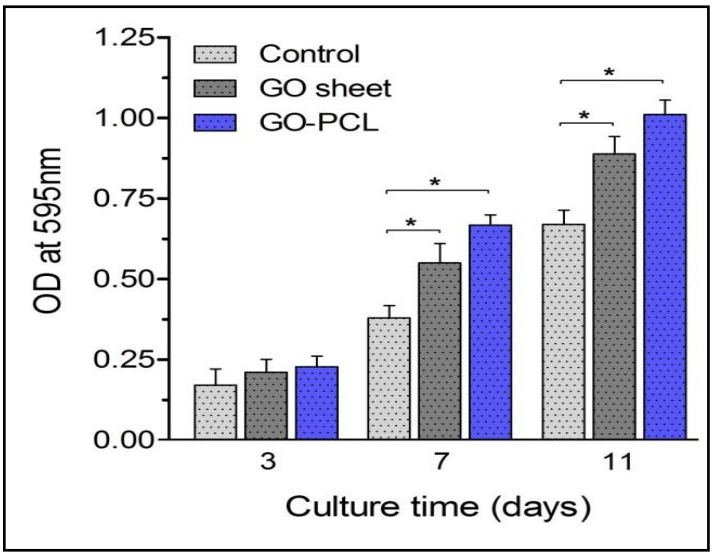

Figure 5.6. WST-8 assay of hMSCs grown on GO sheet, GO-PCL and control (tissue culture plate) substrates after 3, 7 and 11 days of culture. Superior cellular metabolic activity has been observed on GO-PCL based composite meshes. Results presented as the means ± SD. * indicates significant difference (n=5; p<0.05). Metabolic activity was increased with time with the scaffolds showing the trend GO-PCL>GO>control substrate.

5.1.6. Cell proliferation assay (via DNA quantification)

The proliferation of hMSCs on the prepared scaffolds was evaluated by DNA quantification assay. Figure (5.7) shows an increasing rate in DNA content of hMSCs with time as observed in different GO based substrates prepared for investigation.

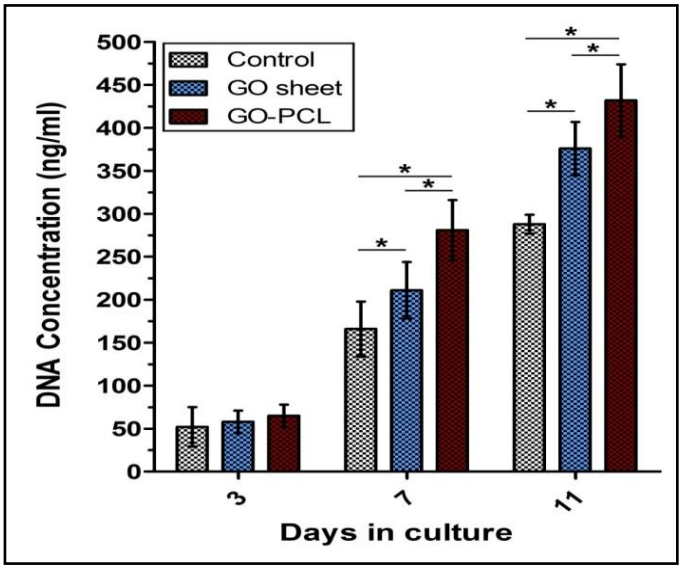

Figure 5.7. Cell proliferation represented in terms of DNA quantification on GO sheet, GO-PCL mesh and control (tissue culture plate) substrates. An increased trend in DNA content is observed on all the GO based matrixes. Results represented as mean ± SD, * indicates significant difference (*n=5; p < 0.05*). Proliferation of hMSCs were increased with time with the scaffolds showing the trend GO-PCL>GO>control substrate.

The corresponding DNA contents of hMSCs cultured on tissue culture plate (TCP) taken as control, GO sheet and GO-PCL composite meshes on 3 to 11 days of culture are ~50ng/ml to ~285ng/ml, ~58ng/ml to ~375ng/ml and ~65 to ~430ng/ml, respectively. GO based substrates have shown significantly higher amount of DNA content representing the higher proliferation rate of hMSCs on these novel substrates indicating their superior cell supportive property. Proliferation of hMSCs was increased with time with the scaffolds showing the trend GO-PCL>GO>control.

5.2. Differentiation Potential of hMSCs on GO-PCL Composite Scaffolds

5.2.1. Myoblast differentiation potential

After confirming viability and proliferation of cord blood derived hMSCs onto the novel GO-PCL composite scaffolds, hMSCs were further allowed for myoblast differentiation on these substrates. Along with differentiation of hMSCs, elongated bipolar morphology of myoblasts have been observed as depicted in FESEM micrographs (Figure 5.8. (a→b)).

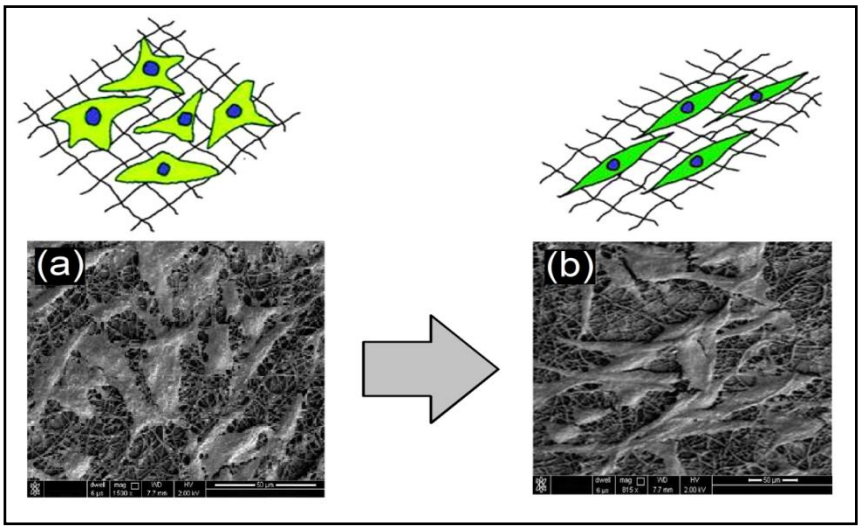

Figure 5.8. Morphology of hMSCs (a) changes towards bipolar structure (b), same as myoblasts, on GO-PCL electrospun composite scaffold that indicates differentiation of hMSCs to myoblast cells (morphology wise).

These myoblasts were further used for various characterizations as described below. Myoblasts morphology on GO-PCL scaffold indicates myogenic differentiation potential of the scaffold.

5.2.2. Myoblast viability and proliferation

Figure 5.9. shows viability and proliferation of myoblast cells on GO sheets, GO-PCL mesh and controls. Cell viability (from WST-8 assay analysis) was found to increase significantly for GO sheets and GO-PCL meshes compared to the control surfaces (*:p<0.05).This was ascribed to be due to the better myogenic differential potential contributed by the favourable physicochemical properties of graphene oxide. This result implied that GO sheets and GO-PCL meshes were cytocompatible and supported cell viability that increased the biocompatibility of GO-PCL composite scaffolds.

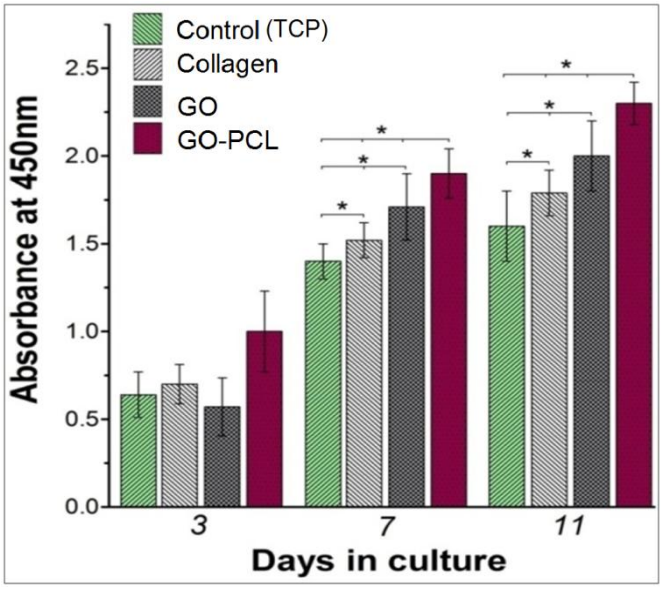

Figure 5.9. Viability and proliferation of myoblasts observed by tetrazolium salt (WST-8) assay. Superior viability of cells has been found on GO-PCL composite meshes compare to GO sheet and other controls (collagen and tissue culture plate) indicating better myogenic potential and hence biocompatibility. Results presented as the means ± standard deviation). * indicates significant difference (*n=5; p<0.05*).

5.2.3. Immunophenotypic characterization of myoblast cells

Flow cytometric analysis of cells adhered on thin GO sheets and GO-PCL meshes was performed to confirm the positive expression of myogenic markers CD56 and desmin indicating skeletal myoblast cells phenotype (Figure 5.10). Myogenic markers expressed better on GO-PCL meshes than that on the GO sheets indicating GO-PCL composite mesh as a better candidate for skeletal muscle tissue regeneration. Electrospun GO-PCL composite mesh provided increased interconnectivity along with electroconductivity and biocompatibility of PCL compare to plane GO sheet resulting better cell-scaffold interaction.

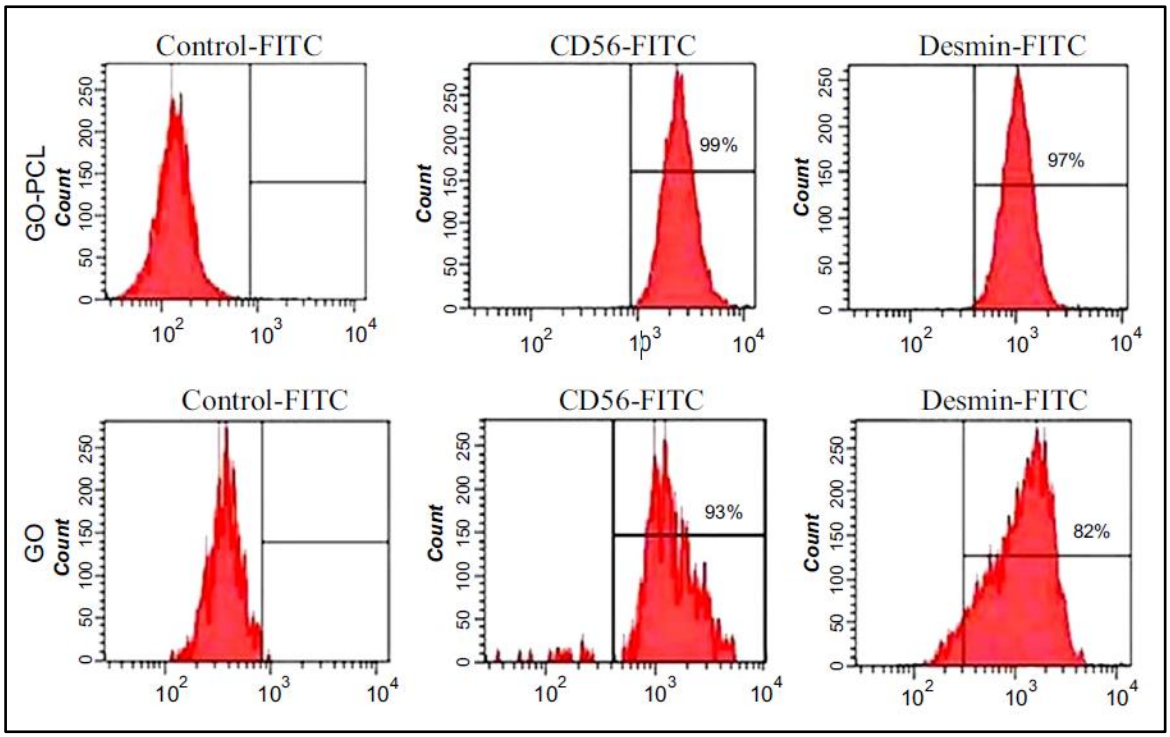

Figure 5.10. Flow cytometric analysis of hSkMCs obtained from GO–PCL mesh and GO sheet (by trypsinization method) after 7 days of culture. Cells highly expressed for skeletal muscle markers CD56 and desmin that confirmed myoblast cell phenotype.

5.2.4. Aspect ratio analysis

Aspect ratio of myoblast is important to obtain the elongated structure of the cells that further differentiate to myotubes through cells fusion. After 3 days of culture, the aspect ratios measured on GO-PCL meshes, GO sheets and controls were found to be ~6.6, ~5.4 and (~4.7 for collagen mesh and ~4.3 for tissue culture plate (TCP)), respectively, (Figure 5.11). Compared to GO sheets and controls, a more elongated bipolar morphology of skeletal myoblasts was observed on GO-PCL electrospun meshes due to its better physicochemical and biological properties indicating its improved myogenic potential.

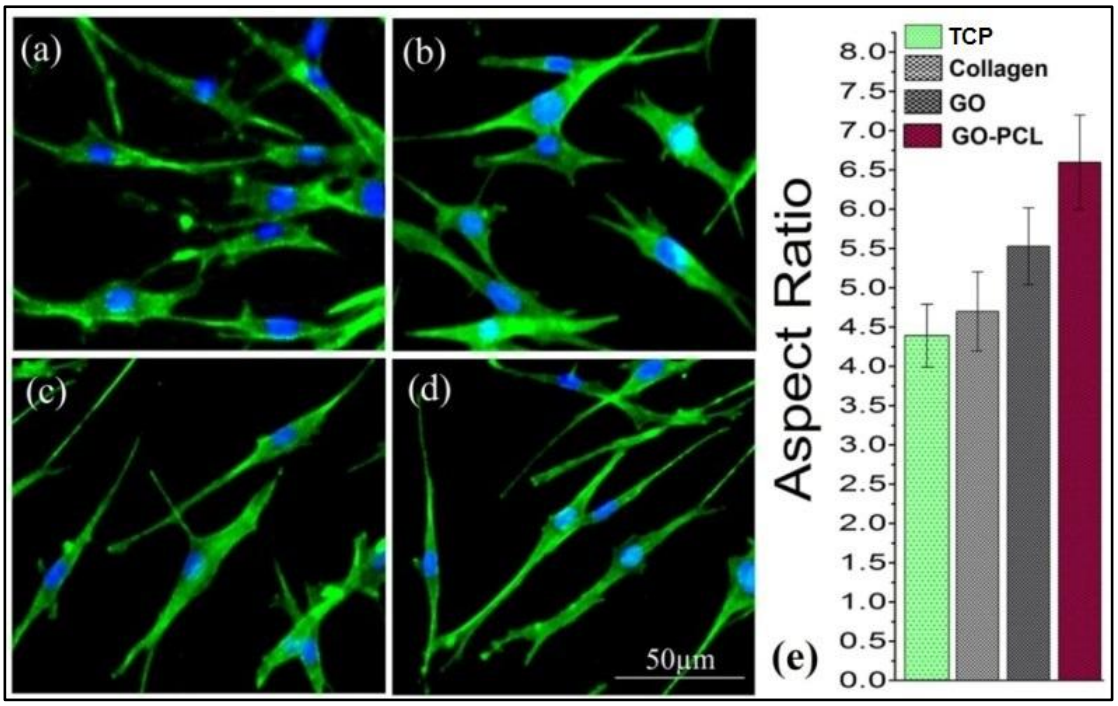

Figure 5.11. Analysis of cytoskeleton development of hSkMCs grown on (a) control (tissue culture plate (TCP)), (b) collagen mesh, (c) GO sheets, (d) GO-PCL meshes. (e) Cell aspect ratio quantification from (a-d) after 3 days of culture. Increased aspect ratio indicates better elongation of these cells on GO based substrates.

5.2.5. Formation of myotubes

The myoblast cells were bipolar at the initial stage (Figure 5.12 a-b) and they were fused together on extended time interval (day 11) under proper condition and formed myotubes that were further clarified by FESEM micrograph (Figure 5.12 c) as well as immunostaining assay (Figure 5.12 d-l). These figures showed improved myoblasts cell proliferation, differentiation and formation of myotubes onto GO-PCL meshes compare to GO-sheet and control, which might be attributed to the interconnectivity of fibrous meshes and enhanced σ and ε of the composite induced by the addition of GO. Thus the presence of GO in the polymer composites played an important role for guiding cellular interaction, resulting in a higher proliferation and myotubes formation.

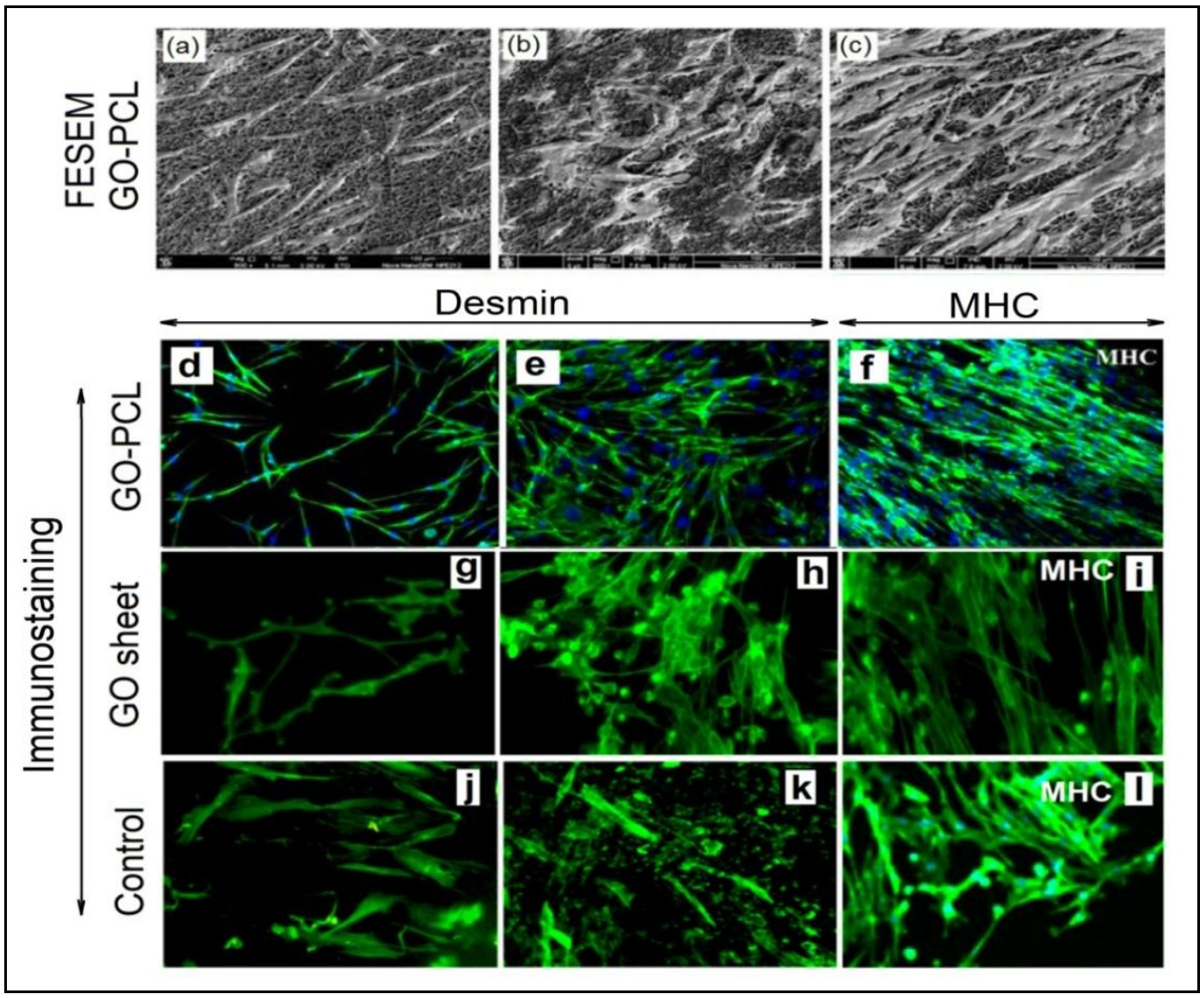

Figure 5.12. FESEM micrographs of GO-PCL electrospun scaffolds representing cells attachment as well as spreading at increasing time interval (Day3(a)-Day7(b)) and also formation of myotubes at extended time of differentiation (Day11(c)). For better comparison, Immunostaining (with Desmin-FITC and MHC-FITC conjugated) images of the corresponding FESEM images have also been shown alongside (d-l) with GO sheet and control (tissue culture plate (TCP)) substrate.

5.2.6. Immunohistochemical characterization

This process has widely been used for the detection of cells specific antigens (proteins e.g., Desmin, MyoD, Myosin Heavy Chain, Dystrophin etc.) to verify the presence of specific cells/tissues. Immunohistochemical analysis (Figure 5.13 a-l), along with FESEM analysis of the corresponding samples (Figure 5.13 m-p), confirmed differentiation of hMSCs to myoblasts via early expression of myogenin-positive nuclei on controls (tissue culture plate and collagen mesh), GO sheet and GO-PCL mesh (Figures 5.13 a-d).

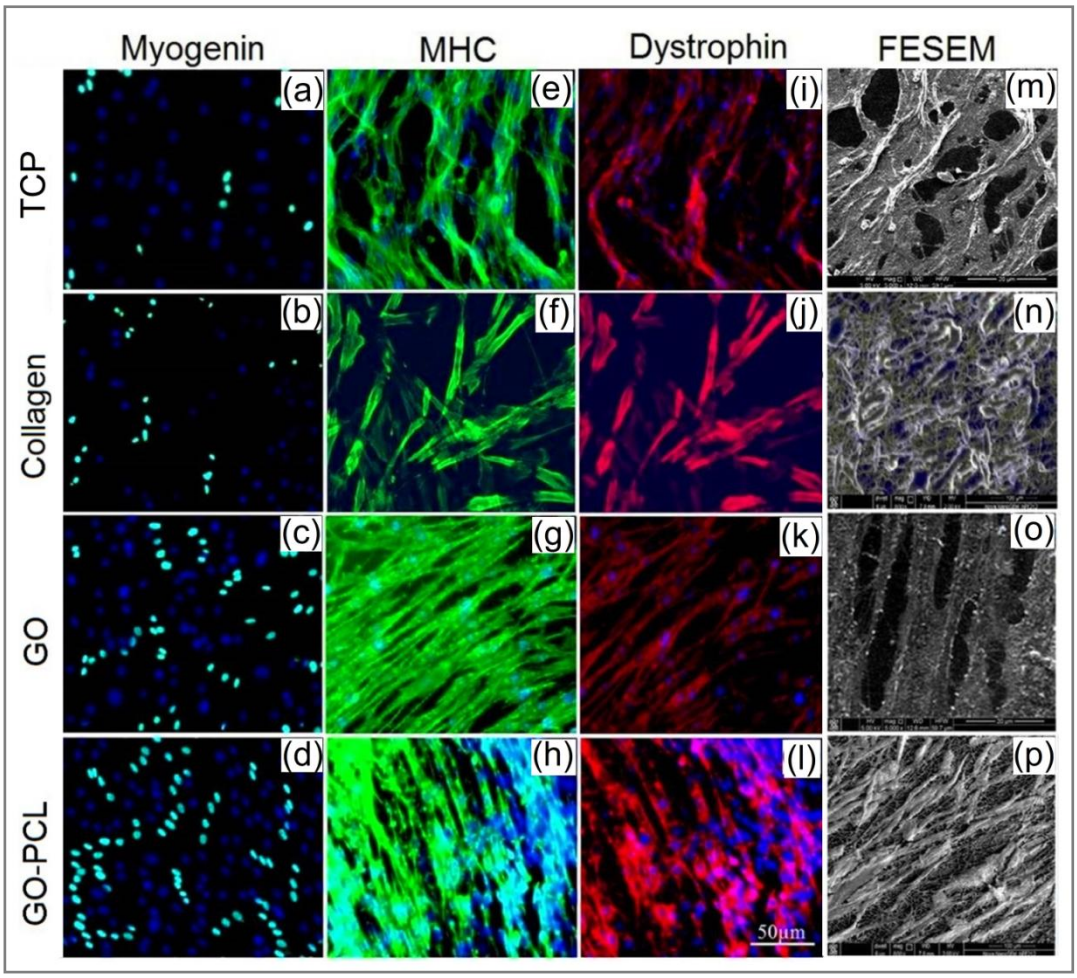

Figure 5.13. Expression of the early myogenic differentiation marker Myogenin-positive nuclei (green) on controls (a,b), GO sheets (c) and GO-PCL meshes (d). Immunostaining of MHC (green), respectively, on controls (collagen and tissue culture plate) (e-f), GO sheets (g) and GO-PCL meshes (h) and Dystrophin (red) similarly on controls (I,j), GO sheets (k) and GO-PCL meshes (l). Nuclei were counterstained with DAPI. FESEM micrographs (m-p) of the corresponding samples were also shown for better demonstration.

Moreover, muscle specific antigens like myosin heavy chain (MHC) shown in figures 5.13 e-h and dystrophin (Figures 5.13 i-l) were expressed more intensely on GO-PCL meshes compared to those on thin GO sheets or control substrates. Myotubes formed on GO sheets and GO-PCL meshes were found to be more aligned compared to those on the control substrates. Quantitative analysis of the percentage of myogenin-positive nuclei showed in (Figure 5.14) that myogenin expression increased more on thin GO sheets and GO-PCL meshes compared to that on control substrates (collagen mesh and tissue culture plate), which also indicated a better differentiation potential of the GO-based substrates. Importantly, GO-PCL meshes showed the highest percentage of myogenin positive nuclei (~19%) (Figure 5.14). Significantly higher expression of early

myogenic marker (myogenin) indicated superior myogenic differentiation potential of GO-PCL electrospun meshes compared to GO sheets and controls.

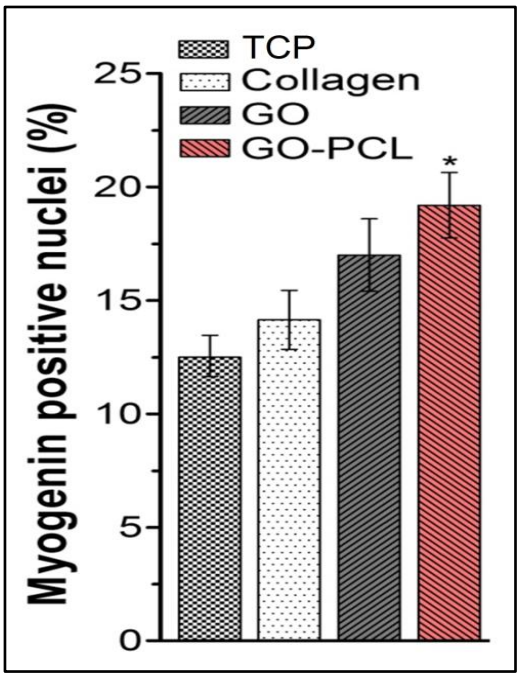

Figure 5.14. Quantitative analysis of percentage myogenin-positive nuclei (cells cultured in differentiation medium for 5 days before staining). * represents significant difference ($p<0.05$) compare to collagen mesh and tissue culture plate (TCP) taken as controls.

As discussed above graphene oxide nanoplatelets impregnated GO-PCL composite meshes showed excellent cell scaffold interaction as such they are potential candidates for electro-responsive skeletal muscle tissue (SMT) regeneration. This is because of the extraordinary physicochemical properties, nanostructural feature and surface charge of GOnPs which contributed to the enhancement of conductivity of the meshes and hence the biocompatibility as a whole. Enhanced biocompatibility of GO-polymer composites was also revealed from the expression of myogenic protein, gene and IGF-1 cell signalling pathway analysis as discussed in the subsequent section.

5.3. Expression of Myogenic Protein and IGF-1 Cell Signaling Pathway Analysis

The ability of cells to correctly respond to their microenvironment is the basis of tissue repair and development [285,287]. Here, myogenic protein expression on GO sheet and electrospun GO-PCL scaffolds and cell signaling pathway (Insulin-like Growth Factor-1 (IGF-1)) analysis have been investigated. Better myogenic protein expression was

observed on GO based polymer composites representing their superior myogenic differential potential. It was also observed that late myogenic protein, myosin heavy chain (MHC) related to the formation of myotubes, expressed more on GO-PCL composite scaffolds compare to GO sheet and control (tissue culture plate). Myogenic gene (Desmin, MyoD and MHC) expression was also found to be better on GO based polymer composite substrate. In addition, IGF-1 pathway, important for skeletal myoblast cells growth and maturation [319,320], was also studied with various intermediate proteins (IRS-1/PI(3)K/Akt/MyoD) expression. Inhibition of Akt was investigated to examine the variation of the expression of myogenic protein MyoD, involved in skeletal muscle differentiation [319,320]. The expression of MyoD was observed to reduce along with the inhibition of Akt that indicated the effectiveness of IGF-1 pathway for skeletal myoblast cells differentiation and maturation.

5.3.1. Expression of Desmin, MyoD and MHC proteins on scaffolds

Expressions of myogenic proteins such as Desmin, MyoD and MHC were assessed on GO-PCL meshes, GO sheet and control (tissue culture plate) using Western Blot analysis. Figure (5.15) showed expressions of Desmin and MyoD on these substrates after 5 days of culture. Both of these proteins expressed well on GO based substrates. The electroconducting GO-PCL composite mesh showed the highest expression due to better interconnectivity that enhanced cellular growth and hence their protein expressions.

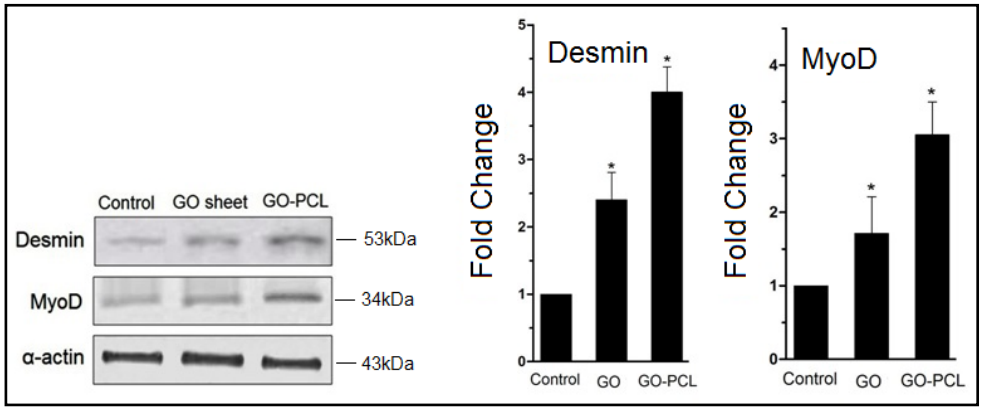

Figure 5.15. Expression of myogenic protein Desmin and MyoD (left) and expression of fold change on GO-PCL mesh, GO sheet and control (tissue culture plate) (right) for the corresponding proteins. * indicates significant difference compare to control ($p < 0.05$).

From the present observation (Figure 5.15), the expression levels of Desmin and MyoD proteins were found to be enhanced on graphene based scaffolds, compared to

that of control as follows: 2.4-fold on GO, 4-fold on GO-PCL for Desmin and 1.8-fold on GO, 3.1-fold for GO-PCL for MyoD. Data reported as fold change from control (means ± SE). *indicates significant differences (n=5; p<0.05).

After 11 days of culture on the same substrates, expression of MHC (a late myogenic marker) was assessed using Western Blot analysis (Figure 5.16). Expression of MHC, related to formation of myotubes was found to be better on GO and GO-PCL meshes compared to control substrate.

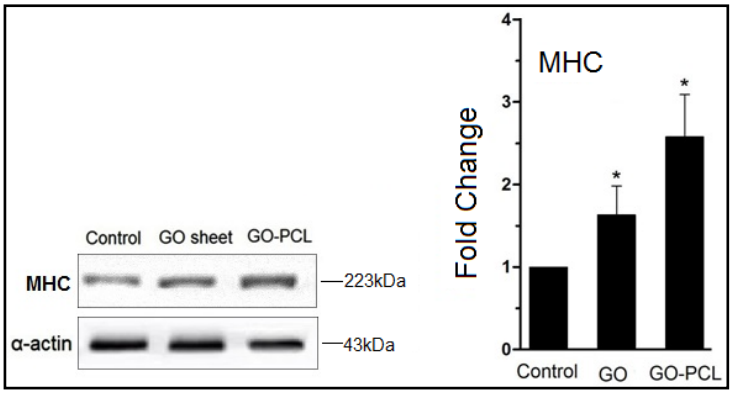

Figure 5.16. Expression of myogenic protein (MHC) (left) and expression of fold change on control, GO and GO-PCL substrates (right). * indicates significant difference from control (p< 0.05).

Here, better expression of this protein in GO-PCL mesh also indicates better myotube formation on this substrate. Similar result was also observed from previous studies (flow cytometry analysis, cell viability assay etc.) described earlier in this chapter. The expression levels of MHC protein were found to enhance on GO-PCL composite and GO sheet compared to that observed with control: 1.6-fold on GO and 2.5-fold on GO-PCL mesh. Data were reported as fold change from control (means ± SE). * indicates significant difference (n=5; p<0.05).

5.3.2. Myogenic gene expression

Real-time RT-PCR was used to analyze the expression level of MyoD, Desmin and MHC on GO sheet, GO-PCL scaffolds and control. It was found, similar to protein expression, these myogenic genes expressed better on GO-PCL composite and GO sheet.

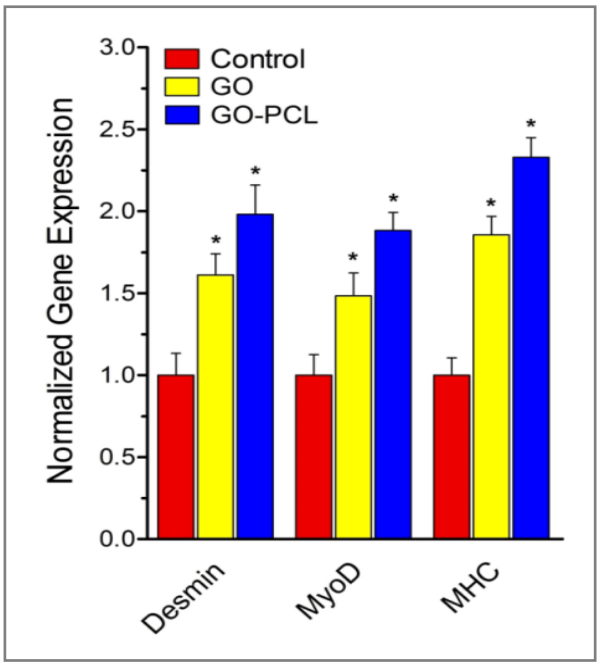

Figure 5.17. Expression of myogenic genes (Desmin, MyoD and MHC) in myoblasts grown on electrospun GO-PCL mesh, GO sheet and control (tissue culture plate) substrates. * indicates significant difference from control ($p < 0.05$).

Highest expression was found on myoblast cells grown on GO-PCL meshes. Quantitative RT-PCR analysis was performed after differentiation for 5 days for Desmin and MyoD and 11 days for MHC (as MHC express late). As shown in figure (5.17), the expression level of all of the tested genes were enhanced on graphene derivative and GO-polymer composites, compared with that of the control as 1.60-fold on GO and 1.98-fold on GO-PCL for Desmin; 1.48-fold on GO and 1.88-fold on GO-PCL for MyoD; 1.86-fold on GO and 2.33-fold on GO-PCL for MHC. * denotes a significant difference compared to control substrate.

Significant up-regulation of myogenic gene expression indicated that the GO based substrates enhanced both early and late stages of myogenic differentiation, subsequently stimulating the formation of myotubes. In addition, higher expression of myogenic proteins and genes on GO-PCL substrates again confirmed its superiority perhaps due to its higher conductivity and dielectric constant associated with GO surface charge.

5.4. Cell Signaling Pathway Analysis

5.4.1. Insulin-like growth factor 1 (IGF-1) pathway study

IGF-1 is one of the most important pathways that have been studied extensively in the field of muscle growth [285,319,320]. Researchers studied IGF-1/IRS-1/PI(3)K/Akt/MyoD pathway and concluded its importance for skeletal muscle differentiation and maturation [285,319,320]. In the present study it was attempted to verify this pathway using the novel graphene based composite scaffolds (Figure 5.18). IGF-1 is one of the primary mediators of the effects of growth hormone (GH) in body that stimulates growth via growth promoting effects on almost every cell, especially muscle cells present in the body. IGF-1 is also capable of regulating cellular growth and development. In addition, IGF-1/PI3K/Akt pathway prevents expression of muscle atrophy, very much important for proper development of muscle tissue [4]. So, skeletal muscle healing is associated with IGF-1.

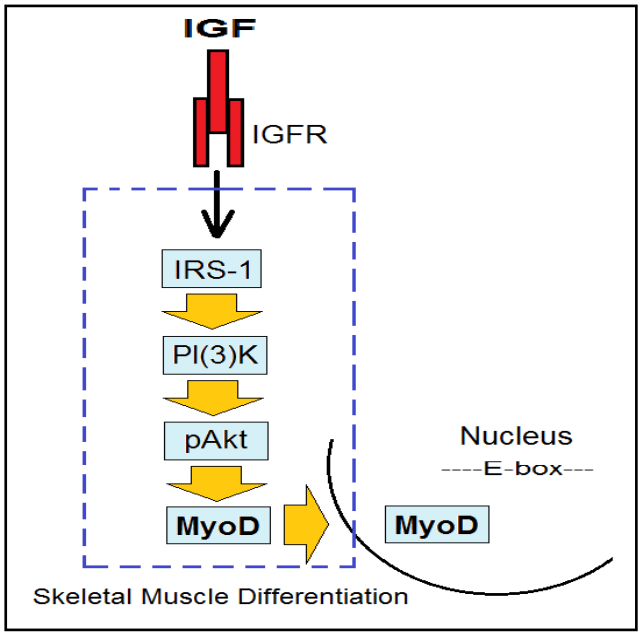

Figure 5.18. A Schematic representation of IGF-1 cell signaling pathway that involves in skeletal muscle differentiation and maturation.

5.4.2. Protein expression for IGF pathway

To study IGF pathway, expression of IRS-1/PI(3)K/Akt/MyoD proteins is important. Initially, the expression of IRS-1/PI(3)K/Akt/MyoD proteins on GO, GO-PCL and control (tissue culture plate) substrates (Figure 5.19) was analysed. All of these proteins expressed better on GO and GO-PCL, while the expression was highest for GO-PCL. This

indicates that the GO-PCL substrate is the most suitable candidate for myoblast differentiation of hMSCs.

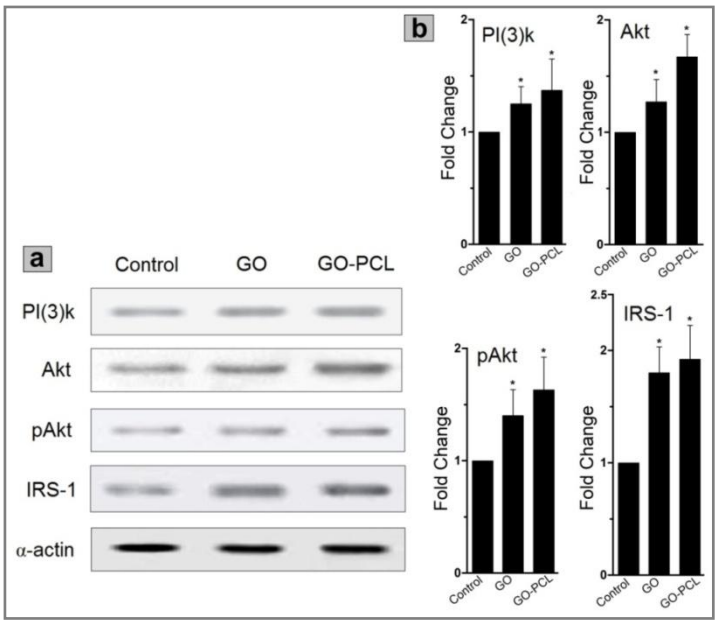

Figure 5.19. Expression of PI(3)k, Akt, pAkt, IRS-1 (a) and expression of fold change for these corresponding signaling proteins (b) on control (tissue culture plate), GO sheet and GO-PCL meshes. * indicates significant difference ($p < 0.05$).

To evaluate IGF-1 pathway, Akt is the most important protein that regulates skeletal muscle differentiation and hypertrophy. It was also reported that IGF-1 dependent Akt-phosphoralization increased along with a higher rate of myogenic differentiation. Properties of MyoD, responsible for skeletal muscle differentiation, are controlled by Akt and blockage of Akt that prevents formation of skeletal muscle transcript some [285,319,320]. The present investigation demonstrates that the investigated pathway proteins expressed better on GO-PCL composite meshes than those on GO sheet or control (tissue culture plate). Up-regulation of such pathway proteins on GO-PCL further emphasizes the IGF-1 pathway which is related to skeletal muscle development. Thus, it reveals the importance of GO-PCL composite meshes for skeletal muscle tissue engineering applications.

5.4.3. Effect of Akt inhibition on MyoD expression

As mentioned above, Akt is a major component that regulates IGF-1 pathway. Inhibition of Akt deters IGF-I stimulated nuclear translocation of Akt and also suppresses the growth of various cells. Akt is a vital component of the cell survival pathway as it

functions by resisting apoptosis via improving communication between cells that are damaged [320-322]. Inhibition of Akt results in much higher rate of apoptosis and a decrease in IGF-1 cell signaling. Inhibition of Akt was done using 10-DEBC hydrochloride, a selective and precise cell permeable Akt phosphorylation inhibitor that shows no activity at PDK1, SGK1 or PI 3-kinase [323,324]. In the present experiment, the expression of MyoD, a vital myogenic protein that helps in myogenic differentiation has been studied by pre and post Akt inhibition. The results showed (Figure 5.20) that after inhibition of Akt, the expression of MyoD intensity decreased rapidly. Akt inhibitor inhibits IGF-I-stimulated nuclear translocation of Akt that results in much reduction of MyoD protein assessed by Western Blotting. This finding indicates the importance of IGF-1/IRS-1/PI(3)K/Akt/MyoD cell signaling pathway for the system of present investigation.

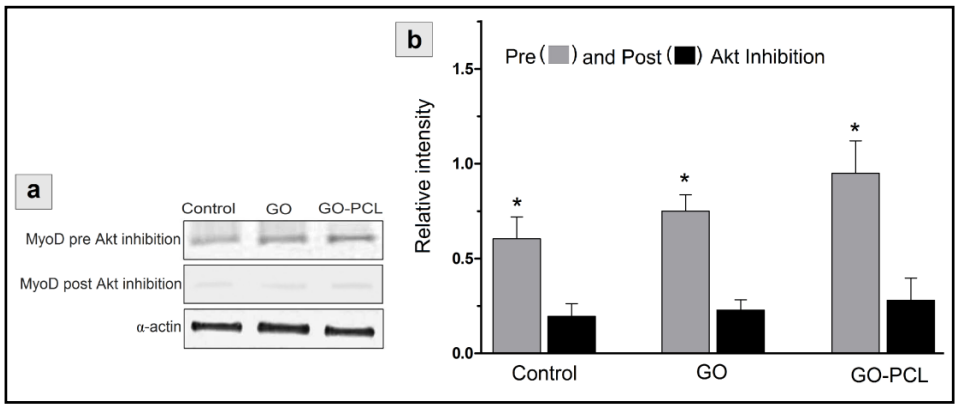

Figure 5.20. Expression of MyoD (a) and the corresponding relative intensity (b) indicating pre and post inhibition of Akt. * indicates significant difference from post Akt inhibition ($p < 0.05$).

The expressions of myogenic proteins on graphene oxide based substrates (GO sheet and GO-PCL scaffold) have been assessed. It has been demonstrated that myogenic proteins expressed better on the GO-PCL composite meshes than GO sheet and the control (tissue culture plate). This highlighted the superiority of graphene based substrates for myoblast differentiation. Favourable physicochemical and biological properties established these scaffolds as potential platforms for myogenic differentiation and maturation for tissue engineering and other biomedical applications. In addition, we have also shown preliminary study of IGF-1 pathway that is important for skeletal muscle differentiation and maturation as well. This pathway proteins (IRS-1/PI(3)K/Akt/MyoD) also expressed better on graphene based substrates, particularly on

GO-PCL scaffolds. Moreover, selective inhibition of Akt has reduced the expression level of MyoD, a myogenic protein important for skeletal muscle differentiation.

Hence, it was noticed that lower expression of MyoD along with Akt inhibition indicated the importance of the IGF-1 cell signaling pathway observed from this preliminary investigation. Further elaborate study seems to be more interesting.

5.5. Conclusion

In conclusion, the present study clearly demonstrated that pure GO sheet and GO added GO-PCL fibrous scaffolds are suitable for myoblast differentiation. Electrospun GO-PCL scaffolds are excellent biocompatible substrates for human skeletal myoblast cells differentiation of cord blood derived mesenchymal stem cells. GO-PCL composite with increased conductivity and dielectric constant (compared to PCL) showed enhanced myoblast differentiation and oriented multinucleated myotubes formation, like natural orientation, which is highly desirable for the in-vivo regeneration of electro-responsive skeletal muscle tissue. Myogenic proteins also expressed better on GO-PCL composite meshes. Preliminary investigation of IGF-1 cell signalling pathway examined on the prepared substrates further confirms the superiority of GO-PCL composite scaffolds for myoblast differentiation. Thus the present result also supports that GO-PCL electrospun scaffold is a potential candidate for skeletal muscle tissue regeneration. Therefore, in demand of cell specific substrates GO based polymer composite meshes might be considered as one of the most favourable scaffolds for electro-responsive skeletal muscle tissue engineering applications.

Moreover, it would be worthwhile to mention that the easily available cord blood derived multipotent hMSCs used for the myoblast differentiation might also be similarly employed on these GO based biocompatible substrates for the regeneration of other lineages for future biomedical applications in a cost effective way.

CHAPTER-6

Characterization of the Fabricated Electrospun GO-PLGA Composite Meshes

6. Characterizations of the Electrospun GO-PLGA Composite Scaffold

This chapter deals with the experimental characterization of the samples from the studies of XRD, SEM, FTIR, Raman spectra, mechanical property, contact angle, electrical and dielectric properties. GO added GO-PLGA electrospun scaffold meshes was also demonstrated as a potential substrate for skeletal muscle tissue regeneration.

6.1. Characterization of GO- PLGA Scaffold Materials

6.1.1. Morphology of the GO film and GO-PLGA electrospun scaffold meshes

Preparation of GO-PLGA composite and electrospun meshes have already been discussed in chapter 3. Figure (6.1) represents GO solution (figure 6.1a) used for making GO films (figure 6.1b) composed of GO and typical SEM micrograph of electrospun GO-PLGA composite meshes shown in figure 1.6c. The average fiber diameter estimated (using the method discussed in chapter 3) 540 ±130nm and the corresponding porosity lied within 80±10%. However, porosity of the meshes depends on the fiber diabetes. The GO concentration dependent percolation behavior of conductivity and dielectric constant of the composite films was also studied in the present case at room temperature.

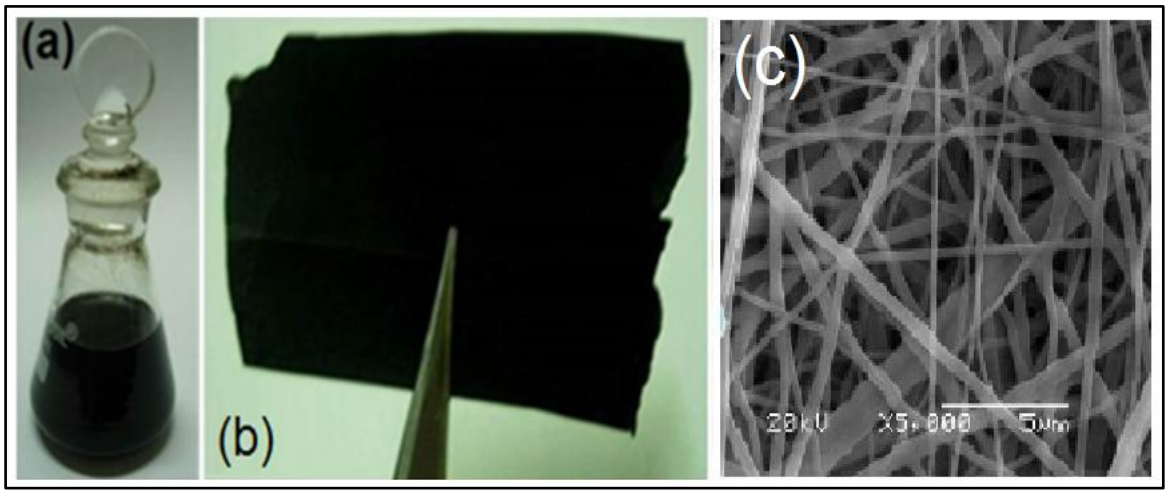

Figure 6.1. (a) GO solution, (b) GO film composed of GO and (c) scanning electron micrograph of a typical; electrospun GO-PLGA meshes.

6.1.2. Percolation threshold behaviour exhibited by GO-PLGA composite

To make electroconducting electrospun GO-PLGA composite scaffolds (like GO-PCL composite), GOnPs concentration within non-toxicity limit (20μg/ml solution) was taken within the percolation threshold concentration (f_c~ 0.75wt% observed in case of PLGA) shown in figure (6.2). Percolation threshold f_c was determined, as usual, from the measurements of GO concentration dependent conductivity and dialectic constant measurements. GO concentration dependent dielectric constant (ε) and conductivity (σ) showed maximum values near the percolation threshold.

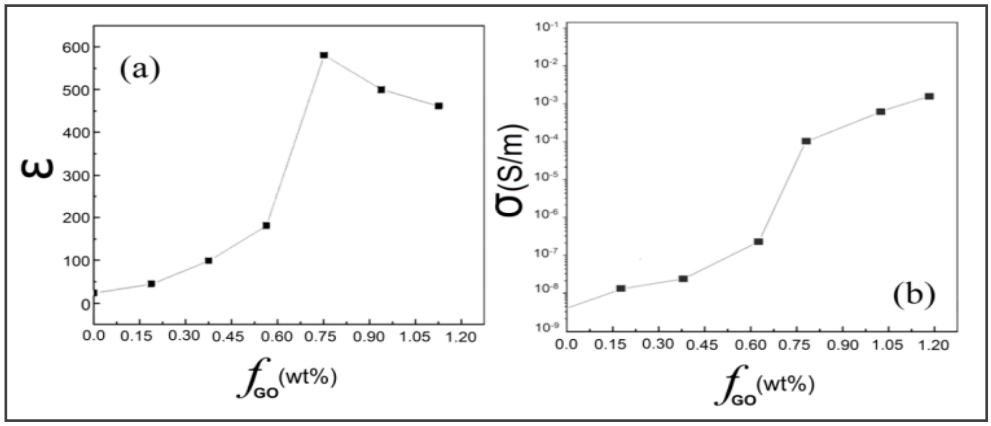

Figure 6.2. GO concentration (f_{GO}) dependent dielectric permittivity (ε) and conductivity (σ) showing maximum ε and σ around 0.75wt%.

PLGA and GOnPs also found to form homogeneous composite showing very low GO concentration. GO-PLGA composite exhibited maximum ε and σ values around f_c. The f_c value(~ 0.75wt%) of GO-PLGA was found to be slightly lower than that of the GO-PCL composite (~0.79wt%) (shown in chapter-4) but it is comparable to the corresponding value of GO-PVA (~0.76wt%) composite [289]. The percolation behavior of the GO-PLGA composites (figure 6.2) also follow the theoretical formulae [290] as discussed in chapter-4. As mentioned above, for myoblast differentiation, GO-PLGA polymer composite scaffold was also prepared with GO concentration (~20μg/ml) within nontoxicity and the percolation threshold limits.

6.1.3. Phase behaviour of GO-PLGA fibrous meshes

Figures (6.3a and b) showed X-Ray diffraction patterns of PLGA and GO-PLGA meshes. As reported earlier (chapter-4), the X-Ray diffraction patterns of GO indicated the

characteristic GO peak appearing at 2θ =11.1^{o} with d-spacing of ~0.78 nm. The corresponding XRD patterns of PLGA shown in figure (6.3a) indicated amorphous character with a hum around 2θ~19.2^{o} while the XRD patterns of GO-PLGA composite exhibited diffraction peak (Figure 6.3b) at 21.65^{o} indicating crystalline phase of the polymer. For the GO-PLGA composite, XRD data only showed the sharper diffraction peak with no peak for GO similar to the case observed earlier in GO-PCL [4] and GO-PVA [214] composites which was attributed [4] to the disappearance of the regular and periodic structure of graphite oxide and formation of fully exfoliated structures and the homogeneous distribution of GOnPs in the polymer matrix. The well-dispersed low concentration GOnPs acted as nucleating agents and thus the crystallinity of the composites was improved which enhanced conductivity hereby improving biocompatibility of the composite [4].

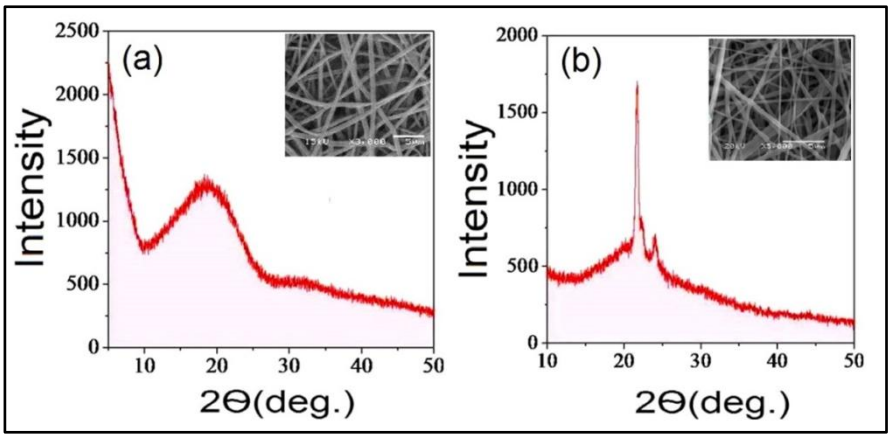

Figure 6.3. XRD pattern of PLGA (a) and GO-PLGA (b) composite meshes indicating sharp crystalline peaks. Insets of (a) and (b) show the SEM micrographs of electrospun meshes of PLGA and GO-PLGA composite, respectively.

6.1.4. Raman spectroscopy

Raman spectra of GOnPs sheet shown in figure (6.4a) indicated the characteristic feature of GO peaks at frequencies around 1338 and 1600cm^{-1}, respectively, for the G and D band usually assigned to the E_{2g} phonon of Csp^2 atoms and a phonon breathing mode of symmetry A_{1g} [325,326].

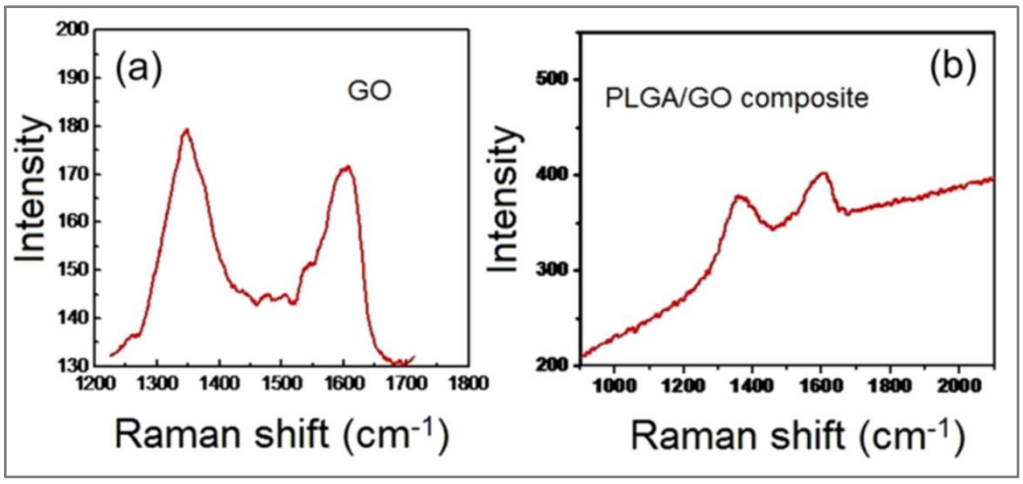

Figure 6.4. Raman spectra of GO (a) and GO-PLGA composite showing the presence of E_{2g} (D) and A_{1g} (G) peak corresponding to the graphene oxide GO and GO-PLGA composite meshes.

The presence of GO peak corresponding to 2D graphene band around 2700cm^{-1} was hardly observed in the present system as also mentioned in chapter 4 in case of GO-PCL system. This indicated the absence or traces amount of pure conducting graphene in the synthesized GOnPs and GO-PLGA composites also observed from the GO-PLGA Raman spectra (figure 6.4b). The characteristic frequency corresponding to the well-studied G and D bands are in good agreement with the literature values of graphene oxide [321] and also indicate little lattice distortion of the GO nanostructure. The intensity ratio I_D/I_G of the two peaks was widely used as characterizing the defect quantity within the GO materials [294]. By controlling the amount of defect quantity, the electronic and mechanical properties of the GO sheets might also be tuned [295]. The D band was reported to be associated with the structural imperfections created by attachment of hydroxyl and epoxide groups on the carbon basal plane [301]. The G band corresponds to the ordered sp^2 bonded carbon GO conduction was also reported to occur through sp^2 regions via Klein tunnelling [301]. Figure (6.4a) indicated GO Raman spectra shown for the comparison as in the case of GO-PCL system.

6.1.5. FTIR spectra

The Fourier transform infrared (FTIR) spectra of pure PLGA and GO-PLGA composites are shown in figures (6.5 a and b), respectively, for comparison. The absorption bands observed in the GO-PLGA at 1727 cm^{-1} (Figure 6.5b) indicates carbonyl stretching. The bands appeared at 1295 cm^{-1} and 1240 cm^{-1} represent the C-O and C-C stretching bonds.

The bands at 1239 cm^{-1} and 1175 cm^{-1} were the asymmetric C-O-C stretching bonds indicating characteristic absorption [303] of PLGA.

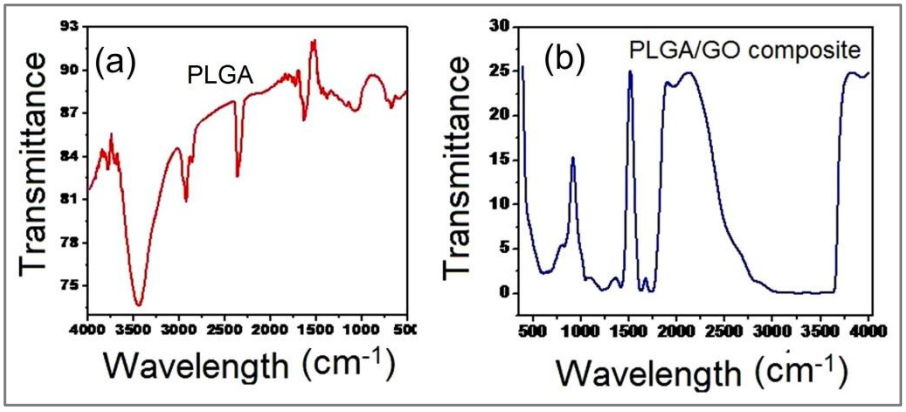

Figure 6.5. FTIR spectra of PLGA (a) and GO-PLGA (b). The corresponding spectra of GO have been shown in chapter-5. The intense band at 3438cm^{-1} was attributed to stretching of the O-H band of CO-H. The band at 1639cm^{-1} was associated with stretching of the C=O bond of carbonyl groups.

The FTIR spectrum of GO-PLGA (Figure 6.5b) indicated an intense band at 3438cm^{-1} which was attributed to stretching of the O-H bond of CO-H. The band at 1639cm^{-1} was associated with stretching of the C-O bond of carbonyl groups. Deformation of the C-O bond was observed at the band appeared at 1017cm^{-1}. From FTIR spectroscopy, evidences of different types of oxygen functionalities on GO were exhibited. The ultra violet (UV) spectrum of water solution GO exhibited a peak at 371nm, characteristic feature of the π-π* transition of aromatic C-C bonds [4]. Similar peaks were also observed in GO-PCL as well as in GO-PLGA around 460nm. The ionic bonds, the π-π stacking forces created by the sp^2 bonding and hydrophobic interaction between molecules allowed graphene to adsorb proteins and low molecular weight chemicals which are important for biocompatibility [246,308] of GO. Chen and Eda and his co-worker suggested that the fluorescence of prepared GO may originate from the optical transitions from structural disorder-induced states in the π-π* gap of sp^2 sites [327,328].

6.1.6. Mechanical property of GO-PLGA composite scaffold

Figure (6.6) showed the stress-strain curves of GO-PLGA composite mesh. From the stress-strain curves of GO-PLGA mesh, tensile stress is estimated to be ~2.87± 0.05 (MPa) which is comparatively higher to that of the GO-PCL mesh as discussed earlier in

chapter 5. This value is also comparable to that of the GO-PCL electrospun fibers [67]. In GO-PCL composite, the tensile strength was also reported to increase with increasing GO concentrations [67]. This indicates that mechanical property of the composite depends on the GO concentration. The changes of conductivity and other properties (discussed in chapter 5) also indicate that physical and mechanical properties of the composites depend on GO concentration.

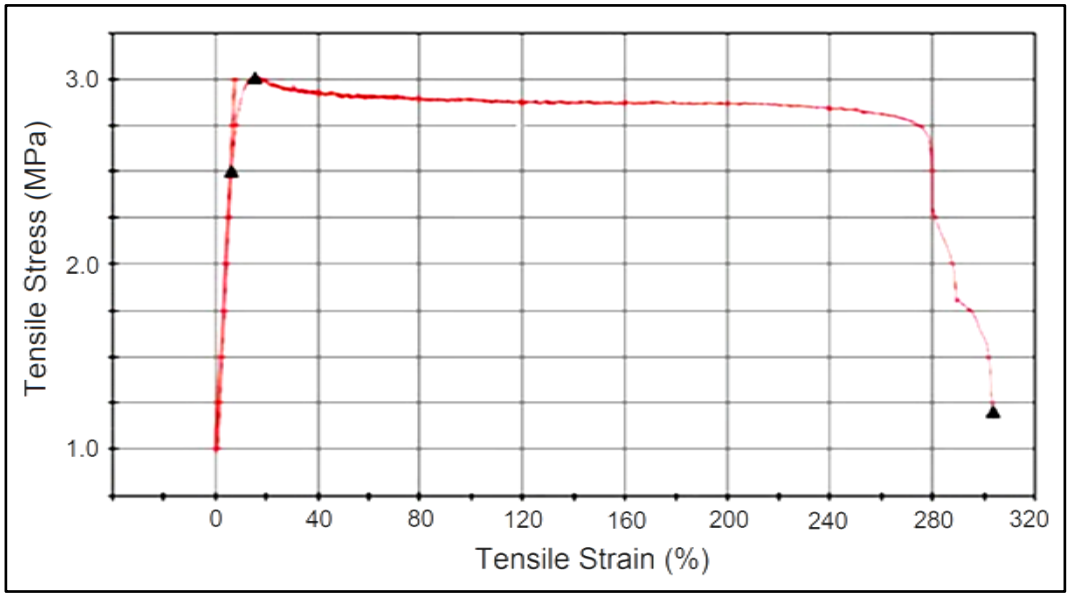

Figure 6.6. Showed the stress strain curve of a typical GO-PLGA scaffold mesh. The corresponding curve for the GO has been shown in part-1 of this chapter.

6.1.7. *In-vitro* biodegradability study

As already mentioned (chapter-2), degradation behaviour of scaffold plays an important role in the formation of new tissue at the site of an implant. The in-vitro degradation pattern of PLGA and GO-PLGA composite scaffolds as shown in the figure (6.7) indicates electrospun PLGA meshes degrade upto ~28% where as electrospun GO-PLGA mesh degrade ~17% after 30 days of time interval. Therefore, degradation rate of electrospun GO-PLGA mesh is more optimized and suitable for cellular growth compares to quicker degradation rate of PLGA mesh. Optimized degradation of scaffolds eases the longevity of the scaffold implants at the site of the implant [309]. GO-PLGA composite scaffold can thus provide support to the growing tissue for long period of time in an optimized way which may be beneficial for *in-vivo* applications as well.

6.1.8. Contact angle (CA) measurement

The wetting (CA_w) and dewetting (CA_{dw}) contact angles of sessile water drops on spin coated thin GO sheet, PLGA and GO-PLGA scaffold meshes were shown in Figure (6.7 inset) for comparison. In the case of thin GO sheets, CA_w =58.7o and hysteresis (CA_w-CA_{dw}) was estimated as ~5.5^o which is a measure of the solid–liquid surface interaction and chemical heterogeneity [310].

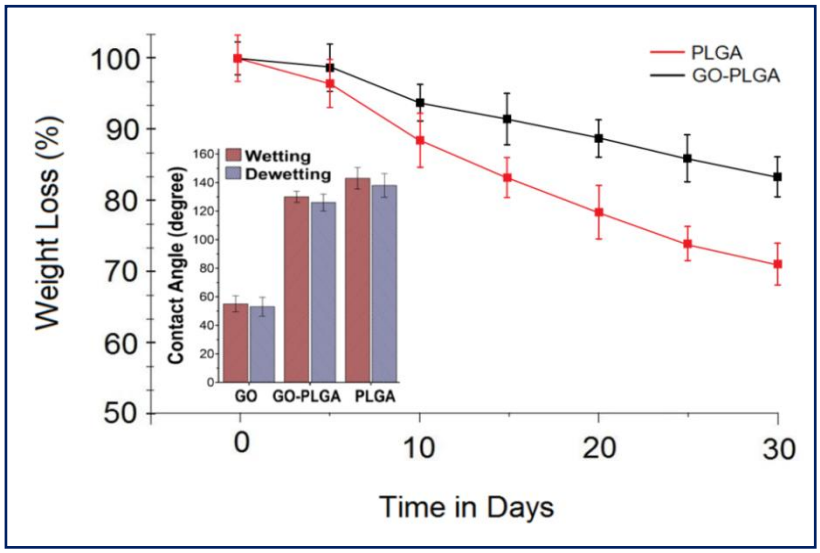

Figure 6.7. *In-vitro* degradation pattern of electrospun PLGA and GO-PLGA composite scaffolds in SBF (simulated body fluid) for 30 days. Inset shows contact angle (CA) of GO, PLGA and GO-PLGA meshes. The wetting and dewetting difference is a measure of the molecular interaction of the liquid and the scaffold.

Both CA_w and CA_{dw} values of GO-PLGA meshes (130 and 126^o, respectively) were reduced compared to that of PLGA meshes (~143^o). Small CA hysteresis for the composite meshes was due to few micron level surface inhomogeneity, which is favourable for cell adhesion and proliferation [329]. Such moderately wettable composite surface like GO-PLGA meshes are favourable for cell growth and proliferation [330,331]. GO-PLGA-Collagen hybrid fiber also showed [4] decrease of CA from 147 to 127^o. Due to the presence of GO with abundant hydroxyl group, CA of GO-PLGA significantly ($p<0.05$) decreased while its hydrophilicity of the GO-PLGA meshes increased. It is suggested that in GO-PLGA composite fiber meshes cell adhesion might be enhanced as they are more hydrophilic and have higher surface energy in presence of GO than pure PLGA fiber. Observed contact angles of GO is less than that of conducting

GOnPs-PLGA meshes indicating better biocompatibility of GO-PLGA due to enhanced hydrophilicity.

6.1.9. Swelling behavior

Figure (6.8) shows the swelling ratio of the PLGA and GO-PLGA scaffolds. Compared to PLGA mesh, the swelling ratio of the GO-PLGA scaffolds increased from 223 to 305%, indicating that the addition of GOnPs improves the hydrophilicity of the scaffold.

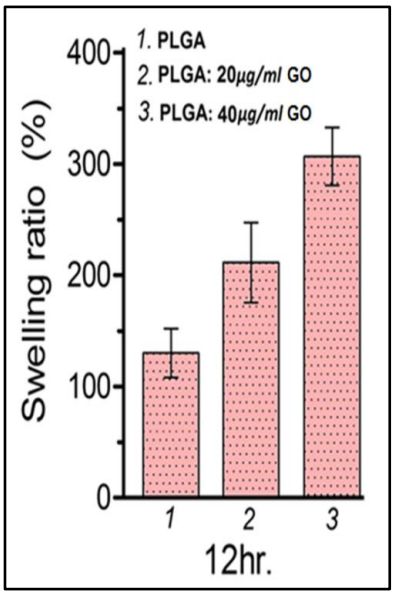

Figure 6.8. Swelling ratio of PLGA and GO-PLGA meshes. The ratio increases with addition of GO in PLGA. Figure shows that GO addition in PLGA in DMF solution (20 μg/ml and 40 μg/ml of PLGA solution) enhance hydrophilicity of the scaffolds.

This attributed to the GO-PLGA bonding. Additionally, according to the report of Li and co-workers [332,333], the capillary effect might also lead to better water adsorption. Therefore, it can be seen from figure (6.8) that the GO addition contributes to a higher swelling ratio in GO-PLGA meshes. Both swelling and hydrophilicity are important properties of the tissue engineering scaffolds, their enhanced values with the addition of GO in the polymers would enhance the cells viability and proliferation [332,333].

6.1.10. Stability of conductivity and dielectric constant of GO-PLGA meshes

Stability of conductivity and biodegradation of PLGA and GO-PLGA meshes were assessed by immersing them in PBS solution for up to one week. Upon immersion in PBS

solution, both effective σ and ε values of PLGA and GO-PLGA were found to decrease with increase of immersion (Figure 6.9) in the PBS solution (discussed in experimental chapters-3 and 4). However, the σ and ε values in case of GO-PLGA composite meshes decreased at a slower rate with respect to those of pure PLGA meshes (Figure 6.9) indicating that GO-PLGA meshes are more stable than PLGA meshes.

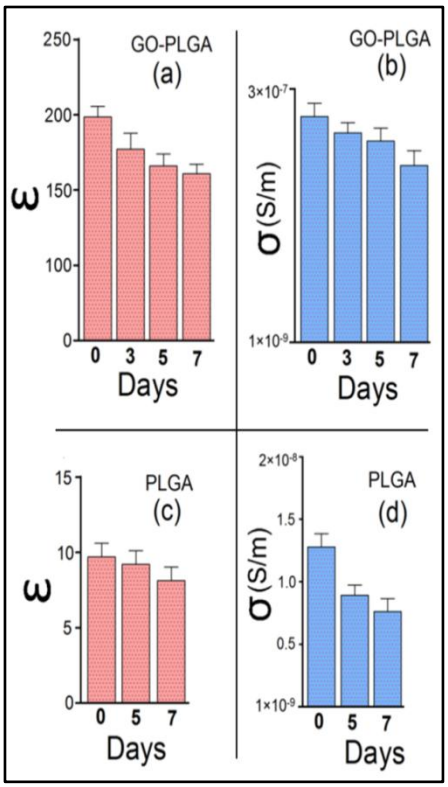

Figure 6.9. (a) Room temperature (RT) effective dielectric constant (ε) and (b) effective conductivity (σ) data of GO-PLGA composite meshes before (indicated by 0 days) and after immersion in PBS solution for upto 7 days. Similar ε (c) and σ (d) data from PLGA meshes before (0 days) and after immersion (maximum 7 days) in PBS solution discussed in chapter 3 (all measurements were performed at 1kHz).

These results specifying that the addition of GO increased σ, ε and stability of GO-PLGA which also indicate better biocompatibility of GO- PLGA (compared to PLGA with much lower ε and σ values). Similar results were also reported earlier in case of GOnPs-PCL composites meshes [4] where GOnPs addition to PCL significantly increased both conductivity and dielectric permittivity. At percolation threshold, the conductivity of GO-PLGA reached more than two orders of magnitude higher value than that of PLGA. A slight decrease in ε and σ of GO-PLGA (Figure 6.9) after immersion up to one week might be associated with small amounts of material leaching from GO-PLGA

scaffolds as in the case of PANi added PCL scaffolds as reported earlier [84]. By varying the GO concentration in PLGA or similar biopolymers, conductivity and degradation rate could also be varied. It was also shown earlier that after immersion for one week, no significant morphological change of the GO film was observed as shown in chapter-5. Due to the presence of GOnPs, mechanical stability and bioactivity of GO-PLGA composite remained quite stable even after immersion in PBS solution, which was important for belter cell scaffold interaction similar to the case of GO-PCL composite meshes studied earlier [4] as discussed in the following sections.

6.2. Conclusion

Electrospun GO-PLGA biocompatible nanocomposite also showed low percolation threshold (~0.75wt%) similar to that of GO-PCL and enhanced conductivity compared to pure PLGA. The electrospun GO-PLGA scaffolds prepared with GOnPs concentration within the non-toxicity limits were characterized from the study of structural, mechanical properties, contact angle, SEM and vibration spectroscopy properties. GO-PLGA also showed similar favourable characteristic properties suitable for skeletal muscle tissue regeneration. Due to the addition of GO mechanical property and contact angle increased while the biodegradability decrease to a little extent. This study also confirmed that both σ and ε did not change appreciably after immersion in PBS solution for about a week as observed in case of the GO-PCL meshes. This indicated that the cellular interaction associated with the biocompatibility of such composites appears to remain almost unaltered even after immersion in PBS solution over one week. The mechanical property, hydrophilicity, controllable non-toxic degradation and unique physical properties also pointed out that covalently-linked GO-polymer based composites [71] are suitable for skeletal muscle tissue engineering and other biomedical applications.

CHAPTER-7

Myoblast Differentiation on Electrospun GO-PLGA Meshes

7. Myoblast Differentiation on Electrospun GO-PLGA Meshes

This Part deals with the study of myoblast differentiation of hMSCs on the developed electrospun GOnPs-PLGA (or GO-PLGA) composite scaffold meshes. Like GO-PCL, GO-PLGA meshes also showed excellent myogenic differentiation and cell viability. These results further demonstrated the high potential of electroconducting GO-PLGA composite meshes for skeletal muscle tissue regeneration using hMSCs similarly to the case of GO-PCL composite meshes with immense potentiality.

7.1. *In-Vitro* Cell Study

7.1.1. hMSCs isolation, culture and characterization

Isolation of human umbilical cord blood derived hMSCs have already been described in chapter 5 .

7.1.2. hMSCs seeding, attachment and spreading

After seeding of hMSCs (by static seeding method with ~2×10^4 cells/ml), attachment and spreading of these cells were evaluated by scanning electron microscopic (SEM) micrographs on increasing time interval. SEM micrographs revealed excellent cell adherence as well as proliferation on the developed scaffolds after three, five and seven days of culture as shown in figure (7.1). Cellular attachment and well spreading of the cells also indicate their compatibility to the scaffold environment.

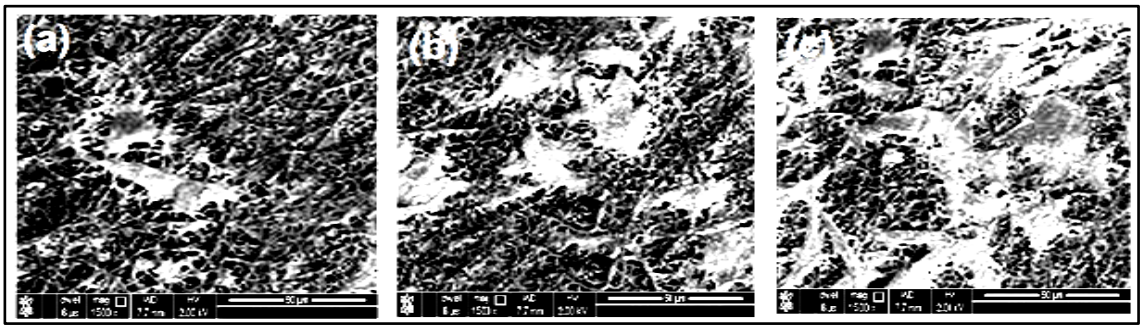

Figure 7.1. Attachment and spreading of hMSCs on GO-PLGA composite scaffolds examined on 3^{rd}(fig. a), 5^{th}(fig. b), and 7^{th}(fig. c) days of culture. Proliferation of cells has been found with increasing time interval indicating cells are compatible with scaffold environment.

7.1.3. Cell metabolic activity

The metabolic activity of the cultured cord blood derived hMSCs seeded on the prepared GO-PLGA scaffold was further evaluated quantitatively by WST-8 assay as shown in

figure (7.2). Difference in the increase of O.D (optical density) values with culture period were observed for hMSCs grown on different substrates (GO-PLGA meshes and tissue culture plate (TCP) as control).

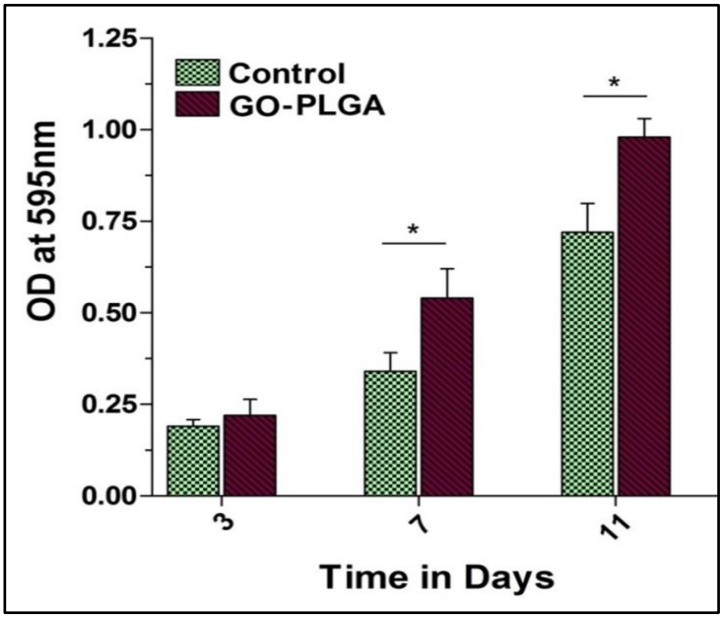

Figure 7.2. WST-8 assay of hMSCs grown on GO-PLGA composite scaffolds after 3, 7 and 11 days of culture. Superior cellular metabolic activity has been observed on GO-PLGA composite meshes. Results presented as the means ±SD. * indicates significant difference (n=5; $p<0.05$). Metabolic activity was increased with time with the scaffolds showing the trend PLGA>control substrate.

However, the higher O.D value representing higher metabolic activity was obtained with GO-PLGA composite scaffolds than the control. The increase in metabolic activity achieved with GO-PLGA composite mesh could be attributed to the addition of GOnPs that provided essential physicochemical properties suitable for better cellular interaction. The amount of formazan dye generated (by the activities of dehydrogenases) was directly proportional to the number of living cells. Thus, GO-PLGA scaffolds proved superior biocompatibility compared to GO sheet and the control.

7.1.4. Cells proliferation assay (via DNA quantification)

The proliferation of hMSCs on the prepared scaffolds was evaluated by DNA quantification assay. Figure (7.3.) showed an increasing rate in DNA content of hMSCs with time as observed in different GO based substrates prepared for investigation. The corresponding DNA contents of hMSCs cultured on tissue culture plate (taken as control)

and GO-PLGA composite meshes on 3 to 11 days of culture were ~50ng/ml to ~275ng/ml, and ~62 to ~350ng/ml, respectively.

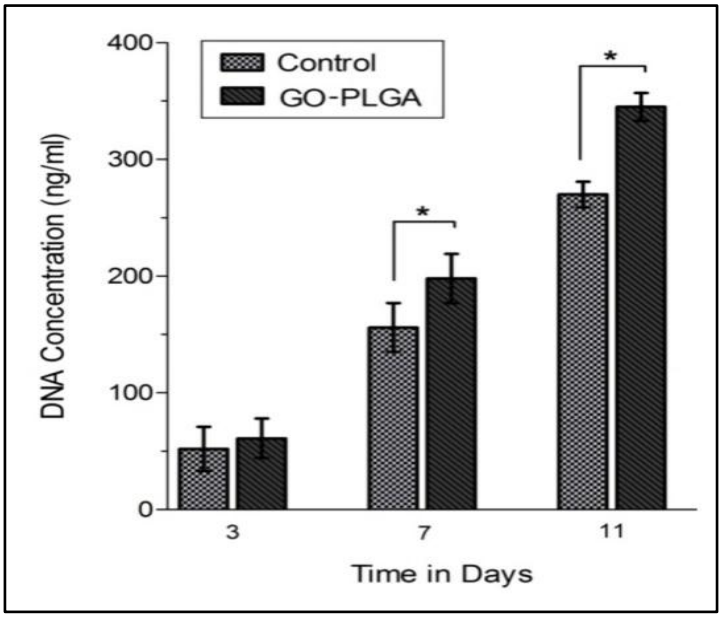

Figure 7.3. Cell proliferation represented in terms of DNA quantification on GO-PLGA mesh and control substrates (tissue culture plate). An increased trend in DNA content is observed on GO-PLGA composite matrixes. Results represented as mean ± SD, * indicates significant difference ($n=5$; $p < 0.05$). Proliferation of hMSCs was increased with time with the scaffolds showing the trend GO-PLGA >control substrate.

Electrospun GO-PLGA meshes have shown significantly higher amount of DNA content representing highest proliferation rate of hMSCs. Proliferation of these cells was increased with time with the scaffolds showing the trend of GO-PLGA>control (tissue culture plate) substrate.

7.2. Differential Potential of hMSCs on GO-PLGA Composite Meshes

7.2.1. Myoblast differentiation and spreading

After confirming excellent viability and proliferation of hMSCs onto the novel GO-PLGA composite scaffolds, these cells were further allowed for myoblast differentiation. Along with differentiation of hMSCs, elongated bipolar morphology of myoblasts was observed

on GO-PLGA composite scaffolds which were further confirmed by Immunohistochemical (Desmin, MyoD, MHC, Dystrophin) as well as FESEM analysis.

7.2.2. Myoblast viability

The viability of Myoblast cells on GO-PLGA composite scaffolds were analysed by WST-8 assay. Figure (7.4) showed myoblast viability on GO-PLGA mesh along with control (tissue culture plate) and GO sheet (for comparison). Cell viability was found to increase significantly on GO sheets and GO-PLGA meshes compared to that on the control surfaces (*:$p<0.05$). This result implies that GO-PLGA mesh is cytocompatible and supported myoblast proliferation as in the case of GO-PCL composite meshes studied earlier [4,28]. It was thus seen that electrospun GO-polymer meshes with low GO concentration (not toxic to human cells) provided favourable circumstance for the growth and proliferation of myoblast cells.

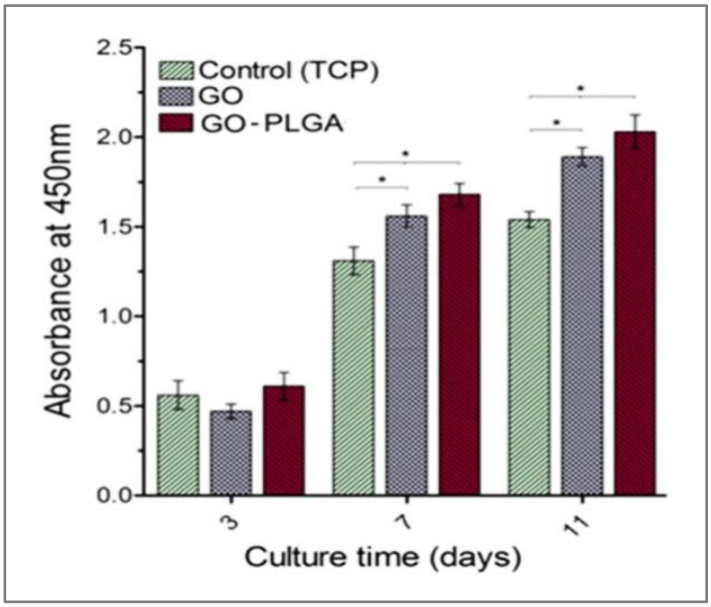

Figure 7.4. Myoblast cells viability and proliferation observed by tetrazolium salt (WST-8) assay. Results presented as mean ± standard deviation. * indicates significant difference (*n=5, p<0.05*). Viability was found to increase with time on the samples showing the trend of GO-PLGA>GO>control substrate (tissue culture plate).

7.2.3. Immunophenotypic characterizations

The flow cytometry analysis of the myoblasts grown onto the GO-PLGA mesh confirmed the positive expressions of myogenic markers CD56 and Desmin indicating the

differentiation of hMSCs to myoblast cells. Expression of these myogenic markers indicates myoblast cells phenotype (Figure 7.5).

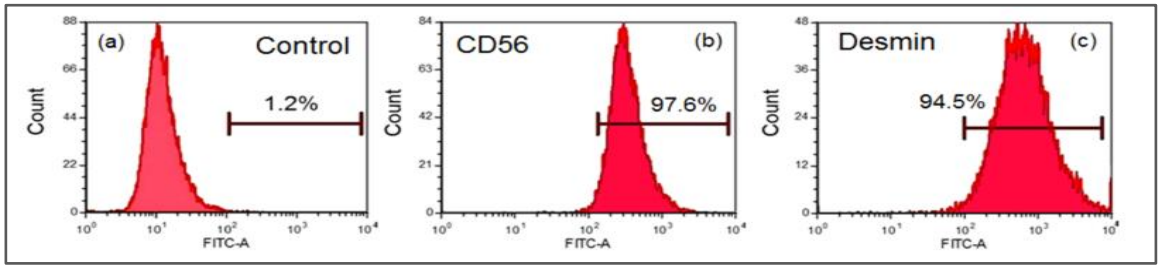

Figure 7.5. Flow cytometric analysis of myoblasts grown onto the GO-PLGA composite scaffold. Positive expression of myogenic markers CD56 and Desmin represents myoblast cells phenotype.

7.2.4. Formation of myotubes

The formation of Myotubes on GO-PLGA meshes was examined by FESEM as well as immunostaining as represented in figure (7.6). The myotubes are observed to be the highest and more aligned on the GO-PLGA scaffold meshes compared to that on control substrate indicating better compatibility of myotubes formation. A better interconnectivity of the GO-PLGA fibrous meshes along with enhanced conductivity and dielectric constant, due to the presence of GO, might play a combined role at the cell anchoring sites for better myoblast proliferation and myotubes orientation on GO-PLGA meshes as discussed as in the case of GO-PCL.

7.2.5. Immunohistochemical analysis

Similar to the GO-PCL composite meshes studied in the previous chapter, Immunohistochemical study has also been performed with myoblasts grown on electrospun GO-PLGA scaffold meshes. The experimental results confirmed the differentiation of hMSCs into skeletal myoblasts by the expressions of Desmin and MyoD, and formation of myotubes by the expression of MHC on GO-PLGA composite meshes and controls (pure PLGA mesh and tissue culture plate, TCP) as evidenced from Figure (7.6). Immunostaining of Desmin and MyoD after 3-7 days of culture expressed almost similarly on both control and GO-PLGA substrates. But, the formation of MHC on GO-PLGA mesh was much better compare to pure PLGA and TCP control substrates.

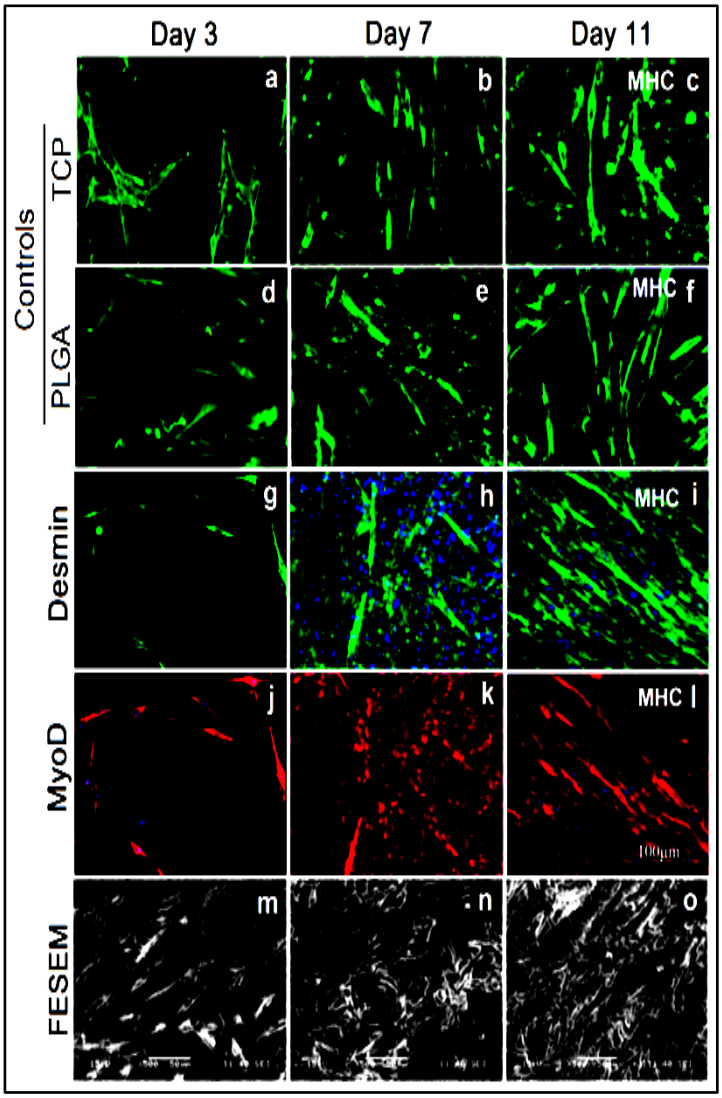

Figure 7.6. Immunostaining of Desmin, MyoD and MHC (myosin heavy chain) on controls (a-f) and GO-PLGA electrospun composite mesh (g-l). Corresponding FESEM micrographs (m-o) of these samples were shown for better demonstration. It is revealed that GO-PLGA showed better myoblast differentiation compared to that on control groups (pure PLGA mesh and TCP).

The formations of myotubes on this composite scaffold were also more aligned, similar to natural tissue orientation. This indicates better myotubes formation hence better myogenic maturation potential of GO-PLGA mesh. But, GO-PCL composite meshes showed even superior myoblast proliferation as well as differentiation potential

compared to GO-PLGA meshes. This might be due to the fact that PLGA released acidic by-products upon its degradation that hamper cellular interaction. Moreover, conductivity, a highly desirable material property for skeletal muscle regeneration, of GO-PCL was higher than GO-PLGA mesh that also makes GO-PCL more suitable for electro-responsive skeletal muscle tissue regeneration.

7.2.6. Myogenic protein and gene expression

For myogenic gene expressions, such as Desmin, MyoD and MHC quantitative real-time RT-PCR was used after differentiation for five days for Desmin and MyoD and seven days for MHC. The expression levels for all the tested myogenic genes were enhanced on GO-PLGA meshes as compared with control substrate (tissue culture plate). Significant up-regulation of these myogenic gene expressions (Figure 7.7) indicated that GO based substrates improved myogenic differentiation compared to the control substrate and subsequently stimulated the formation of myotubes.

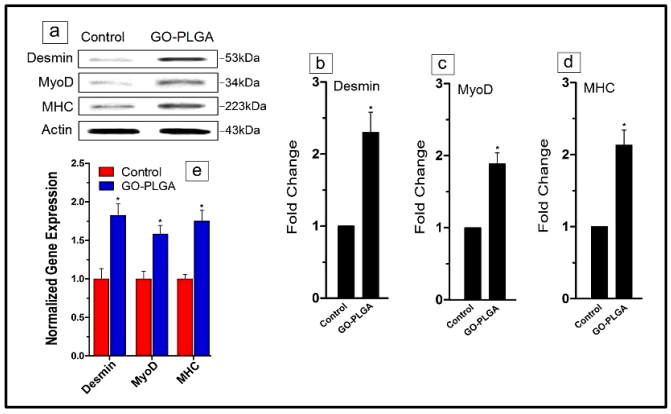

Figure 7.7. Expression of myogenic proteins Desmin, MyoD and MHC (a) and expression of fold change on control and GO-PLGA substrates (b-d) for the corresponding proteins. Expressions of myogenic genes (analysed by quantitative real-time RT-PCR) in myoblasts grown on GO-PLGA mesh and control substrates (e). * indicates significant difference compared with control ($p < 0.05$). Up regulation of myogenic proteins and genes indicates the better myogenic differential potential of the scaffolds.

Similar enhanced myoblast differentiation potential was also observed in the case of GO-PCL composite meshes (chapter-5) where increased in conductivity and dielectric constant were reported to be little higher than those of GO-PLGA which might

be due to the fact that PLGA is less conducting with lower dielectric constant than those of PCL. Therefore, the excellent biocompatibility and myoblast differentiation potentiality of GO added GO-PLGA meshes might also be associated with the surface charge increasing conductivity of the GO based polymer composites.

7.3. Conclusion

Fabricated electrospun PLGA-GO electrospun fibrous meshes with GO concentration within low percolation threshold and toxicity limits exhibited excellent biocompatibility. Well dispersed GOnPs with adhered surface charge enhanced both conductivity and dielectric constant of the composites due to quantum tunnelling between the graphene oxide nano-flakes. The increased hydrophilicity of the GO added PLGA meshes provided favourable environment for cell attachment and proliferation. Initial enhancement of myoblast attachment, proliferation and differentiation were stimulated by the presence of GOnPs in the PLGA-GO scaffolds. Such spontaneous myogenic differentiation was due to the presence of GO in the polymer matrix which gave rise to better cell scaffold interaction (arising due to GO surface charge and other inherent physicochemical properties) favourable for cells growth and proliferation. Thus the enhancement of mechanical property, hydrophilicity, conductivity and excellent biocompatibility make the GO-polymer composite an ideal scaffold material. Moreover, one important characteristic of graphene is that it adsorbs protein and low molecular weight chemicals which are important for enhanced cell-scaffold interaction. For growth or cellular communication, cells secrete different substances that are adsorbed onto GO surface and affect cell proliferation and differentiation [127,306]. The present results demonstrated enhanced biocompatibility of PLGA-GO fibrous meshes showing excellent myoblast differentiation and self-aligned myotubes formation with cord blood derived mesenchymal stem cells. Increased biocompatibility of GO-polymer composites was attributed to the surface charge and nano-flake structure of GO as in the case of GO-PCL meshes. Therefore, in demand of cell specific substrates, the use of GO-based polymer composites (both GO-PCL and GO-PLGA) scaffold meshes might be considered as one of the most potential substrates for the next generation tissue engineering and other biomedical applications.

CHAPTER-8

Phenomenological Origin of Excellent Biocompatibility of GO Based Polymer Composites

8. On the Origin of Excellent Biocompatibility of GO Based Polymer Composites

In the previous chapters (5 and 7), it was showed that GO sheet, GO-PCL and GO-PLGA electrospun meshes are promoted for myoblast differentiation of cord blood derived mesenchymal stem cells and thus suitable for tissue engineering and other biomedical applications. The origin of such excellent biocompatibility of GO based composite polymers had not been elucidated. Study of GO surface charge, current (I)- voltage (V) and capacitance (C)- voltage characteristics indicated the presence of GO surface charge which actually provided excellent cues for excellent biocompatibility of such GO based polymer composites for electro-responsive skeletal muscle tissue engineering applications.

It was observed from the results of myoblast differentiation of hMSCs on GO-PLGA and GO-PCL (chapter-5) meshes that conductivity enhancement of the GO-polymer scaffold materials (compared to PLGA or PCL) favoured biocompatibility. Conductivity of insulating polymers was increased by the addition of GO. Electroconducting scaffolds were also reported to stimulate bone [334], cardiac [335] and skeletal muscle [4] tissue. On the contrary, although GO is a low-conducting and high dielectric nanomaterial with surface charge [4,312], it provides excellent necessary supporting cues towards biocompatibility of the composites.

Therefore, the conductivity of GO (~10^{-7} S/m at RT) might not be responsible for the excellent potentiality of the GO-polymer composite for myoblast differentiation of stem cells. This is also in contrast to the behaviour displayed by PCL-PANi where increased conductivity, by blending PCL with conducting polyaniline (PANi), enhances the biocompatibility and cell proliferation of electrospun PCL-PANi composite fibers [84].

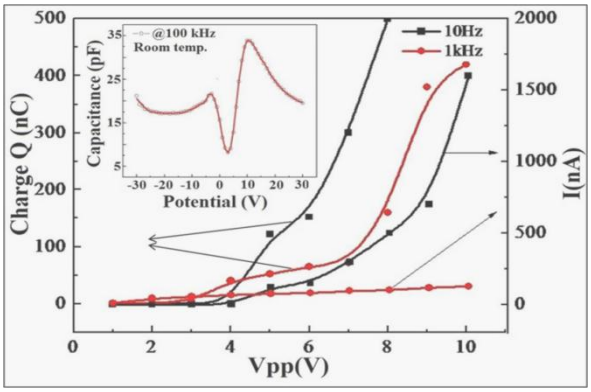

Figure 8.1. The variations of surface charge (Q) and current (I) with applied voltage (Vpp) measured at two different fixed frequencies. Inset shows capacitance (C) – voltage (V) characteristic curve of thin GO sheet at 100 kHz (all measurements at room temperature).

However, addition of GO in insulating polymers like PCL or PLGA was observed to largely increase both ε and σ values (figure 4.13 in chapter 4 and figure 6.2 in chapter 6) similar to that of GO-PCL composite reported earlier [4,312]. The ε value of GO-PLGA used for myoblast differentiation reached to a high value of ~200 at 1 kHz which was much higher than the corresponding measured value of PLGA (~8-10). The dielectric constant of GO-PLGA, at percolation with 0.75wt% GO, is more than 600 which was around 900 in case of GO-PVA composite [307] and around 800 in case of GO-PCL composite. The σ value of GO-PLGA composite also increased by about two orders of magnitude compared to pure PLGA. This increase in conductivity and dielectric constant led to the enhancement of biocompatibility of GO-PLGA as in the case of GO-PCL meshes.

Therefore, the origin of such conductivity enhancement is needed to be explored. Within the non-toxicity limits, conductivity enhancement in case of GO-PCL [4,312] was little higher than that observed in case of GO-PLGA. Interestingly, both dielectric constant and conductivity of PLGA are little less than those of pure PCL which might be responsible for GO-PCL meshes showing slightly better myoblast differentiation potential compared to GO-PLGA meshes on their surface. However, polymer structure and GOnPs-polymer interaction might also have some contribution to the biocompatibility of the composite other than conductivity.

It is worthy to note that GOnPs possess high charge trap density (~1.2×10^{18} cm^{-3}/eV) [311] and high charge mobility [312]. Moreover, GO was also reported to be piezoelectric (PE) that stimulates cells growth [4, 302]. Surface charge and dielectric constant are related to the PE behavior (PE coefficient d_{33} is related to dielectric constant [336]) of the materials [337-341]. PE properties are the unique universal properties of living tissues, and play a significant role in several physiological phenomena [342-346]. The biocompatibility of GO added GO-polymer composites might, therefore, be attributed to the presence of GO surface charge. The presence of significant GO surface charge was visualized from the measurements of the surface charge related C-V (capacitance –voltage), I-V (current-voltage) and I-Q (current –charge) characteristics of GO sheet at ambient temperature as shown in figure (8.1).

These curves showed the presence of appreciable surface charge and surface current associated with the high mobility of the charges which increased with frequency and applied external voltage. Almost similar trend of variations of I-V and Q-V curves (Figure 8.2) with frequency and applied voltage indicated that same surface charge was responsible for the development of surface current. The C-V characteristic curve (inset of Figure 8.2) also indicated the presence of surface charge on GO sheet. If the charges on the GO nanoplatelets are denoted by +q and −q , respectively, and V gives the voltage between the two nanoplatelets, then the capacitance, C, is given by (C = q/V) which gives the voltage/ current relationship (I= C [dV(t)/dt]). Static surface charge of GO sheet was also visualized from the repelling character of the GO flakes kept in a plastic container.

8.1. Surface Charge Related Properties of GO and GO-Polymer Composites

The GO added to a polymer like PLGA matrix also retained the GO surface charge and formed conducting pathways that stimulated cell growth (myoblast differentiation, proliferation and myotubes formation in GO-PLGA, GO-PCL meshes). Recognizing the fact that GOnPs are coated with thin layers of PLGA or PCL, the tunnelling conduction (like proton tunnelling) between nanoplatelets prevailed above the percolation concentration (tunnelling is a quantum mechanical phenomenon where a particle tunnel

through barrier classically does not surmount [342,346]. This mechanism of enhancement of conductivity in GO is quite different from the mechanism of enhancement of PANi added conductivity in PCL or PVA [347-349] where conductivity increment arose from the electrode polarisation rather than the interfacial polarization within the material like GO.

In the GO-polymer electrospun meshes substantial electronic disorder occurred because of the distortion of graphene oxide nanoplatelets (as also revealed from the analysis of the Raman spectra) which might give rise to the variable sp^2 and sp^3 carbon ratio in GO and increase conductivity (since conductivity depends on the sp^3/sp^2 ratio [207].

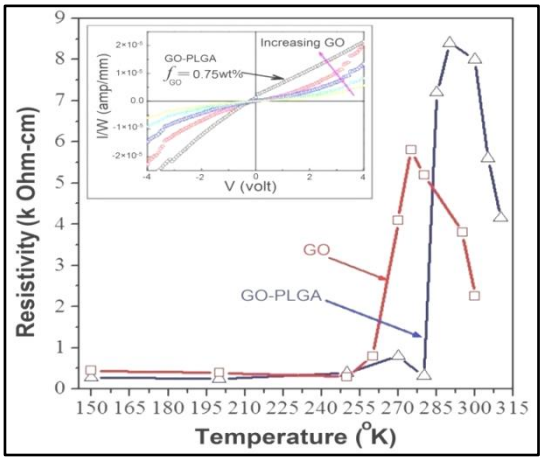

Figure 8.2. Thermal variations of resistivity of thin GO sheet and GO-PLGA composite indicating a metal insulator like transition around room temperature. Inset indicates the room temperature current (I) - dc voltage (V) characteristics of GO-PLGA composites with increasing GO concentrations (maximum with f_c=0.75wt%).

Chien and Eda [327,328] also pointed out that the disorder-induced states and the newly formed graphitic domain of sp^2 clusters during reduction were responsible for GO photoluminescence (PL). Interesting metal insulator like transitions were observed in the GO sheet and GO-PLGA composite around room temperature (275 and 305K, respectively)as shown in figure (4.51). Similar transition was also observed in GO around 275K [328]. A drastic change of the sp^2/sp^3 ratio around 300K might be associated with conducting pathways between the GO flakes around this temperature, which gave rise to such anomalous large increase of conductivity of GOnPs around room temperature in

the composite leading to the enhancement of biocompatibility. Table 8.1 showed some of the physical and mechanical properties of the GO-PCL and GO-PLGA composite meshes. Figure (8.2) was also reflected in the resistivity versus temperature curve of GO-PLGA. Resistivity (inverse of conductivity) of GO-PLGA decreased with decreasing GOnPs concentrations, which was attributed to the percolation in DC conductivity as shown in figure (8.2) as well as the progressive destruction of its layered structure. The current-voltage (I-V) characteristics for the GO-PLGA composite film samples measured at RT exhibited non-linear behavior (figure 8.2 inset) which decreased with increase of GO concentrations. No saturation of the current was indicated. This feature resembled the width – normalized current (I/W) as a function of source drain bias voltage (V) from a single reduced GOnPs flake [326] The C-V, V-Q, and I-V characteristics related to the applications involving device or biosensors and biocompatibility of the GO based polymer composites are, therefore, mainly controlled by the GO surface charge, Q, and the nano-flake structure of GOnPs. This means, Q related electro-responsive parameters (conductivity, PE and dielectric constant) provided the supporting cues for the biocompatibility of GO-polymer composite materials for different biomedical and TE applications.

Table 8.1. Summary of some important physical parameters of prepared GO-Polymer composite scaffolds prepared with GOnPs concentration with the percolation and non-toxicity limits*

SL. No	GO-polymer composite scaffolds	Conductivity (σ) (T=300K, f=1kHz) (S/m)	Dielectric Constant(ε) (T=300K, f=1kHz)	Contact angle (degree)		Tensile strength (MPa)	Hydrophilicity (%)	Decrease of σ and ε after immersion in PBS solution for seven days is less than 2 % indicating stability of these composite meshes [84].
				Wetting	Dewetting			
1	GO-PCL	2.7×10^{-6}	300	78±5	75±5	3.99±0.5	34	
2	GO-PLGA	2.8×10^{-7}	198	130±5	126±5	2.95±0.5	30	

* Remark: Both conductivity and dielectric constant of GO-PCL is Higher than those of GO-PLGA meshes indicating better biocompatibility of GO-PCL for electro-responsive skeletal muscle TE applications.

This new observation of GO oxide and GO-Polymer composite might be utilized for the controlled and directional differentiation and proliferation of skeletal myoblast

or similar cell types (by controlling the GO surface charge orientation along the particular direction which could be done electromagnetically). Along with surface charge, physiochemical aspects of GO sheet, GO-PCL and GO-PLGA meshes also play important role for the admirable myoblasts differentiation and proliferation. Well-dispersed GOnPs with surface charge acted as nucleating agents for cells proliferation and aligned myotubes formation on the GO-PLGA or GO-PCL meshes. From FTIR spectroscopy, the evidence of different types of oxygen functionalities on GO were exhibited. The ultra violet (UV) spectrum [214] of GO exhibited characteristic feature of the π-π transition of aromatic C-C bonds. The ionic bonds, the π-π* stacking forces created by the sp^2 bonding and hydrophobic interaction between molecules allow graphene to adsorb proteins and low molecular weight chemicals (during cell growth, cells secrete various substances that are adsorbed by GO surface affecting cell growth and proliferation [308] which provided important supporting cues for the biocompatibility of GO and GO-Polymer meshes. Therefore, molecular interaction between GO and the living cells mediated by the GO surface charge carriers might be associated with the hidden mechanism of biocompatibility of GO based scaffolds, while electronic charge transfer process among the embedded GOnPs makes the same system also suitable for applications in electronic devices in a unified way.

8.2. Conclusion

The addition of GO has been shown to enhance the conductivity and dielectric constant of the composites due to quantum tunnelling between the graphene oxide nano-flakes. Enhanced biocompatibility of GO based polymer composites might be attributed to the surface charge and nano-flake structure of graphene oxide. Though GO-PCL and GO-PLGA (with the same concentration of GOnPs) exhibited excellent myoblast differentiation of cord blood stem cells, superior myoblast alignment and myotubes formation were observed in case of GO-PCL meshes with higher conductivity and dielectric constant (associated with GO surface charge) compared to those of the GO-PLGA meshes. Further study of conductivity variation of influencing cell-scaffold interaction might be interesting.

S U M M A R Y

A N D

CONCLUSION

CHAPTER-9

Overall Summary and Conclusion

9. Summary and Conclusion

Skeletal muscle is one of the most important tissue types that are responsible for the movement of various body parts. Due to various causes like diseases, trauma, burns, accidents etc. skeletal muscle tissues are damaged which requires repair and regeneration. In such a case, Tissue Engineering (TE) can help in the regeneration of new muscle tissue maintaining its original structure as well as functionality. One of the most important requirements of successful skeletal muscle tissue engineering is to develop suitable biocompatible scaffolds which provide the favourable environment for the proliferation and differentiation of myoblast cells for new muscle tissue regeneration. These scaffolds should provide guiding cues for skeletal muscle tissue regeneration within desired time frame. So far, a number of biocompatible polymer composites have been developed for such applications. But various problems related to biodegradability, mechanical stability, cell scaffold interaction, hydrophilicity and conductivity of the scaffold materials hindered wide application of such polymer scaffolds for typical electro-responsive skeletal muscle tissue regeneration. No single polymer based scaffold has, however, been found to provide most of the desirable properties to successfully regenerate skeletal muscle tissues. Therefore, development of suitable scaffold material that would be more appropriate for such application is a continuous process and seems to be highly appealing and various attempts are being made worldwide.

The present thesis dealt with fabrication of a novel graphene oxide (GO) based electro conductive biopolymer nanocomposite scaffold with improved mechanical, electrical and biological properties that provided suitable cues for the in-vitro electro-responsive skeletal muscle tissue regeneration. The most interesting and encouraging results obtained from the present research work is described here.

In the first phase, GO sheet (composed of GOnPs) and GO-PCL nanofibrous scaffolds were fabricated by electrospinning method (chapter-3) and characterized (chapter-4) from the studies of SEM, TEM, structural, vibration spectroscopy (FTIR and Raman), mechanical and surface (contact angle, hydrophilicity and swelling behavior), properties and measurements of fiber diameter and pore size (discussed in chapter-4). It

has been shown that the addition of GOnPs in bioactive polymer PCL, enhances its conductivity (σ) and dielectric constant (ε) which in turn enriches biocompatibility of the GO-PCL composite scaffolds (with ~34% hydrophilicity, ~80% porosity and tensile strength ~3.99MPa) are suitable for skeletal muscle tissue regeneration. The GO-PCL composite showed maximum values of room temperature conductivity (σ) and dielectric permittivity (ε) at low (~0.79wt% GO) percolation threshold, which made this composite suitable for skeletal muscle TE applications .

In the second phase (chapter-5), possibility of using abundantly available cord blood derived mesenchymal stem cells for myoblast differentiation was explored. Cord blood derived stem cells were successfully proliferated and differentiated into skeletal myoblast cells (hSkMCs) on the electrospun fibrous mesh of GO-PCL composite and also on spin coated thin GO sheets. Compared to GO sheet as the control, GO-PCL electrospun scaffolds were found to exhibit enhanced myoblast differentiation and also promoted myotube formations similar to natural orientations. The addition of GO to PCL provided the necessary physicochemical and biological cues required for electro-responsive skeletal muscle tissue regeneration. Observing admirable biocompatibility of GO-PCL mesh for the future skeletal muscle tissue engineering applications, IGF-1 cell signalling pathway, which is related to myoblast differentiation and hypertrophy, was also studied with GO-PCL meshes. Up regulation of IGF-1 pathway molecules indicated better myogenic differential potential. Therefore, it was demonstrated that GO added electrospun GO-PCL composite meshes are highly prospective scaffolds for hMSCs proliferation and differentiation for skeletal muscle tissue regeneration.

In the third phase (chapter-6) efforts have been given to prepare and characterize GO-PLGA electrospun fibrous meshes similarly to the case of GO-PCL meshes. Morphological, structural and other characterizations of the GO-PLGA scaffolds have been made from the studies of XRD, SEM, FESEM, Raman, FTIR, mechanical property (tensile strength ~2.95MPa), contact angle (~130), biodegradation and hydrophilicity (~30%) behaviour. Moreover, electrical conductivity and dielectric constant (associated with surface charge) of the scaffolds were measured and percolation behaviour of the GO-PLGA composite meshes was investigated. Similar to the case of GO-PCL, GO-PLGA meshes were also found to be suitable for myoblast differentiation of cord blood derived

mesenchymal stem cells (chapter-7). Myoblast viability, proliferation and formation of myotubes were also verified by various biological characterizations. The analysis of aligned myotubes formation and expression of muscle specific proteins and genes were also observed elucidating the potentiality of this composite scaffold for TE applications. These results confirmed that GO-PLGA meshes are also found to be potential candidates for skeletal muscle tissue regeneration using cost effective and easily available hMSCs.

Interestingly, from the results of present investigations (discussed in chapters 5-7), it was revealed, for the first time, that though the novel GO-PCL and GO-PLGA composite meshes exhibited excellent myoblast proliferation potential, GO-PCL electrospun meshes showed better myogenic potential compared to those of GO-PLGA meshes. This might be due to the different chemical composition of the two different polymers and their interaction with the GO. Moreover, GO-PCL composite was found to be more conducting ($2.7x10^{-6}S/m^2$) (which is in favour of skeletal muscle regeneration) than the corresponding GO-PLGA ($2.8x10^{-7}S/m^2$) composite. The dielectric constant of the GO-PCL (ε ~300) composite (associated with surface charge of the composite, discussed in chapter 8) was also found to be higher than that of GO-PLGA (ε ~198) meshes indicating GO-PCL more appealing candidate (compared to GO-PLGA) for electro-responsive skeletal muscle TE application using hMSCs. In addition, unlike PLGA, the degradation of PCL does not release any toxic by-product (i.e. lactic acid and glycolic acid) thereby favouring enhanced biocompatibility of GO-PCL.

In the final phase (chapter-8), an attempt has also been made to explore the origin of biocompatibility of GO and GO polymer composites from the studies of some physical properties (i.e. electrical conductivity and dielectric constant related to GO surface charge) of GO and GO-polymer composites. Though PCL and PLGA are insulators (very low conductivity ~$2\text{-}5x10^{-9}S/m^2$), GO-polymer composites are much higher conducting compared to those of either pure polymer or GO itself. This was attributed to the contribution of GO surface charge and percolation behaviour exhibited by the GO-polymer composites, with the formation of nanoclusters that actually led to the enhancement of conductivity and better cellular interaction leading to boost the biocompatibility of GO-polymer composites. This conclusion was drawn from the study (chapter 8) of surface charge–voltage and current–voltage characteristics of GO sheet

and GO-polymer composite indicating the importance of GO surface charge (Q) for the enhancement of conductivity and dielectric constant of the composites. It was further concluded that the ionic bonds, the π-π* stacking forces created by the sp^2 bonding and hydrophobic interaction between molecules allowed graphene to adsorb proteins and low molecular weight chemicals that are adsorbed by GO surface affecting cells growth and proliferation which might also provide important supporting cues for the biocompatibility of GO and GO-Polymer meshes.

Overall, in this dissertation, it has been demonstrated that graphene oxide-polymer composites are excellent biocompatible scaffold materials suitable for the skeletal muscle tissue regeneration. Graphene oxide enhances the cellular behaviour, including attachment, proliferation, and even myoblast differentiation. The extraordinary properties, nanostructural features and surface charge jointly provide the necessary guiding environment for the admirable myoblast differentiation and oriented myotubes formation on the developed electrospun composite scaffolds. Among the derived scaffolds, GO-PCL was found to be the best showing superior scaffold properties and myoblast differential potential making it most favourable candidate which can be used as a template for the skeletal muscle tissue regeneration. Moreover, it was established that, as an alternative to bone marrow derived stem cells, the use of abundantly available human umbilical cord blood (commonly considered as a biological waste) derived mesenchymal stem cells would also be beneficial to develop tissue constructs in an economical and more efficient way.

It is finally concluded that development of such novel graphene oxide based composite scaffolds, GO-PCL in particular, might pave the way for their application for the next generation skeletal muscle regeneration by developing tissue grafts for clinical applications.

9.1. Future Scope of Research

In the present dissertation, we have confirmed excellent in-vitro biocompatibility and myogenic differentiation potential of GOnPs sheet, GO-PCL and GO-PLGA nanocomposite electrospun meshes using human cord blood derived mesenchymal stem cells.

The suggested future research study can be summarized as follows:

- In-vivo biocompatibility study using animal model.
- Biocompatible reduced graphene oxide (rGO), another derivative of graphene, might also form important rGO-polymer composite suitable for myoblast differentiation.
- Generation of skeletal muscle tissue constructs using bioreactor and its optimizations.
- Scale up of the fabrication of electrospun GO-PCL composite scaffold.
- Developing appropriate preservation strategies (such as cryopreservation) for long term storage of the developed constructs for future use.

Bibliography

[1] Hollister SJ. Porous scaffold design for tissue engineering.Nature Materials. 4: 518-24. 2005.

[2] Kamihira M. Recent Progress of Biochemical and Biomedical Engineering in Japan II (Advances in Biochemical Engineering/Biotechnology Vol. 91), Springer-Verlag ,Transgenic birds for the production of recombinant proteins (pp171～189),2004.06.

[3] Mc Keon KD, Flagg DH and Freeman JW.Coaxial electrospun poly(ε-caprolactone), multiwalled carbon nanotubes, and polyacrylic acid/polyvinyl alcohol scaffold for skeletal muscle tissue engineering. J. of Biomed.Mater. Res. Part A. 99: 493-499, 2011.

[4] Chaudhuri B, D Bhadra, L. Moroni and K Pramanik. Biocompatibility of electrospun graphene oxide–poly(ε-caprolactone) fibrous scaffolds with human cord blood mesenchymal stem cells derived skeletal myoblast. Materials Letters. 126: 109-112, 2014.

[5] Niomi M. Mechanical biocompatibility of titanium alloys for biomedical supplications.Journalof mechanical behavior of biomedical materials.1: 30-42, 2008.

[6] Freymann U, Petersen W and Kaps C. Cartilage regeneration revisited: entering of new one-step procedures for chondral cartilage repair. OA Orthopaedics,1:6, January 05,2013.

[7] Sun L,Wang X and Kaplan DL. A 3D cartilage — inflammatory cell culture system for the modelling of human osteoarthritis. Biomaterials. 32: 5581–5589, 2011.

[8] Kumbar SG, Nukavarapu SP, James R, Nair LS and Laurencin CT. Electrospun poly (lactic acid - co - glycolic acid) scaffolds for skin tissue engineering. Biomaterials.29: 4100-4107, 2008.

[9] Engelmayr GC Jr, Cheng M, Bettinger CJ, Borenstein JT, Langer R and Freed LE. Accoridan-like honeycombs for tissue engineering of cardiac anisotropy.Nature Materials.7: 1003-1010, 2008.

[10] Klumpp D, Horch Re, Kneser U and Beier JP. Chapter 17 - Skeletal muscle tissue engineering.issue Engineering Using Ceramics and Polymers (2nd Edition). 524-540, 2014.(Also See: Engineering skeletal muscle tissue-new perspectives in vitro and in vivo. J Cell. Mol. Med. 14: 26229-9, 2010.

[11] Cezar CA and Mooney DJ. Biomaterial-based delivery for skeletal muscle repair.Adv.Drug Deliv.Rev. 84:188-97, 2015.

[12] Vindigni V, Mazzoleni F, Rossini K, Fabbian M, Zanin ME, Bassetto F, and Carraro U. Reconstruction of ablated rat rectus abdominis by muscle regeneration.Plastic and Reconstructive Surgery.114: 1509-1515, 2004.

[13] Jarvinen TA, Jarvinen TN, Kääriäinen M, Kalimo H et al. Muscle injuries – biology and treatment. Am. J. Sports Med. 33:745–764, 2005.

[14] Rothenburger M, Volker W, Vischer JP, Berendes E, Glasmacher B, Scheld HH, and Deiwick M. Tissue engineering of heart valves: formation of a three-dimensional tissue using porcine heart valve cells. ASAIO Journal.48:586-591, 2002.

[15] Han S, Wang B, Jin W, Xiao Z, Li X, Ding W, Kapur M et al. The linear-ordered collagen scaffold-BDNF complex significantly promotes functional recovery after completely transacted spinal cord injury in canine. Biomaterials.41: 89-96, 2015.

[16] Mohammadi MS, Bureau MN, and SN. Chapter 11 - Polylactic acid (PLA) biomedical foams for tissue engineering. Biomedical Foams for Tissue Engineering Applications.313-334, 2014.

[17] Okamoto M, and John B. Synthetic biopolymer nanocomposites for tissue engineering scaffolds.Progress in Polymer Science. 38: 1487-1503, 2013.

[18] Xin X, Hussain M, and Mao JJ. Continuing differentiation of human mesenchymal stem cells and induced chondrogenic and osteogenic lineages in electrospun PLGA nanofiber scaffold.Biomaterials. 28: 316-325, 2007.

[19] Offeddu GS, Ashworth JC, Cameron RE, and Oyen ML. Multi-scale mechanical response of freeze-dried collagen scaffolds for tissue engineering applications.Journal of the Mechanical Behavior of Biomedical Materials. 42: 19-25, 2015.

[20] Bhardwaj N, and Kundu SC. Silk fibroin protein and chitosan polyelectrolyte complex porous scaffolds for tissue engineering applications.Carbohydrate Polymers.85: 325-333, 2011.

[21] Smart SK, Cassady AL, Lu GQ, and Martin DJ. The biocompatibility of carbon nanotubes.Carbon.44: 1034-47, 2006.

[22] Kalbacova M. Kalbac M, Dunsch L, and Hempel U. Influence of single walled carbon nanotube films on metabolic activity and adherence of human osteoblasts .Carbon. 45: 2266-72, 2007.

[23] Zhang D, Yi C, Qi S, Yao X, and Yang M. Effects of carbon nanotubes on the proliferation and differentiation of primary osteoblasts, Nanotechnology. 18: 475102-10, 2007.

[24] Fang L, and Liu Z. Graphene in Biomedicine: Opportunities and Challenges. Nanomedicine. 6:317-24,2011

[25] Kim H, Abdala AA, and Macosko CW. Graphene/polymer nanocomposites. Macromolecules. 43: 6515-6530, 2010.

[26] Balint R, Cassidy NJ, and Cartmell SH. Conductive polymers: Towards a smart biomaterial for tissue engineering.Acta Biomaterialia. 10: 2341-53, 2014.

[27] Choi JS,Lee SJ, Christ GJ, Atala A, and Yoo JJ.The influence of electrospun aligned poly(ε-caprolactone)/collagen nanofiber meshes on the formation of self-aligned skeletal muscle myotubes. Biomaterials. 29: 2899-2906, 2008.

[28] Chaudhuri B, Moroni L, Bhadra D, and Prakmanik K. Myoblast differentiation of human mesenchymal stem cells on graphene oxide and electrospun graphene oxide–polymer composite fibrous meshes: importance of graphene oxide conductivity and dielectric constant on their biocompatibility. Biofabrication.7: 015009 doi:10.1088/1758-5090/7/1/015009. 2015.

[29] Giannitelli SM, Accotob D, Trombettaa M, and Rainer A. Current trends in the design of scaffolds for computer-aided tissue engineering. ActaBiomaterialia.10: 580-94, 2014.

[30] Simion LL, O'Brien M, and Mashayekhi K. OA A clinical perspective to mesenchymal stem cell based musculoskeletal regeneration. Musculoskeletal Medicine.1: 8, 2013.

[31] Ryu TK, Oh MJ, Moon SK, Paik DH, Kim SE, Park JH, and Choi SW. Uniform tricalcium-phosphate beads with an open porous structure for tissue engineering. Colloids and Surfaces B: Biointerfaces. 112: 368-373, 2013.

[32] Sun W,Starly B, Nam J, and Darling A. Bio-CAD modelling and its applications in computer-aided tissue engineering.Computer-Aided Design.37: 1097-1114, 2005.

[33] Moroni L,de Wijn JR, and van Blitterswijk CA. Integrating novel technologies to fabricate smart scaffolds. J. of Biomaterials ci. Pol. Ed. 19: 534-572, 2008.

[34] Yoshida A, Chitcholtan K, Evans JJ, Nock V, and Beasley SW. In vitro tissue engineering of smooth muscle sheets with peristalsis using a murine induced pluripotent stem cell line. J. Pediatr Surg. 47: 329-335, 2012.

[35] Ferland DJ, Darios ES, and Watts SW. The persistence of active smooth muscle in the female rat cervix through pregnancy.American Journal of Obstetrics and Genecology. 212: 244e1-244e8, 2015.

[36] Wang M, Zhang G, Wang Y, Liu T, Zhang Y, An Y, and Li Y. Crosstalk of mesenchymal stem cells and macrophages promotes cardiac muscle repair. Int. J. of Biochem & Cell Biology. 58, 53-61, 2015

[37] Marieb EN. (2001). Human Anatomy and Physiology: Benjamin Cummings.(5th Edition).

[38] Wakelam MJ. The fusion of myoblasts.Biochemical Journal.228, 1-12, 1985.

[39] Marieb EN. Human Anatomy and Physiology: Benjamin Cummings.(5th Edition), 2001.

[40] Yin H, Price F, and Rudnicki MA. Satellite cells and the muscle stem cell niche. Physiol. Rev. 93: 23–67, 2013.

[41] Zheng Y, and Feng Y. From human embryonic and induced pluripotent stem cells to skeletal satellite cells for muscle dystrophies therapy. Journal of Reproduction and Contraception. 26: 53-60, 2015.

[42] Urciuolo A, Quarta M, Morbidoni V, Gattazzo F, Molon S, Grumati P et al. Collagen VI regulates satellite cell self-renewal and muscle regeneration. Nat. Commun. 4: 1964.doi: 10.1038/ncomms2964, 2013.

[43] Bentzinger CF, Wang YX, von Maltzahn J, Soleimani VD, Yin H, and Rudnicki MA. Fibronectin regulates Wnt7a signaling and satellite cell expansion. Stem Cell.12: 75–87, 2013.

[44] Gurtner GC, Werner S, Barrandon Y, and Longaker MT. Wound repair and regeneration. Nature. 453: 314-321, 2008.

[45] Bischoff R. Regeneration of single skeletal muscle fibers in vitro. The Anatomical Record. 182: 215-236, 1975.

[46] Boukpessi T, Menashi S, Camoin L, Tencate JM, Goldberg M, and Chaussain-Miller C. The effect of stromelysin-1 (MMP-3) on non-collagenous extracellular matrix proteins of demineralized dentin and the adhesive properties of restorative resins.Biomaterials. 29: 4367-4373, 2008.

[47] Bedair H, Liu TT, Kaar JL, Badlani S, Russell AJ, Li Y, and Huard J. Matrix metalloproteinase-1 therapy improves muscle healing. Journal of Applied Physiology. 102: 2338-2345, 2007.

[48] Wang W, Pan H, Murray K, Jefferson BS, and Li Y. Matrix Metalloproteinase-1 promotes muscle cell migration and differentiation. The American Journal of Pathology. 174: 541-549, 2009.

[49] Zammit PS, Partridge TA, and Yablonka-Reuveni Z. The skeletal muscle satellite cell: the stem cell that came in from the cold. Journal of Histochemistry and Cytochemistry. 54: 1177-1191, 2006.

[50] Zhang Z, Ortiz O, Goyal R, and Kohn J. Chapter 23 - Biodegradable Polymers.Principle of Tissue Engineering (4th Edition).441-473, 2014.

[51] Shin YC, Lee JH, Jin L, Kim MJ, Kim YJ, Hyun JK, Jung TG, Hong SW, and Han DW. Stimulated myoblast differentiation on graphene oxide-impregnated PLGA-collagen hybrid fiber matrices.Journal of Nanobiotechnology.13: 21 (DOI 10.1186/s12951-015-0081-9), 2015.

[52] Hosseinabadi ME, Ashrafizadeh F, Etemadifar M, and Venkatraman SS. Evaluating and Modeling the Mechanical Properties of the Prepared PLGA/nano-

BCP Composite Scaffolds for Bone.Tissue Engineering. Journal of Mat Sci and Technology.27: 1105-1112, 2011.

[53] Tian HC, Liu JQ, Wei DX, Kang XY, Zhang C, Du JC, Yang B et al. Graphene oxide doped conducting polymer nanocomposite film for electrode-tissue interface. Biomaterials. 35: 2120-2129, 2014.

[54] McNamara LE, Sjostrom T, Seunarine K, Meek RMD, Su Band Dalby MJ. Investigation of the limits of nanoscale filopodial interactions.Journal of Tissue Engineering. 5: 1-5, 2014.

[55] Liu Y, Yu D, Zeng C, Miao Z, and Dai L. Biocompatible graphene oxide-based glucose biosensors.Langmuir. 26: 6158-60, 2010.

[56] Akhavan O, Ghaderi E, and Emamy H. Nontoxic concentrations of PEGylated graphene nanoribbons for selective cancer cell imaging and photothermal therapy. Journal of Mater Chem. 22: 20626-33, 2012.

[57] Zhao H, Ji X, Wang B, Wang N, Li X, Ni R, and Ren J. An ultra-sensitive acetylcholinesterase biosensor based on reduced graphene oxide-Au nanoparticles-β-cyclodextrin/Prussian blue-chitosan nanocomposites for organophosphorus pesticides detection. Biosensors and Bioelectronics. 65: 23-30, 2015.

[58] Kalbacova M, Broz A, Kong J, and Kalbac M. Graphene substrates promote adherence of human osteoblasts and mesenchymal stromal cells. Carbon. 48: 4323-9, 2010.

[59] Ryoo SR, Kim YK, Kim MH, and Min DH. Behaviors of NIH-3T3 fibroblasts on graphene/carbon nanotubes: proliferation, focal adhesion, and gene transfection studies. ACS Nano. 4: 6587-98, 2010

[60] Nayak TR, Andersen H, Makam VS, Khaw C, Bae S, Xu X, Ee PL, Ahn JH, Hong BH, Pastorin G, and Özyilmaz B. Graphene for controlled and accelerated osteogenic differentiation of human mesenchymal stem cells. ACS Nano. 5: 4670-8, 2011

[61] Park SY, Park J, Sim SH, Sung MG, Kin KS, Hong BH, and Hong S. Enhanced differentiation of human neural stem cells into neurons on graphene.Adv Mater. 23: H 263-7, 2011.

[62] Chen GY, Pang DW, Hwang SM, Tuan HY, and Hu YC.A graphene-based platform for induced pluripotent stem cells culture and differentiation.Biomaterials. 33: 418-27, 2012.

[63] Thevi KJ,Saarani NN, Kadir MRA, and Hermawan H. Triple-layered PLGA/nanoapatite/lauric acid graded composite membrane for periodontal guided bone regeneration. Mat. Sci. Eng. C. 43: 253-63, 2014.

[64] Wan C, and Chen B.Poly(ε-caprolactone)/graphene oxide biocomposites: mechanical properties and bioactivity. Biomed.Mater.6: 055010-8, 2011.

[65] Zhao X, Zhang Q, and Chen D. Enhanced Mechanical Properties of Graphene-Based Poly(vinyl alcohol) Composites. Macromolecules. 43: 2357-63, 2010.

[66] Vadukumpully S, Paul J, Mahanta N, and Valiyaveettil S. Flexible conductive graphene/poly(vinyl chloride) composite thin films with high mechanical strength and thermal stability. Carbon. 49: 198-205, 2011.

[67] Ku SH, and Park CB. Myoblast differentiation on graphene oxide.Biomaterials. 34: 2017-23, 2013.

[68] Grounds MD. Towards understanding skeletal muscle regeneration.Pathol. Res. Pract. 187: 1-22, 1991.

[69] Grounds MD, White JD, Rosenthal N, and Bogoyevitch MA. The role of stem cells in skeletal and cardiac muscle repair.J. Histochem. Cytochem.50: 589-610, 2002.

[70] Peter GA, Heidi RH, Karen LC, and Rocky ST. Chapter 54 - Mesenchymal Stem Cells in Musculoskeletal Tissue Engineering. Principles of Tissue Engineering (4th Edition).1171-1199, 2014.

[71] Murray E, Thompson BC, Sayyar S, and Wallace GG. Enzymatic degradation of graphene/polycaprolactone materials for tissue engineering.Polymer Degradation and Stability. 111: 71-77, 2015.

[72] Anon, E., X. Serra-Picamal, P. Hersen, N.C. Gauthier, M.P. Sheetz, X. Trepat, and B. Ladoux. Cell crawling mediates collective cell migration to close undamaged epithelial gaps. Proc. Natl. Acad. Sci. U S A. 109:10891-10896. 2012.

[73] Zhou M, Zhai YM, and Dong SJ. Electrochemical sensing and biosensing platform based on chemically reduced graphene oxide.Anal . Chem.81:5603-5613, 2009.

[74] Danby R, and Rocha V.Chapter 7 – Clinical Use of Umbilical Cord Blood Cells. Cord Blood Stem Cells and Regenerative Medicine. 77-100, 2015.

[75] Christopher JB, Bruggeman JP, Misra A, Borenstein JT, and Langur R. Biocompatibility of biodegradable semiconducting melanin films for nerve tissue engineering.Biomaterials. 30: 3050-7, 2009.

[76] Chandy T. Chapter 11 – Biocompatibility of materials and its relevance to drug delivery and tissue engineering. Biointegration of Medical Implant Materials Science and Design.301-325, 2010.

[77] Stoll GH, Nimmerfall F, Acemoglu M, Bodmer D, Bantle S, Müller I, Mahl A, Kolopp M, and Tullberg K. Poly(ethylene carbonate)s, part II-1: degradation mechanisms and parenteral delivery of bioactive agents. Journal of Controlled Release. 76: 209-25, 2001.

[78] Janvikul W, Uppanan P, Thavornyutikarn B, Kosorn W, and Kaewkong P. Effects of surface topography, hydrophilicity and chemistry of surface-treated PCL

scaffolds on chondrocyte infiltration and ECM production. Procedia Engineering.59: 158-165, 2013.

[79] Kim K, Yu M, Zong X, Chiu J, Fang D, Seo YS, Hsiao BS, Chu B, and Hadjiargyrou M. Control of degradation rate and hydrophilicity in electrospun non-woven poly(d,l-lactide) nanofiber scaffolds for biomedical applications. Biomaterials. 24: 4977-4985, 2003.

[80] Wu F, Liu C, Neill BO, Wei J, and Ngothai Y. Fabrication and properties of porous scaffold of magnesium phosphate/polycaprolactone biocomposite for bone tissue engineering. Appl. Surface Sci. 258: 7589-7595, 2012.

[81] Mozafari M, Mehraien M, Vashaee D, and Tayebi L. Electroconducting nanocomposite scaffold: A new strategy into tissue engineering and regenerative medicine. Nanocomposites-new trend and development. Ed. By Ebrahimi F. IBSN 978-953-51-07620, 2012.

[82] Rivers TJ, Hudson TW, and Schmidt CE. Synthesis of a novel, biodegradable electrically conducting polymer for biomedical applications.Adv.Funct. Mater.12:33-37, 2002.

[83] Kai D, Prabhakaran MP, Jin G, and Ramkrishna S. Biocompatibility evaluation of electrically conductive nanofibrous scaffolds for cardiac tissue engineering. Journal Mat Chem B: 1: 2305-14, 2013.

[84] Chen MC, Sun YC, and Chen YH. Electrically conductive nanofibers with highly oriented structures and their potential application in skeletal muscle tissue engineering.Acta Biomaterialia. 9:5562-72, 2013.

[85] McKeon KD, DH Flagg, and JW Freeman. Coaxial electrospun poly(ε-caprolactone), multiwalled carbon nanotubes, and polyacrylic acid/polyvinyl alcohol scaffold for skeletal muscle tissue engineering.Journal Biomed.Mater. Res. A. 99: 493-499, 2011.

[86] Sanigrahi J, Bhadra D, and Chaudhuri BK. Crystalline graphite oxide/PVDF nanocomposite gate dielectric: Low-voltage and high field effect mobility thin-film transistor. Phys. Status Solidi.210: 546-552, 2012.

[87] Gaharwar AK, Peppas NA, and Khademhosseini A. Nanocomposite hydrogels for biomedical applications. Biotech.& Bioengg. 111, 441-453, 2014.

[88] Marcia T, Carvalho PP, Gomes ME, and Reis RL. Chapter 11 - Biomaterials in Preclinical Approaches for Engineering Skeletal Tissues.Translational Regenerative Medicine.127-139, 2015.

[89] Croll TI, Oconnor AJ, Stvens GW, and White JC. Controllable Surface Modification of Poly(lactic-co-glycolic acid) (PLGA) by Hydrolysis or Aminolysis I: Physical, Chemical, and Theoretical Aspects. Biomacromol.5: 463-473, 2004

[90] Li D, Wang Y, and Xia Y. Electrospinning of polymeric and ceramic nanofibers as uniaxially aligned arrays. Nano Lett. 3: 1167–71, 2003.

[91] Tang X, Thankappan SK, Lee P, Fard SE, Harmon MD, Tran K, and Yu X. Chapter 21 - Polymeric Biomaterials in Tissue Engineering and Regenerative Medicine. Natural and Synthetic Biomedical Polymers.351-371, 2014.

[92] Neffe AT , Julich Grunter KK, and Lendlein AI. Chapter 4 - Combinations of biopolymers and synthetic polymers for bone regeneration. Biomaterials for Bone Regeneration.87-110, 2014.

[93] Li H, and Chang J. Preparation and characterization of bioactive and biodegradable Wollastonite/poly(D,Llactic acid) composite scaffolds. Journal of Materials Science: Materials in Medicine. 15: 1089–1095, 2004.

[94] Kokubo T. Apatite formation on surfaces of ceramics, metals and polymers in body environment. Acta Materialia. 46: 2519–2527, 1998.

[95] Wang M. Developing bioactive composite materials for tissue replacement.Biomaterials. 24: 2133–2151, 2003.

[96] Kothapalli CR, Shaw MT, and Wei M. Biodegradable HA-PLA 3-D porous scaffolds: Effect of nano-sized filler content on scaffold properties. Acta Biomaterialia. 1: 653–662, 2005.

[97] Ravichandran R, Sundarrajan S, Venugopal JR, Mukherjee S, and Ramakrishna S. Application of conducting polymers and their issues in biomedical engineering.Journal of Royal Soc. Interface.7: S559-S579, 2010.

[98] Billiet T, Vandenhaute M, Schelfhout J, Van Vlierberghe S, and Dubruel P. A review of trends and limitations in hydrogel-rapid prototyping for tissue engineering.Biomaterials. 33: 6020-6041, 2012.

[99] Flaibani M, and Elvassore N. Gas anti-solvent precipitation assisted salt leaching for generation of micro- and nano-porous wall in biopolymeric 3D scaffolds. Mat. Sci. Engg. C. 32: 1623-39, 2012.

[100] Nie L, Chen D, Suo J, Zou P, Feng S, Yang Q, Yang S, and Ye S. Physicochemical characterization and biocompatibility in vitro of biphasic calcium phosphate/polyvinyl alcohol scaffolds prepared by freeze-drying method for bone tissue engineering applications. Colloids and Surfaces B: Biointerfaces. 100: 169-176, 2012.

[101] Ho MH, Kuo PY, Hsieh HJ, Hsien TY, Hou LT, Lai JY, and Wang DM. Preparation of porous scaffolds by using freeze-extraction and freeze-gelation methods.Biomaterials.25, 129-138, 2004.

[102] Tabata Y. Biomaterial technology for tissue engineering applications. J. R. Soc. Interface. 6: S311–S324, 2009.

[103] Bhardwaj N, and Kundu SC. Electrospinning: A fascinating fiber fabrication technique. Biotechnology Advances. 28: 325-47, 2010.

[104] Lee JW, Serna F, Nickels J, and Schmidt CE. Carboxylic acid-functionalized conductive polypyrrole as a bioactive platform for cell adhesion.Biomacromolecules. 7: 1692–5, 2006.

[105] Hou Q Grijpma DW, and Feijen J porous polymeric structure for tissue engineering prepaed by a quagulation ,compression molding and solt leaching technique. Biomateial. 24:1937-1947,2003.

[106] Li J, and Mak AF. Transfer of collagen coating from porogen o scaffold: collagen coating with PLGA scaffold .Composite. Part B:Engg.38:317-323 ,2007

[107] Quin L, and Zhang H. conrol freezing and freeze dryin:A versatile route for porous and micro/nanostructurematerials. J Chm. Tech bio tech. 86:172-184, 2011]

[108] Tsai AP, Ho MH, Wang AM, Liu CE, Hsieh CH, Tseng HC, and Hsieh HJ. Analysis of freeze gelation and crosslinking processes for preparing porous chitosan scaffolds. Carbohydrate Polymers. 67:124-132, 2007]

[109] Chen PH,Kuo TY, Kuo JY, Tseng YP, Wang DM, Lai JY, and Hsieh HJ et al. Novel Chitosan Pectin composite membranes with enhanced strength, hydrophilicity and controllable disintegration. Carbohydrate Polymers. 82:1236-1242,2010.

[110] Caplan AI, and Bruder SP. Mesenchymal stem cells: building blocks for molecular medicine in the 21st century. Trends in Mol. Med. 7:259-264, 2001.

[111] Odorico JS, Kaufman DS, and Thomson JA. Multilineage differentiation from human embryonic stem cell lines.Stem Cells. 19: 193-204, 2001.

[112] Fuller B, and Paynter S. Fundamentals of cryobiology in reproductive medicine.Reproductive BioMedicine Online.9: 680-691, 2004.

[113] Fuller BJ. Cryoprotectants: the essential antifreezes to protect life in the frozen state. CryoLetters. 25: 375-388, 2004.

[114] Woelders H,and Chaveiro A. Theoretical prediction of 'optimal'freezing programmes.Cryobiology.49:258-271. 2004

[115] Wharton DA, Gordon G, and Craig JM.Freezing survival and cryoprotective dehydration as cold tolerance mechanisms in the Antarctic nematode Panagrolaimus davidi.Journal of experimental biology.206; 215-221, 2003.

[116] Sahagian ME, and Douglas GH.Fundamental aspects of the freezing process.Food Science And Technology-New York-Marcel Dekker, 1-50. 1996

[117] Mazur P, and Ulrich S. Osmotic responses of preimplantation mouse and bovine embryos and their cryobiological implications.Cell biophysics. 8: 259-285, 1986.

[118] McGrath JJ, Cravalho EG, and Huggins CE.An experimental comparison of intracellular ice formation and freeze-thaw survival of HeLa S-3 cells.Cryobiology. 6: 540-550, 1975.

[119] Miller RH, and Peter M. Survival of frozen-thawed human red cells as a function of cooling and warming velocities.Cryobiology. 13: 404-414, 1976

[120] Karlsson JO,and Toner M. Long-term storage of tissues by cryopreservation: critical issues.Biomaterials. 17: 243-256, 1996.

[121] Massip A, Mermillod P, and Dinnyes A. Morphology and biochemistry of in-vitro produced bovine embryos: implications for their cryopreservation. Human Reproduction. 10: 3004-3011, 1995.

[122] Gadea J, Molla M, Selles E, Marco MA, Garcia-Vazquez FA, and Gardon JC. Reduced glutathione content in human sperm is decreased after cryopreservation: Effect of the addition of reduced glutathione to the freezing and thawing extenders. Cryobiology.62:40-46, 2011.

[123] Rozman-Pungercar J, Kopitar-Jerala N, Bogyo M, Turk D, Vasiljeva O, Stefe I, Vandenabeele P, Brömme D, Puizdar V, Fonović M, Trstenjak-Prebanda M, Dolenc I, Turk V, and Turk B. Inhibition of papain-like cysteine proteases and legumain by caspase-specific inhibitors: when reaction mechanism is more important than specificity. Cell Death & Differentiation.10: 881-888, 2003.

[124] Ferrusola CO. Fernandez L, Salazer SC, Macias GB, Rodrique MH, Tapia JA, and Pena FJ. Inhibition of the mitochondrial permeability transition pore reduces “apoptosis like” changes during cryopreservation of stallion spermatozoa. Theriogenology. 74: 458-465, 2010.

[125] Hunt CJ. Cryopreservation of human stem cells for clinical application: a review. Transfusion Medicine and Hemotherapy. 38:107-123, 2011.

[126] Balachandran H. Optimization Of Methods For In-vitro Expansion And Cryopreservation Of Mammalian Stem Cells. Umi-uta-1320.pdf(6.233MB)or URI http/hdl.handle.net/10106/526,, 2007.

[127] Benson EE.Cryopreservation theory. Plant Cryopreservation: A Practical Guide, p. 15-32.2008.

[128] Lee SB, Kim YH, Chong MS, Hong SH, and Lee YM. Study of genatin coated artificial skin: fabrication of gelatine scaffolds by saly leaching method. Biomaterials. 26: 1961-68, 2005.

[129] Le Bl, and Ringdén O. Immunomodulation by mesenchymal stem Cells and clinical experience. J. Int. Med. 262: 509-525, 2007.

[130] Penn MS. Importance of the SDF-1:CXCR4 axis in myocardial repair. Circ. Res. 104: 1133–35, 2009.

[131] Tidball JG.Inflammatory cell response to acute muscle injury.Med. Sci. Sports Exercise. 27: 1022-32, 1995.

[132] Tao XR, Li WL, Su J, Jin CX, Wang XM, Li JX, Hu JK, Xiang ZH, Lau JT, and Hu YP. Clonal mesenchymal stem cells derived from human bone marrow can differentiate into hepatocyte-like cells in injured livers of SCID mice. Journal Cellul.Biochem. 108: 693–704, 2009.

[133] Beiner JM, and Jokl P. Muscle contusion injuries: current treatment options. J Am Acad. Orthop Surg. 9: 227-237, 2001.

[134] Lee MH, Arcidiacono JA, Bilek AM, Wille JJ, Hamill CA, Wonnacott KM, Wells MA, and Oh SS. Considerations for tissueengineered and regenerative medicine product development prior to clinical trials in the United States. Tissue Engg.Part B Rev. 16: 41, 2009.

[135] Robert MN. Regenerative medicine: the emergence of an industry. J. Royal. Soc. Interface. 7: S771–S775, 2010.

[136] Bian W, and Bursac N. Tissue engineering of functional skeletal muscle: challenges and recent advances. IEEE Eng. Med. Biol. Mag. 27, 109-113, 2008.

[137] Juhas M, and Bursac N.Engineering skeletal muscle repair.Current Opinion in Biotechnology. 24: 880–886, 2013.

[138] Jones BJ, Brooke G, Atkinson K, and McTaggart SJ. Immunosuppressant by placental indoleamine 2,3- dioxygenase: a role for mesenchymal stem cells. Placenta. 28: 1174–81, 2007.

[139] Lysaght MJ, and Hazlehurst AL. Tissue engineering: the end of the beginning. Tissue Engineering. 10: 309-20, 2004.

[140] Jaklenec A, Stamp A, Deweerd E, Sherwin A, and Langer R. Progress in the Tissue Engineering and Stem Cell Industry ‘‘Are we there yet?’’. Tissue Engineering Part B. 18, 155-167, 2012.

[141] Nerem RM. Regenerative medicine: the emergence of an industry. J. R. Soc. Interface 7 Suppl. 6: S771, 2010.

[142] Mason C, Brindley DA, Culme-Seymour EJ, and Davie NL. Cell therapy industry: billion dollar global business with unlimited potential. Regen. Med. 6, 265-272, 2011.

[143] Mason C,and Manzotti E. Regenerative medicine cell therapies: numbers of units manufactured and patients treated between 1988 and 2010. Regen Med. 5: 307-313, 2010.

[144] Lonza R, Langer R, andVacanti J.The Growth of Tissue Engineering.The Tissue-Engineering Industry (chapter-84).Principles of Tissue Engineering, (3rdEdition).1266-1270.2007.

[145] Lysaght MJ, and Reyce J. The growth of tissue engineering.Tissue Engineering. 7: 485-493, 2001.

[146] Johnson PC, Bertram TA, Tawil B, and Hellman KB. Hurdles in tissue engineering/regenerative medicine product commercialization: a survey of North American academia and industry. Tissue Engg. Part A. 17: 5-15. 2011.

[147] Rizzi R, Bearzi C, Mauretti A, Bernardini S, Cannata S and Gargioli C. Tissue engineering for skeletal muscle regeneration. Muscles Ligaments Tendons J. 2: 230-234, 2012.

[148] Koffler J, Kaufman-Francis K, Shandalov Y, Egozi D, Pavlov DA, Landesberg A, and Levenberg S. Improved vascular organization enhances functional integration of engineered skeletal muscle grafts. Proc. Natl. Acad. Sci. U.S.A. 108, 14789–14794 10.1073/pnas.1017825108 , 2011.

[149] Carosio S, Barberi L, Rizzuto E, Nicoletti C, Del Prete Z, and Musarò A. Generation of ex vivo-vascularized Muscle Engineered Tissue (X-MET). Scientific Reports. 3: 1420, 2013.

[150] Grayson WL, Martens TP, Eng GM, Radisic M, and Novakovic GV.Biomimetic approach to tissue engineering.Semin. Cell Dev. Biol. 20: 665–673, 2009.

[151] Moresi V, Pristerà A, Scicchitano BM, Molinaro M, Teodori L, Sassoon D, Adamo S, and Coletti D. Tumor necrosis factor-alpha inhibition of skeletal muscle regeneration is mediated by a caspase-dependent stem cell response. Stem Cells.26, 997–1008, 2008.

[152] Musarò A, Giacinti C, Pelosi L, Dobrowolny G, Barberi L, Nardis C, Coletti D, Scicchitano BM, Adamo S, and Molinaro M. Stem cell-mediated muscle regeneration and repair in aging and neuromuscular diseases. Eur. J. Histochem. 51(Suppl 1): 35–43, 2007.

[153] Sharples AP, Player DJ, Martin NR, Mudera V, Stewart CE, and Lewis MP. Modelling in vivo skeletal muscle ageing in vitro using three-dimensional bioengineered c onstructs.Aging Cell.11: 986–995, 2012.

[154] Moresi V, Garcia-Alvarez G, Pristerà A, Rizzuto E, Albertini MC, Rocchi M, Marazzi G, Sassoon D, Adamo S, and Coletti D. Modulation of caspase activity regulates skeletal muscle regeneration and function in response to vasopressin and tumor necrosis factor. PLOS ONE.4: e5570 10.1371, 2009.

[155] Perniconi B, Costa A, Aulino P, Teodori L, Adamo S, and Coletti D. The pro-myogenic environment provided by whole organ scale acellular scaffolds from skeletal muscle. Biomaterials. 32: 7870–82, 2011.

[156] Rossi CA, Pozzobon M, and De Coppi P. Advances in musculoskeletal tissue engineering: moving towards therapy. Organogenesis. 6: 167–172, 2010.

[157] Charge SBP and Rudnicki M A. Cellular and molecular regulation of muscle regeneration.Physiological Reviews.84: 209-238, 2004.

[158] Tatsumi R, Anderson JE, Nevoret C J, Halevy O, and Allen RE.HGF/SF is present in normal adult skeletal muscle and is capable of activating satellite cells. Developmental Biology.194: 114-28, 1998.

[159] Yablonka-Reuveni Z, Rivera A J. Influence of PDGF-BB on proliferation and transition through the MyoD-myogenin-MEF2A expression program during myogenesis in mouse myoblasts. Growth Factors 15: 1-27,1007.

[160] Graves DC and Yablonka-Reuveni Z.Vascular smooth muscle cells spontaneously adopt a skeletal muscle phenotype: a unique Myf5(-)/MyoD(+) myogenic program. J. Histochem. Cytochem.48: 1173-93, 2000.

[161] Lanza R, Langer R and Vacanti JP.Principles of tissue engineering. Amsterdam, the Netherlands: Elsevier Academic Press, 2007.

[162] Khademhosseini A, Vacanti J, Langer R. Next generation tissue constructs and challenges to clinical practice. Sci. America. 300: 64-71, 2009.

[163] Sun W and Lal P. Recent development on computer aided tissue engineering - a review. Comp. Metho. Prog.Biomed.67: 85–103, 2002.

[164] Mulder ELW.de, Buma P, and Hannink GJ. Anisotropic porous biodegradable scaffold for skeletal muscle regeneration.Materials. 2: 1674-96, 2009.

[165] Moroni L, Wijna JR. de, and Blitterswijk CA van. 3D fiber-deposited scaffolds for tissue engineering: Influence of pores geometry and architecture on dynamic mechanical properties. Biomaterials.27: 974-985, 2006.

[166] Yan X, and Gu P. A review of rapid prototyping technologies and systems.Computer Aided Design. 28: 307-318, 1996.

[167] Mondrinos MJ, Dembzynski R, Lu L, Byrapogu VK, Wootton DM, Lelkes PI, and Zhou J. Porogen based solid freeform fabrication of polycaprolactone-calcium phosphate scaffolds for tissue engineering. Biomaterials.27: 4399-4408, 2006.

[168] Miot S1, Woodfield T, Daniels AU, Suetterlin R, Peterschmitt I, Heberer M, van Blitterswijk CA, Riesle J, and Martin I. Effects of scaffold composition and architecture on human nasal chondrocyte redifferentiation and cartilaginous matrix deposition. Biomaterials.26: 2479-2489, 2005.

[169] Benya PD and Shaffer JD. Dedifferentiated chondrocytes reexpress the differentiated collagen phenotype when cultured in agarose gels. Cell. 30: 215-224, 1982.

[170] Yeong WY, Chua CK, Leong KF, and Chandrasekaran M. Rapid prototyping in tissue engineering: challenges and potential. Trends in Biotechnology.22: 643-652, 2004.

[171] Leong KF, Cheah CM, and Chua CK. Solid freeform fabrication of three-dimensional scaffolds for engineering replacements tissues and organs.Biomaterials.24: 2363-2378, 2003.

[172] Mikos AG, Lyman MD, Freed LE, and Langer R. Wetting of poly [l-Lactic acid) and poly (DL-lactic acid co-glycolic acid) foams for tissue culture. Biomaterials. 15: 55-58, 1994.

[173] Mooney DJ, Kaufmann PM, Sano K, McNamara KM, Vacanti JP, and Langer R. Transplantation of hepatocytes using porous, biodegradable sponges.Transpl. Proc. 26: 3425-3426, 1994.

[174] Hsu YY, Gresser JD, Trantolo DJ, Lyons CM, Gangadharam PR, and Wise DL. Effect of polymer foam morphology and density on kinetics of in vitro controlled release of isoniazid from compressed foam matrices. J. Miomed. Mater.Res. 35: 107-116, 1997.

[175] Hua FJ, Kim GE, Lee JD, Son YK, and Lee DS. Macroporous scaffold by liquid liquid phase separation of a PLLA dioxane water system. J. Biomed. Mat. Res. 63: 161-167, 2000.

[176] Lo H, Ponticiello MS, and Leong KW. Fabrication of controlled release biodegradable foams by phase separation.Tissue Eng. 1: 15-28, 1995.

[177] Oh SH, Kang SG, and Lee JH.Degradation behaviour of hydrophilized PLGA scaffold prepared by melt –modelling particulate-leaching.J. Mat. Sc. Med. 17: 131-137,2006.

[178] Hutmacher DW, Goh JC, and Teoh SH.An introduction to Biodegradable Materials for Tissue Engineering Application.Ann. Acad. Med. Singapore. 30: 183-191, 2001a.

[179] Sun YC, and Chen YH. Electrically conductive nanofibers with highly oriented structures and their potential application in skeletal muscle tissue engineering.ActaBiomaterialia.9: 5562-5572, 2013.

[180] Vandenburgh HH, Karlisch P, and Farr L.Maintenance of highly contractile tissue-cultured avian skeletal myotubes in collagen gel.In Vitro Cell.Dev. Biol. 24: 166–174, 1988.

[181] Huang YC, Dennis RG, Larkin L, and Baar K. Rapid formation of functional muscle in vitro using fibrin gels. J App Phys. 98: 706-713, 2005.

[182] Huang NF, Patel S, Thakar RG, Wu J, Hsiao BS, Chu B, Lee RJ,and Li S. Myotube assembly on nanofibrous and micropatterned polymers. Nano Letters. 6: 537-542, 2006.

[183] Lam MT, Huang YC, Birla RK, and Takayama S. Microfeature guided skeletal muscle tissue engineering for highly organised 3-dimensional free-standing constructs. Biomaterials. 30: 1150-1155, 2009.

[184] Dennis RG, and Kosnik PE 2nd. Excitable and isometric contractile properties of mammalian skeletal muscle constructs engineered in-vitro. In Vitro Cell Dev. Biol. Anim. 36:327-335, 2000.

[185] Engler AJ, Griffin MA, Sen S, Bönnemann CG, Sweeney HL, and Discher DE. Myotubes differentiate optimally on substrates with tissue-like stiffness: pathological implications for soft or stiff microenvironments. J. Cell Biol. 166: 877–887, 2004a.

[186] Engler AJ, Richard L, Wong J, Picart C, and Discher DE. Surface probe measurements of the elasticity of sectioned tissue, thin gels and polyelectrolyte multilayer films: correlations between substrate stiffness and cell adhesion. Surf.Sci. 570, 142–154, 2004b.

[187] Ren K, Crouzier T, Roy C, and Picart C. Polyelectrolyte Multilayer Films of Controlled Stiffness Modulate Myoblast Cell Differentiation. Adv. Funct. Mater.18: 1378–89, 2008.

[188] Levy-Mishali M, Zoldan J, and Levenberg S. Effect of scaffold stiffness on myoblast differentiation.Tissue Engg. Part A. 15, 15–935, 2009.

[189] Powell CA, Smiley BL, Mills J, and Vandenburgh HH. Mechanical stimulation improves tissue-engineered human skeletal muscle. American J. Physiol Cell Physiol.283: C1557-C1565, 2002.

[190] Aviss KJ, Gough JE, and Downes S. Aligned electrospun polymer fibers for skeletal muscle regeneration. Polymer fibers for skeletal muscle regeneration.European Cells and Materials. 19, 193-204,2010.

[191] Riboldi S A, Sampaolesi M, Neuenschwander P, Cossu G, and Mantero S. Electrospun degradable polyesterurethane membranes: potential scaffolds for skeletal muscle tissue engineering. Biomaterials.26: 4606- 4615, 2005.

[192] Bashur CA, Dahlgren LA, and Goldstein AS. Effect of fiber diameter and orientation on fibroblast morphology and proliferation on electrospun poly(D,L-lactic-coglycolic acid) meshes. Biomaterials. 27: 5681-5688,2006.

[193] Dalby M J, Childs S, Riechle MO, Johnstone HJH, Affrossman S, and Curtis ASG. Fibroblast reaction to island topography: changes in cytoskeleton and morphology with time. Biomaterials 24: 927-935,2003.

[194] Bray M-A, Sheehy SP, and Parker KK. Sarcomere alignment is regulated by myocyte shape. Cell Motil Cytoskel. 65: 641-651,2003.

[195] Schiaffino S and Partridge T. Skeletal Muscle Repair and Regeneration, Advances in Muscle Research, Vol 3. Springer Netherlands, Dordrecht, 2008.

[196] Subbiah T, Bhat G S, and Tock R W, Parameswaran S, and Ramkumar SS. Electrospinning of nanofibers.J. Appl. Polym.Sci. 96: 557-569,2004.

[197] Bian W and Bursac N. Engineered skeletal muscle tissue networks with controllable architecture. Biomaterials. 30: 1401-1412,2009.

[198] Blackwood KA, McKean R, Canton I, Freeman CO, Franklin KL, Cole D, Brook I, Farthing P, Rimmer S, and Haycock JW. Development of biodegradable electrospun scaffolds for dermal replacement. Biomaterials.29: 3091-3104,2008.

[199] Wang HB, Mullins ME, Cregg JM, Hurtado A, Oudega M, Trombley MT, and Gilbert RJ. Creation of highly aligned electrospun poly-L-lactide acid fibers for nerve regeneration applications. J NerualEng.**6**: 016001 (15pp), 2009.

[200] Singh L, Kumar V, and Ratner BD. Generation of porous microcellular 85/15 poly(DL-lactide-co-glycolide) foams for biomedical applications. Biomaterials 25: 2611- 2617,2004.

[201] Levenberg S, Rouwkema J, Macdonald M, Garfein ES, Kohane DS, Darland DC, Marini R, Van Blitterswijk CA, Mulligan RC, and D'Amore PA. Engineering vascularised skeletal muscle tissue. Nat Biotechnol. 23: 879-884,2005.

[202] Cooper S T, Maxwell A L, Kizana E, Ghoddusi M, Hardeman E C, Alexander I E, Allen D G, and North KN. C2C12 co-culture on a fibroblast substratum enables sustained survival of contractile, highly differentiated myotubes with peripheral nuclei and adult fast myosin expression. Cell MotilCytoskel. 58. 200-211,2004.

[203] Levi-Mishali M, Zoldan J, and Levenberg S. Effect of scaffold stiffness on myoblast differentiation. Tissue Engg. 15: 935-944.2009.

[204] Stankovich S, Piner RD, Nguyen ST, and Ruoff RS. Synthesis and exfoliation of isocyanate-treated graphene oxide nanoplatelets.Carbon. 44: 3342-3347, 2006.

[205] Farokhzad OC, and Langer R. Impact of nanotechnology on drug delivery. ACS Nano. 3, 16-20, 2009.

[206] Feng L, and Liu Z. Graphene in Biomedicine: Opportunities and Challenges. Nanomedicine.6: 317-24, 2011.

[207] Ryu S, and Kim BS. Culture of neural cells and stem cells on graphene.Tissue Engineering and Regenerative Medicine.10: 39-46, 2013.

[208] Wheeler SE.Understanding substituent effects in noncovalent interactions involving aromatic rings.Acc. Chem. Res. 46: 1029-1038, 2013.

[209] Utesch T, Daminelli G, and Mroginski MA.Molecular dynamics simulations of the adsorption of bone morphogenetic protein-2 on surfaces with medical relevance.Langmuir. 27: 13144–13153, 2011.

[210] Wang K, Ruan J, Song H, Zhang J, Wo Y, Guo S, and Chi D. Biocompatibility of graphene oxide. Nanoscale Res.Lett.6: 1. 2011.

[211] Yang X, Li L, Shang S, and Tao X. Synthesis and characterization of layer-aligned poly(vinyl alcohol)/graphene nanocomposites. Polymer. 51: 3431-3435, 2010.

[212] Novoselov KS, Geim AK, Morozov SV, Jiang D, Zhang Y, Dubonos SV, Grigorieva IV, and Firsov AA. Electric field effect in atomically thin carbon films. Science. 306: 666-70, 2004.

[213] Wang JW, Shen QD, Bao HM, Yang CZ, and Zhang QM. Microstructure and dielectric properties of P(VDF-TrFE-CEF) with partially grafted copper phthalocyanine oligomer. Macromolecules.38: 2247-52, 2005.

[214] Bhadra D, Ph.D. Thesis , Calcutta University, Calcutta. Study of Improved Dielectric Properties of some Technological important flexible oxide-polymer composites. 2015.

[215] Chen G, Ushida T, and Tateishi T. Scaffold design for tissue engineering.Macromol.Bioscience.2: 67-77, 2002.

[216] Sabir ML, Xu X, and Li L. A review of biodegradable polymeric materials for bone tissue engineering applications. J. Mat. Sci. 44:5713-24, 2009.

[217] Yan X, Chen J, Yang J, Xue Q, and Miele P. Fabrication of free-standing, electrochemically active, and biocompatible graphene oxide-polyaniline and graphene-polyaniline hybrid papers. ACS Appl. Mater Interfaces. 9: 2521-29, 2010.

[218] Baker SC, Rohman G, Southgate J, and Cameron NR. The relationship between the mechanical properties and cell behavior of PLGA and PCL scaffolds for blended tissue engineering. Biomaterials.30: 1321-1326, 2009.

[219] Yoon OJ, Jung CY, Sohn Y, Kim HJ, Hong B. Jhon MS, and Lee NE. Nanocomposite nanofibers of Poly (D, L-lacto-co-glycolic acid) and graphene oxide nanosheets. Composites Part A. 42: 1978-1984, 2011.

[220] Markovic ZM, Harhaji-Trajkovic LM, Todorovic-Markovic BM, Kepić DP, Arsikin KM, and Jovanović SP. In vitro comparison of thephotothermal anticancer activity of graphene nanoparticles and carbon nanotubes. Biomaterials.32: 1121-1129, 2011.

[221] Sebaa M, Nguyen TY, Paul RK, Mulchandani A, and Liu H. Graphene and carbon nanotube–graphene hybrid nanomaterials for human embryonic stem cell culture. Materials Lett.92: 122-125, 2013.

[222] Hu H, Ni Y, Montana V, Haddon RC, and Parpura V. Chemically functionalized carbon nanotubes as substrates for neuronal growth. Nano Letts. 4: 507-11, 2004.

[223] Malarkey EB, Fisher KA, Bekyarova E, Liu W, Haddon RC, and Parpura V. Conductive single walled carbon nanotubes modulate neural growth. Nano Letts.9: 264-268, 2009.

[224] Wang K, Ruan J, Song H, Zhang J, Wo Y, Guo S, Cui D. Biocompatibility of graphene oxide. Nanoscale Res. Letts.6: 8, 2011.

[225] Bonaccorsa F, Sun Z, Hasan T, and Ferrari AC. Graphene photonics and optoelectronics.Nat. Photonics. 4: 611-622, 2010.

[226] Heo C, Yoo J, Lee S, Jo A, Jung S, Yoo H, Lee YH, and Suh M. The control of neural cell-to-cell interactions through non-contact electrical field stimulation using graphene electrodes.Biomaterials.32: 19-25, 2011.

[227] Zhang L, Xia J, Zhao Q, Liu L, and Zhang Z. Functional graphene oxide as a nanocarrior for controlling loading and targeted delivery of mixed anticancer drugs. Small.6: 537-544, 2010.

[228] Goenka S, Sant V, and Sant S. Graphene-based nanomaterials for drug delivery and tissue engineering. J. Controlled Release. 173: 75–88, 2014.

[229] Paul A, Hasan A, Kindi HA, Gaharwar AK, Rao VT, Nikkhah M, Shin SR, Krafft D, Dokmeci MR, Shum-Tim D, and Khademhosseini A. Injectable graphene oxide/hydrogel-based angiogenic gene delivery system for vasculogenesis and cardiac repair. ACS Nano.8: 8050–8062, 2014.

[230] Hu W, Peng C, Luo W, Lv M, Li X, Li D, Huang Q, and Fan C. Graphene-based antibacterial paper.ACS Nano.4: 4317-23, 2010.

[231] Seabra AB, Paula AJ, de Lima R, Alves OL, and Durán N. Nanotoxicity of graphene and graphene oxide.Chem. Res. Toxicol.27: 159-168, 2014.

[232] Song Q, Jiang Z, Li N, Liu P, Liu L, Tang M, and Cheng G. Anti-inflammatory effects of three dimensional graphene foams cultured with microglial cells. Biomaterials.35, 6930-6940, 2014.

[233] Talukdar Y, and Kundu SC. The effect of graphene oxide nanostructure in mesenchymal stem cells.Biomaterials.35: 4863-4877, 2014.

[234] Yang X, Li L, Shang S, and Tao X. Synthesis and characterization of layer-aligned poly(vinylalcohol) /graphene nanocomposites. Polymer.51: 3431-3435, 2010.

[235] Dikin DA, Stankovich S, Zimney EJ, Piner RD, Dommett GH, Evmenenko G, Nguyen ST, and Ruoff RS. Preparation and characterization of graphene oxide paper.Nature Letts.448:457-460, 2007.

[236] Zhang YZ, Venugopal J, Huang ZM, Lim CT, and Ramakrishna S. Characterization of the surface biocompatibility of the electrospun PCL collagen nanofibers using fibroblasts.Biomacromolecules. 6: 2583–9, 2005.

[237] Schnell E, Klinkhammer K, Balzer S, Brook G, Klee D, Dalton P, and Mey J. Guidance of glial cell migration and axonal growth on electrospun nanofibers of

poly(ε) caprolactone and a collagen/poly-epsilon-caprolactone blend.Biomaterials. 28: 3012–25, 2007.

[238] Ghasemi ML, Prabhakaran MP, Morshed M, Nasr-Esfahani MH, and Ramakrishna S. Electrical stimulation of nerve cells using conductive nanofibrous scaffolds for nerve tissue engineering. Tissue Eng A. 15: 3605–19, 2009.

[239] Izquierdo R, Garcia-Giralt N, Rodriguez MT, Cáceres E, García SJ, Gómez Ribelles JL, Monleón M, Monllau JC, and Suay J. Biodegradable PCL scaffolds with an interconnected spherical pore network for tissue engineering. J. Biomed. Mater. Res. A. 85: 25-35, 2008.

[240] Mobarakeh LG, Prabhakaran MP, Morshed M, Esfahani MHN, and Ramkrishna S. Bio-functionalized PCL nanofibrous scaffolds for nerve tissue engineering. Mat Sci. Engg C. 30: 1129-36, 2010.

[241] Levenberg S, Rouwkema R, Macdonald M, Garfein ES, Kohane DS, Darland DC, and Marini R. Engineering vascularized skeletal muscle tissue. Nature Biotechnology.23: 879 – 884, 2005.

[242] Wang PY, Wu TH, Tsai WB, Kuo WH, and Wang MJ. Grooved PLGA films incorporated with RGD/YIGSR peptides for potential application on skeletal muscle tissue engineering. Colloids Surf B: Biointerfaces.110: 88-95, 2013.

[243] Beier JP, Klumpp D, Rudisile M, Dersch R, Wendorff JH, and Bleiziffer O. Collagen matrices from sponge to nano: new perspectives for tissue engineering of skeletal muscle. MC Biotechnol. 9, 34, 2009.

[244] Ciofani G, Ricotti L, and Mattoli V. Preparation, characterization and in vitro testing of poly(lactic-co-glycolic) acid/barium titanate nanoparticle composites for enhanced cellular proliferation. Biomed Microdevices. 13: 255–66, 2011.

[245] Chen DW, Hsu YH, Liao JY, Liu SJ, Chen JK, and Ueng SW. Sustainable release of vancomycin, gentamicin and lidocaine from novel electrospun sandwichstructured PLGA/collagen nanofibrousmembranes. Int. J. Pharmaceut. 430, 335–41, 2012.

[246] Lee EJ, Lee JH, Jin L, Jin OS, Shin YC, Sang JO, Lee J, Hyon SH,and Han DW. Hyaluronic acid/poly (lactic-co-glycolic acid) core/shell fiber meshes loaded with epigallocatechin-3-O-gallate as skin tissue engineering scaffolds. J Nanosci.Nanotechnol.14: 8458–63, 2014.

[247] Zhang H, Peng C, Yang J, Lv M, Liu R, He D, Fan C, and Huang Q. Uniform ultra-small graphene oxide nanosheets with low cytotoxicity and high cellular uptake. ACS Appl. Mater. Interface.5: 1761-7, 2013.

[248] Yang K, Wan J, Zhang S, Zhang Y, Lee ST, and Liu Z.In vivo pharmacokinetics, long-term biodistribution, and toxicology of PEGylated graphene in mice.ACS Nano.5: 516-22, 2011.

[249] Akhavan O, and Ghaderi E. Toxicity of graphene and graphene oxide nanowalls against bacteria. ACS Nano. 4:5731-5736. 2010.

[250] Lee K, Silva EA, and Mooney DJ. Growth factor delivery based tissue engineering: general approaches and a review of recent developments. J. R. Soc. Interface. 8: 153-170, 2011.

[251] Chen FM, Zhang M, and Wu ZF.Toward delivery of multiple growth factors in tissue engineering.Biomaterials.31: 6279-6308, 2010.

[252] Vasita R, and Katti DS. Growth factor delivery systems for tissue engineering: A materials perspective. Exp. Rev. Med. Devi. 3: 29-47, 2006.

[253] Chaudhuri B, and Pramanik K. Key aspects of the mesenchymal stem cells (MSCs) in tissue engineering for in vitro skeletal muscle regeneration. Biotechnology and Molecular Biology Review. 7: 5-15, 2012.

[254] Bourque WT, Gross M, and Hall BK. Expression of four growth fracture Repair. Int. J. Dev. Biol. 37, 573-579, 1993.

[255] Leask A, and Abraham DJ. TGF-beta signalling and the fibrotic response.FASEB J. 18: 816–827, 2004.

[256] Bernasconi P, Torchiana E, Confalonieri P, Brugnoni R, Barresi R, Mora M, Cornelio F, Morandi L, and Mantegazza R. Expression of transforming growth factor-beta 1 in dystrophic patient muscles correlates with fibrosis. Pathogenetic role of a fibrogenic cytokine. J. Clin. Invest. 96: 1137–1144, 1995.

[257] Ishitobi M, Haginoya K, Zhao Y, Ohnuma A, Minato J, Yanagisawa T, Tanabu M, Kikuchi M, and Iinuma K. Elevated plasma levels of transforming growth factor beta1 in patients with muscular dystrophy. Neuroreport.11: 4033–4035, 2000.

[258] Husmann I, Soulet L, Gautron J, Martelly I, and Barritault D. Growth factors in skeletal muscle regeneration. Cytokine Growth Factor Rev. 7: 249-258, 1996.

[259] Canalis E, McCarthy TL, and Centrella M. Effects of platelet-derived growth factor on bone formation in vitro. J. Cell. Physiol. 140: 530-537, 1989.

[260] van den Bos C, Mosca JD, Winkles J, Kerrigan L, Burgess WH, and Marshak DR. Human mesenchymal stem cells respond to fibroblast growth factors. Human Cell.10: 45-50, 1997.

[261] Chaudhuri B, Bhadra D, Mondal B, and Pramanik K. Biocompatibility of graphene oxide-PCL fibrous scaffolds with human cord blood mesenchymal stem cells derived myoblasts. Matt Letts.126, 109-112, 2014.

[262] Dennis RG, and Kosnik PE 2nd. Excitable and isometric contractile properties of mammalian skeletal muscle constructs engineered in-vitro. In Vitro Cell Dev. Biol. Anim. 36: 327-335, 2000.

[263] Abedalwafa M, Wang F, Wang L, and Li C. Biodegradable poly-Epsilon-Caprolactone (PCL) for Tissue Engineering Applications: A Review. Rev. Adv. Mater Sci. 34: 123-140, 2013.

[264] Izquierdo R, Garcia-Giralt N, Rodriguez MT, Cáceres E, García SJ, Gómez Ribelles JL, Monleón M, Monllau JC, and Suay J. Biodegradable PCL scaffolds with an interconnected spherical pore network for tissue engineering. J Biomed Mater Res A. 85: 25-35, 2008.

[265] Bouissou C, Rouse JJ, Price R, and van der Walle CF. The influence of surfactant on PLGA microsphere glass transition and water sorption: Remodeling the surface morphology to attenuate the burst release. Pharm Res. 23: 1295–1305. 2006. [PubMed: 16715359].

[266] Ungaro FI, Miro A, La Rotonda MI, Quaglia F. Engineered PLGA nano and micro carriers for pulmonary delivery: challenges and promises. J. Pharm. Pharmacol. 64: 1217-1235, 2012.

[267] Allison SD. Effect of structural relaxation on the preparation and drug release behavior of poly(lactic-co-glycolic)acid microparticle drug delivery systems. J. Pharm. Sci. 97: 2022–2035, 2008.

[268] Hummers WS, and Offema R. Preparation of Graphene oxide J. Am. Chem. Soc. 80: 1339–43, 1958.

[269] Park S, An J, Jung J, Piner RD, and An SJ. Colloidal Suspensions of Highly Reduced Graphene Oxide in a Wide Variety of Organic Solvents. Nano Lett . 9: 1593-7 ,2009.

[270] Moore DM and Reynolds RC , X-ray diffraction and the identification and analysis of minerals, 2nd edition, Oxford University Press, New York, 1997.

[271] Smith BC. Fundamentals of Fourier Transform Infrared Spectroscopy, Second Edition, CRC Press, UK, 2011.

[272] Atkins P and De P. Physical Chemistry, 8th Ed. Oxford Uni. Press, Oxford UK, 2006.

[273] Owen T. Fundamentals of UV-visible spectroscopy.Hewlett-Packard publication number 12-5965-5123E.Printed in Germany 09/1996.

[274] Douglas A*S,* Stanley RC, and Holler FJ. Principles of instrumental analysis 6th ed. Belmont, CA, Thomson Brooks/Cole. 169,2007.

[275] Binnig G and Rohrer H. Scanning tunnelling microscopy.Helv.Phys.Acta. 55: 726-735, 1982.

[276] Tersoff J and Hamann DR. Theory of the scanning tunnelling microscope. Phys. Rev. B, 31: 805,1985.

[277] Maher SA.Raman Spectroscopy, Fullerenes and Nanotechnology.RAC Publication, 2010.

[278] Shan XB."High dielectric constant 0-3 ceramic-polymer composites," Auburn University, 2009.

[279] Winter CH, and Hoffman DM. Inorganic Materials Synthesis: New Directions for Advanced Materials. Oxford University Press. 1999.

[280] Kyung Hwa Hong Hong KH, Oh KW, and Kang TJ.Preparation of conducting nylon-6 electrospun fiber webs by in situ polymerization of polyaniline.J. Appl. Poly. Sci. 96: 983-991, 2005.

[281] Goswami J, Bhatnagar N, Mohanty S, and Ghosh AK. Processing and characterization of poly(lactic acid) based bioactive composites for biomedical scaffold application.Polymer Letters. 7: 767–777, 2013.

[282] Jiang T, Abdel-Fattah WI, and Laurencin CT.In vitro evaluation of chitosan/poly (lactic acid-glycolic acid) sintered microsphere scaffolds for bone tissue engineering. Biomaterials. 27: 4894-4903, 2006.

[283] Gu SY, Wang ZM, Ren J, and Zhang CY. Electrospinning of gelatin and gelatin/poly(l-lactide) blend and its characteristics for wound dressing. Mater Sci. Engg. C. 29:1822–1828 ,2012.

[284] Chaudhuri B and Pramanik K.Isolation of Mononuclear Stem Cells from Human Umbilical Cord Blood and Their Scaffold Interactions.Adv. Sci., Engg.and Med. 5: 427-430, 2013

[285] Lee CS. TRIM72 negatively regulates myogenesis via targeting insulin receptor substrate-1. Cell Death and Differentiation (Nature Publishing Group).17: 1254-1256, 2010.

[286] Gang Ej, Jeong JA, Hong SH, Hwang SH, Kim SW et al. Skeletal myogenic differentiation of mesenchymal stem cells isolated from human umbilical cord blood. Stem Cells.22: 617-624, 2004.

[287] Jennifer LY, Triantaphyllopoulos TK, Todd H, and Raguz S. The Human desmin locus: Gene organization and LCR- mediated transcriptional control. Genomics.37: 733-746, 2006.

[288] Berridge MJ. Cell Signaling Biology(e-Book).doi:10.1042/csb0001001, 2014.

[289] Bhadra D, Sannigrahi J, and Chaudhuri BK. Enhancement of the transport and dielectric properties of graphite oxide nanoparticles-polyvinyl alcohol composite showing low percolation threshold. Polymer composite.33:436-42,2012.

[290] Efros AL, and Shklovskii BI. Critical Behaviour of Conductivity and Dielectric Constant near the Metal-Non-Metal Transition Threshold. Phys. Status Solidi B.76: 475-480, 1976.

[291] Bai Y, Cheng ZY, Bharti V, Xu HS, and Zhang QM. High Dielectric Constant Ceramic Powder Polymer Composites .Appl. Phys. Lett.76: 3804, 2000.

[292] Wang JW, Shen QD, Bao HM, and Yang CZ.Microstructure and dielectric properties of P(VDF-TrFE-CFE) with partially grafted copper phthalocyanine oligomer. Macromolecules.38: 2247, 2005.

[293] Mathur RB, Singh BP, Dhami TL, Kalra Y, Lal N, Rao R, and Rao AM. Influence of Carbon Nanotube Dispersion on the Mechanical Properties of Phenolic Resin Composites.Polymer composition.29: 717,2008.

[294] Jiang S, Ji X, An L, and Jiang B. Crystallization behaviour of PCL in hybrid confined environment. Polymer.42:3901–3907, 2011.

[295] Du XS, Xiao M, Meng YZ, and Hay AS. Direct synthesis of poly(acrylenedisulfide)/carbon nanosheet composites via the oxidation with graphite oxide. Carbon.43: 195-213, 2005.

[296] Chen W, Yan l, and Bangal PR. Preparation of graphene by rapid and mild graphene oxide by microwave.Carbon.48: 1146-52, 2010.

[297] Timko BP, Brigham MD, Naik SR, Karajanagi SS, Levy O, Jin H, Prker KK, Langer R, and Kohane DS. Nanowired three-dimensional cardiac patches.Nat.Nanotechnol.Letts.67: 20-725, 2011.

[298] Tuinstra F, and Koenig JL. Characterization of graphite fiber surfaces with Raman spectroscopy. Compos Mater. 4, 492-99,1970.

[299] Jung L, Dikin DA, Piner RD, and Rouff RS.Tuneable Electrical Conductivity of Individual Graphene Oxide Sheets Reduced at "Low" Temperatures. Nano Letters. 8: 4283-4287,2008.

[300] Eda G, Mattevi C, Yamaguchi H, Kim H, and Chhowalla M. Insulator to semimetal transition in graphene oxide.J. Phys. Chem. C. 113:15768-71,2009.

[301] Ferrari AC, Meyer JC, Scardaci V, Casiraghi C, Lazzeri M, and Mauri F. Raman spectrum of graphene and graphene layers. Phys. Rev. Letts.97:187401-4,2006.

[302] Kim KS, Zhao Y, Jang H, Lee SY, Kim JM, Kim KS, Ahn JH, and Kim P. Large-scale pattern growth of graphene films for stretchable transparent electrodes. Nature.45:7706-710,2009.

[303] Kudin KN, Ozbas B, SchnieppHC,Prud'homme RK, Aksay IA, and Car R. Raman spectra of graphite oxide and functionalized graphene sheets. Nano Lett. 8:,36–41,2008.

[304] Mattevi C, Eda G, Anonli S, Miller S, Mkhoyan KA, and Celik O. Evolution of electrical, chemical, and structural properties of transparent and conducting chemically derived graphene thin films.Adv.Funct. Mater.192: 577–2583,2009.

[305] Xu J, Liu J, Wu S, Yang QH, and Wang P. Graphene oxide mode-locked femptosecond erbium doped fiber lasers. Optic Express. 20:15474-15480,2012.

[306] Katsnelson MI, Novoselov KS, and Geim AK.Chiral tunnelling and Klein paradox in graphene.Nat. Phys. 2: 620-625,2006.

[307] Shimanouchi T. Tables of Molecular Vibrational Frequencies. J Phys. Chem. Ref. Data. 1: 189-216, 1972.

[308] Lee WC, Lim CH, Shi H, Tang LA, Wang Y, Lim CT, and Loh KP. Origin of enhanced stem cells growth and differentiation on graphene and graphene oxide.ACS Nano. 5:7334-41,2011.

[309] Sarem M, Moztarzadeh F, and Mozafari M. "How can genepin assist gelation/carbohydrate chitosan scaffolds to act as replacement of load-bearing sift tissues?", Carbohydrate Pol. 93: 635-643, 2013.

[310] Lee SJ, Khang G, Lee YM, and Lee HB.The effect of surface wettability on induction and growth ofneuritis from PC-12 cell on a polymer surface.Colloid Interface Sci.259:228-235,2003.

[311] Wang S, Ang PK, Wang Z, Tang AL, Thong JT, and Loh KP. High mobility, printable and solution processed graphene electronics. Nano Letts. 10:92-98,2010.

[312] Li JL, Kudin KN, McAllister MJ, Prud'homme RK, and Aksay IA, Car R. Oxygen-driven unzipping of graphitic materials.Phys Rev Lett.96 :176101- 4, 2006.

[313] Yan W, Shang J, and Liu JZ. Piezoelectric properties of graphene oxide: A first-principles computational study. Appl. Phys. Letts. 105:023103-5,2014.

[314] Uddin MJ, Sannigrahi J, Masud MG, Bhadra D, and Chaudhuri BK. High dielectric permittivity and percolative behaviour of polyvinyl alcohol and potassium dihydrogenphosphate composites. J. Appl. Pol. Sci. 125: 2363-6,2012.

[315] Goncaves G, Marques PAP, Timmons AB, Bdkin I, Singh MK, Emami N, and Gracio J. Graphene oxide modified with PMMA via ATRP as a reinforced filler . J. Mat. Chem. 20: 9927-9934,2010.

[316] Ansari S, and Giannelis EP. Functionalized graphene sheet-poly(vinylidene fluoride) conductive nanocomposites. J Poly.Sci.Part B. 47: 888-897,2009.

[317] Uddin MJ, Masud MG, Ghosh A, Middya TR, and Chaudhuri BK. Ammonium dihydrogen phosphate/PVA composite films with high dielectric constant and enhanced thermal stability.Adv.Sci. Eng. Med. 51:26-5,2013.318

[318] Lima CGA, Oliveira RSD, Figueiro SD, Wehmann CF, Goes JC, and Sombra ASB. DC conductivity and dielectric permittivity of collagen chitosan films.Mat Chem.Phys.99: 284-288,2006.

[319] Yi JS, Park JS, Ham YM, Nguyen N, Lee NR, Hong J, Kim BW, Lee H, and Lee CS. MG53-induced IRS-1 ubiquitination negatively regulates skeletal myogenesis and insulin signaling. Nature Communications. 4: 2354, 2013.

[320] Stitt TN, Drujan D, Clarke BA, Panaro F, Timofeyva Y, Kline WO, Gonzalez M, Yancopoulos GD, and Glass DJ. The IGF-1/PI3K/Akt pathway prevents expression of muscle atrophy-induced ubiquitin ligases by inhibiting FOXO transcription factors. Mol. Cell. 14(3):395-403. 2004.

[321] Harada H, Andersen JS, Mann M, Terada N, and Korsmeyer SJ.p70S6 kinase signals cell survival as well as growth, inactivating the pro-apoptotic molecule BAD. Proc. Natl. Acad. Sci. U.S.A. 98: 9666-9670.2001.

[322] Thimmaiah KN, Easton JB, Germain GS, Morton CL, Kamath S, Buolamwini JK, and Houghton PJ.Identification of N10-substituted phenoxazines as potent and specific inhibitors of Aktsignaling. J. Biol. Chem. 280: 31924-31935, 2005.

[323] Jeong SJ, Pise-Masison CA, Radonovich MF, Park HU, and Brady JN. Activated Akt regulates NF-kappaB activation, p53 inhibition and cell survival in HTLV-1-transformedcells. Oncogene. 24: 6719-6728, 2005.

[324] Thimmaiah KN, Horton JK, Seshadri R, Israel M, Houghton JA, Harwood FC, and Houghton PJ. Synthesis and chemical characterization of N-substituted phenoxazines directed toward reversing vinca alkaloid resistance in multidrug-resistant cancer cells. J. Med. Chem. 35: 3358, 1992.

[325] Schniepp HC, Michael JL, McAllister MJ, Sai H, AlonsoMH, and Adamson DH.Functionalized sing graphene sheets derived from splitting graphite oxide. J. Phys. Chem B. 110: 8535-9, 2006

[326] Tuinstra F, and Keono JL. Characterization of graphite fiber surfaces with Raman spectroscopy. Compos Mater 4: 492-99, 1970.

[327] Chien CT, Li SS, Lai WJ, Yeh YC, Chen HA, Chen IS, Chen LC, and Chen KH. Tuneable photoluminescence from grapheme oxide.Angew.Chem.Int. Ed. 51: 1-6, 2012.

[328] Eda G, Lin YY, Mattevi C, Yamaguchi H, Vhen HA, Chen IS, and Chen CW. Blue photoluminescence from chemically derived grapheme oxide.Adv.Mater. 22: 505-509. 2010.

[329] Georgieva N ,Bryaskova R, and Tzoneva R. New polyvinyl alcohol-based hybrid materials for biomedical; application, Mat. Letts.88: 19-22, 2012.

[330] Leenaert O, Partoens B, and Peeters M. Water on graphene: Hydrophobicity and dipole moment using density functional theory. Phys. Rev. B. 79: 235440-5,2009.

[331] Eda G, Ball J, Mattevi C, Acik M, Artiglia L, Granozzi G, Chabal Y, et al. Partially oxidized graphene as a precursor to graphene.J. Mat. Chem 21: 11217-11223, 2011.

[332] Chen ZG , Mo X, He C, and Wang Hl. Intermolecular interactions in electrospun collagen-chitosan complex nanofibers. Carbohydr.Polym.72: 410–418, 2008.

[333] Li Q, Wei Q, Wu N, Cai Y, and Gao W. Structural characterization and dynamic water adsorption of electrospun polyamide/montmorillonite nanofibers. Appl. Polym. Sci. 107: 3535-40, 2008.

[334] Gittings JP ,Bowen CR,Turner IG, BaterF, and Chaudhuri J. Characterization of ferroelectric-calcium phosphate composites and ceramics. J. Eur. Cera. Soc. 27: 4187-490, 2007.

[335] Dvir T ,Timko BP, Brigham MD, Naik SR, and Karajanagi S.Nanowired three dimensional cardiac patches.Nature Nanotechnology. 6: 720–725. 2012.

[336] Chang Z, Yan W, Shang J, and Liu J . Piezoelectric properties of graphene oxide: A computational study. Appl. Phys. Letts. 105: 023103-5,2014.

[337] Nakamura S, Kobayashi T and Yamashita K.Enhanced osteobonding by negative surface charge of electrically polarized Hydroxyapatite.J.Biomed.Meter. Res. 57: 477-484,2001.

[338] Matta, and Cherif F. Quantum biochemistry : Electronics structure and biological activity. Weinheim: Wiley-VCH, 2014.

[339] Majumdar R. Quantum-mechanics: In physics and chemistry with applications in biology ,Newi: PHI Learning,2011.

[340] Line M E, and Glass AM. Principles and applications of ferroelectric and related materials, Oxford , 2001, ISBN :9780198507789.

[341] Taravel MN, and Doamrd A. Collagen and its interaction with chitosan, Part-II.Influence of physicochemical characteristics of collagen.Biomaterials.16: 865-87, 1995.

[342] Sousa VOS, Silva CC, Almeida AFL, Fifueiro SD, Goes JC, de Paiva JAC, Magalhaes CEC and Sombra ASB. Study of the electrical conductivity and piezoelectricity in iron doped collagen films.Solid State Sci. 4: 43-51..2002.

[343] Bowen CR, Gittings J and Turner IG.Dielectric and piezoelectric properties of hydroxyapatite-BaTiO3 composites. Appl. Phys.Letts. 89: 132906-3,2006..

[344] Bendrea AD, Cianga L and Cinga ID. Review paper: Progress in the field of conducting polymers for tissue engineering applications.J. Biomaterials. Appl. 26: 3-84,2011..

[345] Fukada E .Piezielectricity and pyroelectricity of Biopolymers, ferroelectric polymers, Nalwa H S (ed), Marcel Dekker Inc. New York, pp 393-439, 1995.

[346] Mascarenhas S.Bioelectrets in Topics in Appl. Phys. Electrets, 23, Springer-Verlag, Berlin, 1987.

[347] Herbst E .Electrical stimulation of bone growth and repair , ed. Burny F, Herbst E and Hinsonkamp M .Springer-Warlag , Berlin, pp 1-13, 1978.

[348] Hardy JG ,andSchmidt EE. Biomimetic conducting polymer based tissue scaffolds. Current Opinion in Biotechechnology.24: 847-854, 2013.

[349] Dutta P, Biswas S,andDe SK. Dielectric relaxation in polyaniline–polyvinyl alcohol composites ,Mater. Res. Bull. 37:193-200, 2007.

CURRICULUM VITAE

Biswadeep Chaudhuri
Dept. of Biotechnology and Medical Engineering
National Institute of Technology,
Rourkela 769008, Odisha, India

Academics:

- **B.Tech** (Biotechnology), 2008: Heritage Institute of Technology, Kolkata, India
- **M.S.** (Industrial Biotechnology) 2009: Newcastle University, UK
- **Ph.D.** (Research in Tissue Engineering Dec. 2010 – April, 2016) : National Institute of Technology, Rourkela, India

Research Areas: Stem Cells, Biomaterials, Tissue Engineering, Regenerative Medicine, Scaffolds, Polymers.

Technical Skills / Experience:

- Isolation, characterization and maintenance of Human Umbilical Cord Blood derived Mesenchymal Stem Cells
- Stem Cells proliferation as well as lineage specific differentiation
- In vitro Stem Cells viability and proliferation assay (using MTT, WST-8)
- Electrospun fibrous scaffolds preparation using biocompatible polymer composites
- Characterizations of scaffolds using XRD, FTIR, SEM etc.
- Microscopic analysis: Compatible with Confocal (Immunostaining) & Phase Contrast microscope
- FACS - BD LSR Fortessa (Immunophenotypic characterizations of Stem Cells).
- Cell signaling pathway (IGF-1) analysis using Western Blotting , RT-PCR.

❖ Publications:

(1) B. Chaudhuri, D Bhadra , L Moroni and K Pramanik. Myoblast differentiation of human mesenchymal stem cells on graphene oxide and electrospun graphene oxide–polymer composite fibrous meshes: importance of graphene oxide conductivity and dielectric constant on their biocompatibility. Biofabrication.(IOP, SCIENCE).1-13; 7; 015009. 2015. (IF 4.3/ SCI indexed).

(2) B. Chaudhuri, D Bhadra, B Mondal, K Pramanik. Biocompatibility of electrospun graphene oxide–poly(ε-caprolactone) fibrous scaffolds with human cord blood mesenchymal stem cells derived skeletal myoblast. Materials Letters. (ELSEVIER) 109-112, 126, 2014. (IF 2.5 / SCI indexed).

(3) B. Chaudhuri, K Pramanik. Isolation of Mononuclear Stem Cells from Human Umbilical Cord Blood and their scaffolds interaction.Advanced Science, Engineering and Medicine. (AMERICAL SCIENTIFIC PUBLISHERS).5, 427-430, 2013 (IF 0.862)

(4) B. Chaudhuri, K Pramanik. Key aspects of the mesenchymal stem cells (MSCs) in tissue engineering for in vitro skeletal muscle regeneration.Biotechnology and Molecular Biology Review.5-15, 7. 2012 (ISI indexed) (Review paper)

❖ Papers Communicated (2016):

(1) B. Chaudhuri, K. Pramanik. Influence of IGF-1 cell signaling pathway for skeletal muscle differentiation for skeletal muscle tissue engineering applications. Journal of Biomaterial and Tissue Engineering.(Communicated, March2016).

(2) B. Chaudhuri, K. Pramanik. Myoblast differential potential of umbilical cord blood derived mesenchymal stem cells on graphene oxide-PLGA composite electrospun scaffolds for skeletal muscle tissue engineering applications. (Communicated, March 2016)

❖ Conference Papers:

(1) Biswadeep Chaudhuri and K Pramanik., Myoblast differentiation of human cord blood mesenchymal stem cells on thin graphene oxide sheets and electrospun graphene oxide-PLGA composite scaffolds. Proc. Int. Symposium on Polymer Science and Technology, Kolkata (Jan.23-26) P-522, PB10, Page 523, PB11 (2015).

(2) Biswadeep Chaudhuri, G Sardar, Md. Masud, J Uddin, B K Chaudhuri and KPramanik: Observation of enhanced conductivity and dielectric constant in polyvinyl alcohol/polyvinylpyrrolidone blend-hydroxyapatite nd graphene oxide composite; Biocompatibility study using human cord blood stem cells. Indian Science congress 2014.

(3) Biswadeep Chaudhuri, K. Pramanik. Umbilical Cord Blood derived Stem Cells and its applications for Biomedical applications. 1st International Conference of Tissue Engineering and Regenerative Medicine (ICTERM), NIT Rourkela, Dept. of Biotech & Med. Engg - 2011.

Awards:

- Best Research Scholar Award 2015, Dept. of Biotechnology & Medical Engineering, National Institute of Technology, Rourkela, India.
- Best Poster Presentation Award, 2013, International Conference on Tissue Engineering & Regenerative Medicine; Dept. of Biotechnology & Medical Engineering, National Institute of Technology, Rourkela, India.

Membership:

- Indian Science Congress